

12-2016

THE ROLE OF PHOSPHORYLATION IN PAM2 MOTIF-CONTAINING PROTEINS MEDIATED MESSENGER RNA DEADENYLATION

KAI-LIEH HUANG

Follow this and additional works at: https://digitalcommons.library.tmc.edu/utgsbs_dissertations



Part of the [Biochemistry Commons](#), and the [Molecular Biology Commons](#)

Recommended Citation

HUANG, KAI-LIEH, "THE ROLE OF PHOSPHORYLATION IN PAM2 MOTIF-CONTAINING PROTEINS MEDIATED MESSENGER RNA DEADENYLATION" (2016). *The University of Texas MD Anderson Cancer Center UTHealth Graduate School of Biomedical Sciences Dissertations and Theses (Open Access)*. 722. https://digitalcommons.library.tmc.edu/utgsbs_dissertations/722

This Dissertation (PhD) is brought to you for free and open access by the The University of Texas MD Anderson Cancer Center UTHealth Graduate School of Biomedical Sciences at DigitalCommons@TMC. It has been accepted for inclusion in The University of Texas MD Anderson Cancer Center UTHealth Graduate School of Biomedical Sciences Dissertations and Theses (Open Access) by an authorized administrator of DigitalCommons@TMC. For more information, please contact digitalcommons@library.tmc.edu.

**THE ROLE OF PHOSPHORYLATION IN PAM2 MOTIF-CONTAINING PROTEINS
MEDIATED MESSENGER RNA DEADENYLATION**

KAI-LIEH HUANG, M.S.

APPROVED:

Ann-Bin Shyu, Ph.D.
Advisory Professor

Zheng Chen, Ph.D.

Jianping Jin, Ph.D.

William W. Mattox, Ph.D.

Ambro van Hoof, Ph.D.

APPROVED:

Dean, The University of Texas
Graduate School of Biomedical Sciences at Houston

**THE ROLE OF PHOSPHORYLATION IN PAM2 MOTIF-CONTAINING PROTEINS
MEDIATED MESSENGER RNA DEADENYLATION**

A

DISSERTATION

Presented to the Faculty of

The University of Texas Health Science Center at Houston
and
The University of Texas MD Anderson Cancer Center

Graduate School of Biomedical Sciences

in Partial Fulfillment of

the Requirements

for the Degree of

DOCTOR OF PHILOSOPHY

by

KAI-LIEH HUANG, M.S.

Houston, Texas

December 2016

Dedication

I dedicate this dissertation to

my wife

Hui-Chen Jean Lee

&

my parents

Kong Huang & Mei-Lan Chang

&

my children

Bethany L. Huang and Jonathan L. Huang

You two were born during the period of this work.

Acknowledgements

A biggest and most special thank goes to
Dr. Ann-Bin Shyu and Dr. Chyi-Ying A. Chen
for accepting me as their graduate student,
training me to be a methodical scientist,
giving me advice on work and on life, and
supporting my research.

Supervisory committee members:

Thank you all for helping & providing me all sorts of suggestions.

Ambro van Hoof, Ph.D.

Jianping Jin, Ph.D.

William W. Mattox, Ph.D.

Zheng (Jake) Chen, Ph.D.

Candidacy examination members:

Deepa Sampath, PhD

Kelly Hunt, MD

Russell Broaddus, MD/PhD

Advisory committee members:

Alexander Lazar, MD/PhD

Kevin Rosenblatt, MD/PhD

Menashe Bar-Eli, PhD

Raphael Pollock, MD/PhD

Weihua Zhang, PhD

Sponsors for my first few years in GSBS program (including tutorials):

Dina Lev, MD

Hui-Kuan Lin, PhD

Mien-Chie Hung, PhD

Lab members:

Yi-Fang Ho

Yueqiang Zhang

Lingzhi Liu

Amanda B. Chadee

BMB Colleagues:

Ju-Mei Li

Baokun He

Jiandong Chen

Friends:

Ning Tsao

Chia-Chi Chang

Judy Tsai

Shirley Lau

Moonsup Lee

Kari Savannah

.....

Above are the people I met on the journey of my graduate study

Hundreds of thousands of appreciation words in my mind

I just want to let you all know that

You are in my heart, and will remain, for as long as I live.

THE ROLE OF PHOSPHORYLATION IN PAM2 MOTIF-CONTAINING PROTEINS MEDIATED MESSENGER RNA DEADENYLATION

KAI-LIEH HUANG, M.S.

Advisory Professor: ANN-BIN SHYU, Ph.D.

Phosphorylation regulates many cellular processes. However, its role in mRNA deadenylation, a process to remove poly adenosines from the mature mRNA 3' end tail, is unclear. The length of poly(A) tail determines mRNA stability and translation efficiency. Poly(A)-binding protein (PABP), which binds to newly synthesized poly(A) tails homogeneously and is known as a scaffold protein for PAM2 motif-containing proteins, plays a pivotal role in the shortening of poly (A) tails. This study is to examine the role of phosphorylation of PAM2 motif-containing proteins in regulating their interactions with PABP and mRNA deadenylation function.

The PAM2 motif, a region required for binding PABP C-terminal domain, is embedded inside the intrinsically disordered region (IDR) of its containing proteins. IDR is known to be a favored site for phosphorylation, and the PAM2 motif is surrounded by numerous potential phosphorylation sites. To test whether phosphorylation plays a role in controlling the interaction between PAM2-containing proteins and PABP, this study used complementary approaches (to alter the phosphorylation level of PAM2 motif-containing proteins biochemically and to create phospho-mimetic (PM) and non-phosphorylatable (NP) mutants). The results showed that reducing or increasing phosphorylation of these proteins can enhance or diminish their interaction with PABP, respectively. Furthermore, diminished PABP interaction compromises the biological functions of these proteins in deadenylation and miRNA-mediated gene silencing.

Using Tob2-PABP interaction as a model, this study provides more insight into the mechanism by which phosphorylation of PAM2 motif-containing proteins regulates their interactions with PABP. The data presented here suggest that the two PAM2 motifs of Tob2 interact with PABP in a synergistic rather than additive manner. Multiple phosphorylation induced by JNK1 in Tob2 IDR compromises Tob2-PABP interaction. A critical site for phosphorylation of Tob2 was identified. Global mRNA deadenylation can be regulated by phosphorylation status of this site.

Collectively, this work provides a new concept, in which signaling pathways crosstalk may tune global deadenylation rates through phosphorylation of PAM2 motif-containing proteins to modify their PABP affinity.

Table of Contents

Approval Sheet..... i

Title Page ii

Dedication..... iii

Acknowledgements iv

Abstract vi

Table of Contents..... viii

List of Figures xii

List of Tables xv

Chapter 1. Introduction	1
1.1 Messenger RNA biogenesis and poly(A) tail functions	2
1.2 Deadenylation	3
1.3 Poly(A)-binding proteins.....	5
1.4 PAM2 motif-containing proteins	9
1.5 Intrinsically disordered region	10
1.6 Post-translational modification-phosphorylation	11
1.7 Significance of the study	12
 Chapter 2. Materials and Methods	15
2.1 Plasmids construction	16
2.2 PCR-based site-directed mutagenesis	17
2.3 Cell culture, transfection, and protein induction	19
2.4 Stable cell lines establishment	20
2.5 Proliferation assay	22
2.6 Cell cycle analysis	22
2.7 Co-immunoprecipitation and western blot	23
2.8 RNA preparation and RNA-immunoprecipitation	25
2.9 Sample preparation for RNA sequencing	26
2.10 Northern blot	27
2.11 Poly(A) tail distribution assay	28
2.12 Sample preparation for Mass spectrometry	29
2.13 Renilla and firefly dual luciferase assay	29

Chapter 3. Phosphorylation of intrinsically disordered region of PAM2 motif-

containing proteins modulates their interaction with PABP and influences mRNA

fate.....	31
Introduction	32
Results	34
3.1 PAM2 motifs are generally embedded within intrinsically disordered regions	34
3.2 PAM2 motifs in IDRs are generally located next to a cluster of phosphorylation sites.....	38
3.3 Phosphorylation of Tob2 and its ability to interact with PABPC1	39
3.4 Removal of phosphates from Pan3 and Tnrc6c enhances their interaction with PABPC1	42
3.5 Effects of increased phosphorylation of Tob2 and Pan3 on their interactions with PABPC1	43
3.6 Phosphomimetic mutations in the IDRs of Tob2, Pan3, and Tnrc6c diminish their interactions with PABPC1	46
3.7 Phosphomimetic mutations alter Tob2, Pan3, and Tnrc6c functions	48
Discussion.....	51

Chapter 4. Phosphorylation regulates Tob2 function on global mRNA

deadenylation.....	56
Introduction	57
Results	60
4.1 c-Jun N-terminal kinase triggers Tob2 hyper-phosphorylation and weakens Tob2-PABP interaction.....	60

4.2 Identification of JNK1-induced hyper-phosphorylation sites for Tob2-PABP interaction.	62
4.3 S254 phosphorylation of Tob2 enhances mRNA deadenylation in vivo	66
4.4 Multiple phosphorylation outside PAM2 motif of Tob2 reduces PABP interaction	69
4.5 PAM2 motifs work synergistically to interact with PABP	70
4.6 Establishment of Tob2 inducible cell line	71
4.7 Optimization of condition for checking Tob2 S254D effect on deadenylation ...	75
4.8 Tob2 anti-proliferation effect is linked to destabilization of Cyclin mRNAs	80
4.9 CDK1 is likely a major kinase to phosphorylate Tob2 at serine 254	82
Discussion.....	83
 Chapter 5. Retrospectives and Perspectives	89
 Bibliography	94
 Vita	110

List of Figures

Figure 1.1 mRNA life cycle.....	3
Figure 1.2 mRNA decay pathway	4
Figure 1.3 Structure and motifs of human poly(A) binding protein family	6
Figure 1.4 Structure and interaction of PABP C-terminal domain MLLE structure with PAM2 motif	7
Figure 1.5 Current model: MLLE domain of last PABP on poly(A) tail determines which PAM2 motif-containing proteins to interact with	8
Figure 3.1 PAM2 motif-containing proteins contain extensive regions of intrinsic disorder	37
Figure 3.2 Diagram of four representative PAM2-containing PABP-interacting proteins	38
Figure 3.3 Effects of alkaline phosphatase treatment on phosphorylation of four PAM2-containing proteins and their interactions with PABP	41
Figure 3.4 Effects of Calyculin A treatment on phosphorylation of PAM2-containing proteins and their interactions with PABP	45
Figure 3.5 Diagram shows the mutation sites introduced into proteins Tob2, Pan3, and Tnrc6c	48
Figure 3.6 Functional impacts of phosphomimetic (PM) and nonphosphorylatable (NP) mutations on Tob2, Pan3, and Tnrc6	50
Figure 4.1 Co-expressing constitutive activated JNK1 and Tob2 in U2OS cells induces Tob2 hyper-phosphorylation	61
Figure 4.2 Tob2 hyper-phosphorylation can be triggered by UV or Nocodazole	62
Figure 4.3 Identify JNK1-induced hyper-phosphorylation sites by Mass Spectrometry..	63

Figure 4.4 Mutagenesis study to evaluate the impacts of JNK1-induced phosphorylation sites and common highly confident sites on PABP interaction	64
Figure 4.5 Alignment of known PAM2 motif from Homo sapiens.....	65
Figure 4.6 Tob2 serine 254 phospho-mimetic mutation enhances Tob2 function in promoting β -globin reporter mRNA deadenylation	67
Figure 4.7 Tob2 serine 254 phospho-mimetic mutation enhances Tob2 function in promoting global mRNA deadenylation	68
Figure 4.8 JNK reduces Tob2-PABP interaction regardless of S254 status	69
Figure 4.9 The synergism of Tob2 individual PAM2 motif with PABP interaction	71
Figure 4.10 Create tTA-expressing U2OS Tet-off stable cell line	72
Figure 4.11 Examination of the capability of each stable cell line to induce and to repress luciferase gene in the absence and presence of doxycycline, respectively	74
Figure 4.12 Testing the capability of U2OS Tet-off stable cell lines to induce and to repress reporter RNA	75
Figure 4.13 Schematic diagram of pulse-chase bromouridine RNA immunoprecipitation	76
Figure 4.14 Schematic diagram shows the usage of BrU pulse-labeling RNA-IP to study the impact of Tob2 on mRNA stability	77
Figure 4.15 Estimation of the earliest time point where induced Tob2 S254D exerts highest function on promoting deadenylation	78
Figure 4.16 Poly(A) size distribution assay checking the effect of Tob2 S254D in global mRNA population.....	79
Figure 4.17 Tob2 anti-proliferation effect does not affect cell cycle distribution.....	81
Figure 4.18 Mass Spectrometry analysis to identify unique and overlapping interaction proteins of Tob2 WT and S254 mutants	83

Figure 4.19 From co-crystallized structure of PAM2 (from Paip2)-MLLE to hypothesize Tob2 S254 effect on PABP interaction	85
Figure 4.20 A model showing multi-layer regulations of Tob2 function in deadenylation	87
Figure 5.1 Diagram shows the hypothesis of the feedback loop of deadenylation regulation and its effect on cell proliferation	92

List of Tables

Table 3.1 Survey of 13 human proteins known or predicted to interact with PABPC1 through the PAM2 motif, which is generally embedded within intrinsically disordered region (IDR)	35
--	----

Chapter 1

Introduction

1.1 Messenger RNA biogenesis and poly(A) tail functions

mRNAs are ribonucleic acids transcribed from DNA by RNA polymerase II in eukaryotic cells. They only account for ~3% of the population of total RNAs; however, they encode for every protein in a cell (1,2). Immediately following the start of transcription, a 7-methylguanosine nucleotide is added to the 5' end of mRNA (3). This precursor mRNA then goes through splicing (4) to remove non-coding intron sequences while polymerase II continues transcribing. Before the end of transcription, pre-mRNA is cleaved and released by Cleavage and polyadenylation specificity factors (CPSFs) (5). Immediately after the cut, adenosine monophosphates are added to the 3' end by polynucleotide adenylyltransferase at the site downstream of polyadenylation signal sequence AAUAAA. This process is known as polyadenylation (6), which is considered the last step of mRNA maturation in the nucleus.

The majority of mRNAs in a eukaryotic cell are modified by polyadenylation with the notable exception of those coding for histone protein during maturation process. The homogeneous poly(A) tail is known to stretch 250 and 100 adenines in length in mammals and yeast, respectively. Once poly(A) tail starts to form, poly(A)-binding proteins (PABPs) associate with the tail forming a tail complex. This tail-PABPs complex plays critical roles throughout a majority of steps in the mRNA life cycle (Figure 1.1) including, splicing (7), nucleus exportation (8), subcellular localization (9), translation initiation, repression, and termination (10), microRNA-mediated gene silencing (11), and mRNA turnover (1,2,10,12,13).

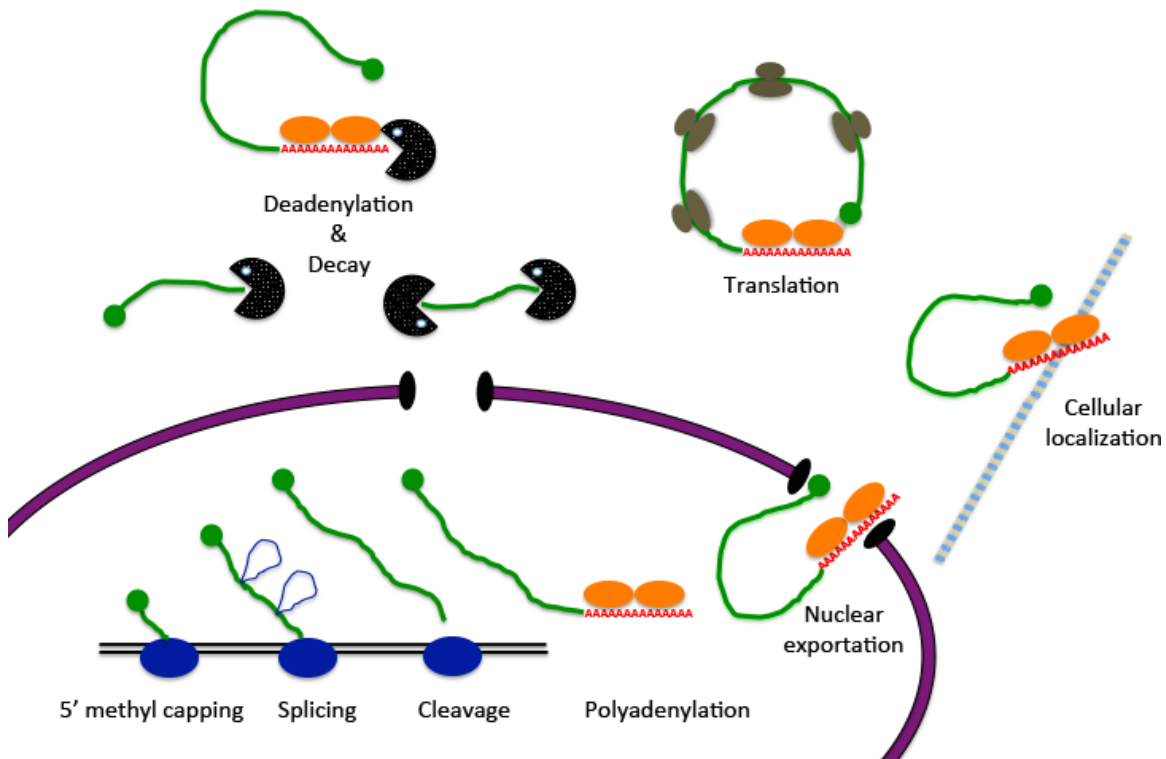


Figure 1.1 mRNA life cycle. Messenger RNA (green line) is transcribed by polymerase II (blue oval). Immediately following synthesis, 5' of mRNA is methyl capped (green solid circle). Splicing (blue loop) occurs while transcribing. At the end of transcription, mRNA is cleaved by CPSF, followed by polyadenylation (red A). PABPs (orange oval) harbor on the poly(A) tail once it is synthesized. The PABPs-poly(A) tail complex is involved in mature mRNA nuclear export, cellular localization, translation, and deadenylation.

1.2 Deadenylation

Removal of a poly(A) tail from 3' end is the major way to regulate mRNA functions in a cell (14,15). This process, deadenylation, is carried out mainly by deadenylase complex Ccr4-Caf1 in all eukaryotic cells. In mammals, a deadenylase complex Pan2-Pan3 is found to be responsible for the shortening of poly(A) tail in the early stage of deadenylation from 250nt to ~110nt. The half length poly(A) tail is then chopped by Ccr4-Caf1 complex from ~110bp to 10bp. This two-phased (16) model was based on the observation that poly(A) tail shortening is in a homogeneous slow distributive enzymatic digestion fashion during the first phase. In this phase, the mRNA

body has no detectable decay. Second phase deadenylation follows when the Ccr4-Caf1 complex hydrolyzes the tail in a processive enzymatic digestion fashion. The mRNA body is decayed during this phase (17). In addition, deadenylation, in most cases, is ahead of, and required for, mRNA body decay. Furthermore, the deadenylation rate may be controlled by cis-acting elements. Followed the default state of deadenylation in which all polyadenylated mRNAs undergo tail shortening, decapping is carried out by Dcp1/2 before Xrn1 performs exonucleolytic digestion from 5' to 3' direction (18-20). This is the major cytoplasmic mRNA decay pathway (Figure 1.2). In some cases, mRNA decay can be independent to deadenylation, where exosome chops the mRNA from 3'→5' fashion, regardless of decapping (21,22).

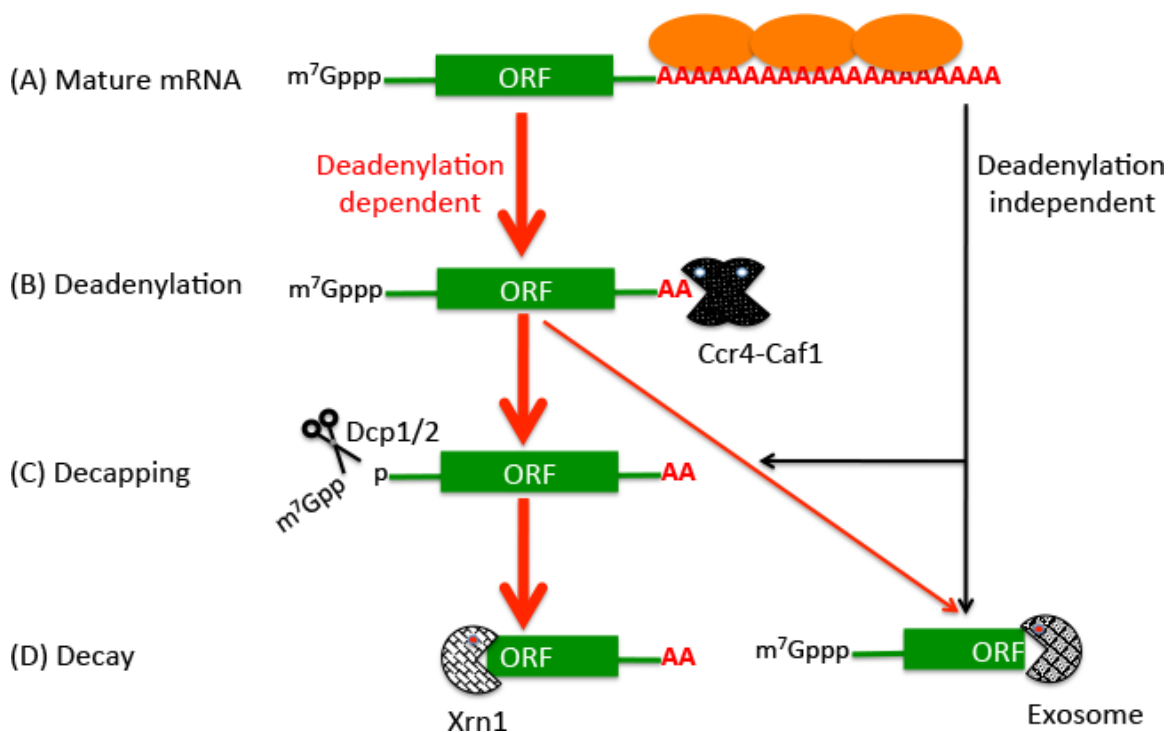


Figure 1.2 mRNA decay pathways. A mature mRNA has 5' methyl cap and 3' poly (A) tail (red A) harbored with PABPs (orange oval). In majority circumstances (red thick arrow), mRNA decay is deadenylation-dependent. It goes as follows: first (B) deadenylation, where Pan2-Pan3 (not depicted) and Ccr4-Caf1 deadenylase complexes digest poly (A) tail to oligomer level, then second (C) decapping, where Dcp1/2 removes the methyl cap, and third (D) decay of mRNA body by Xrn1 takes place. In some cases,

(red thin arrow), nuclease exosome will digest the mRNA body from 3' end after the deadenylation skipping decapping process. In other cases, mRNA decay is deadenylation-independent (black thin arrow). It can either be directly digested by exosome or can be decapped, followed by Xrn1 digestion.

1.3 Poly(A)-binding proteins

Poly(A)-binding protein (PABP) binds to poly(A) tail right after mRNA polyadenylation has occurred. It has been shown that each PABP can interact with ~25 adenylate residues of poly(A) tail (23). Accordingly, there will be around 4 PABPs and 10 PABPs bound on newly synthesized poly(A) tail to control mRNA functions in yeast and mammals, respectively. The PABP gene family is evolutionarily highly conserved and known for its role as a scaffold protein, providing an access point for regulatory proteins to control the length of poly(A) tail (24-26). In mammalian cells, five PABPs have been identified (Figure 1.3). Among them, four (PABPC1, PABPC3, iPABP, and X-linked PABPC5) are cytoplasmic forms and one (PABPN1) is a nuclear form. PABPC3 is testis-specific while iPABP is inducible protein (24). In cytosol, PABPC1 is the most abundant form and contributes significantly to the function of poly(A) tail in cytoplasm including translation initiation/termination, mRNA translocation, and mRNA stability. In the nucleus, PABPN1 controls the length of polyadenylation (27) and contributes to mRNA splicing (28) and nuclear exportation (29).

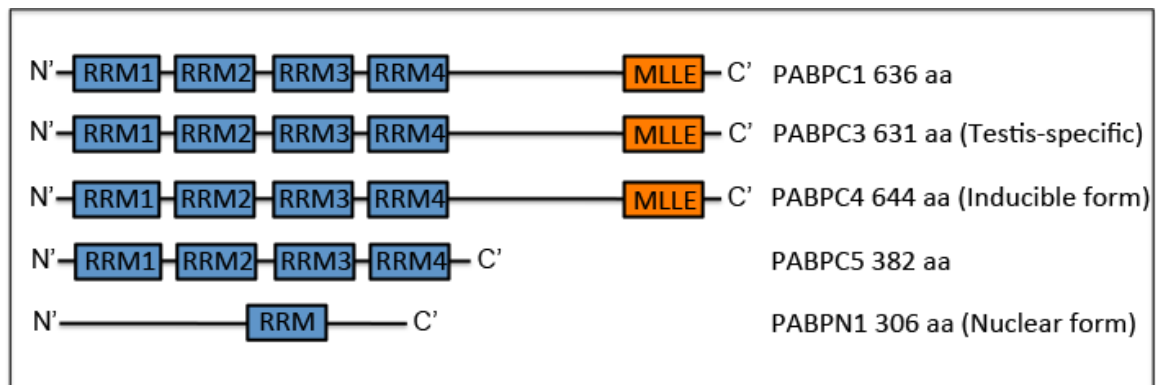


Figure 1.3 Structure and motifs of human poly(A) binding protein family. All members of PABP except nuclear PABPN1 have RRM motifs (blue box) close to N-terminal for poly(A) RNA interaction. Three members have C-terminal MLLE domain for PAM2 motif interaction. Within the cytoplasmic form of PABPs (PABPC1, PABPC3, PABPC4, and PABPC5), PABPC1 expression is predominant and is playing the most critical role. One nuclear PABPN1 is playing roles in pre-mRNA maturation and export.

Structurally, all PABPs in mammals contain RNA-binding motifs (RRM) at N-terminal for RNA binding, while only three PABPs (PABPC1, PABPC3, iPABP) have a unique MLLE motif located in an additional region at the C-terminal end. MLLE represents the conserved signature amino acids in the motif, which is consisted of four and five α -helices in yeast and mammals, respectively (25,30). These helices form a globular structure, which is required for interactions with various regulatory proteins (Figure 1.4). The MLLE motif structure is not only found at PABP C-terminus end, but has also been identified in E3 ligase protein HYD, suggesting the same MLLE-interacting regulatory proteins can be subjected to ubiquitin-mediated protein degradation (24,30), although there is no evidence so far.

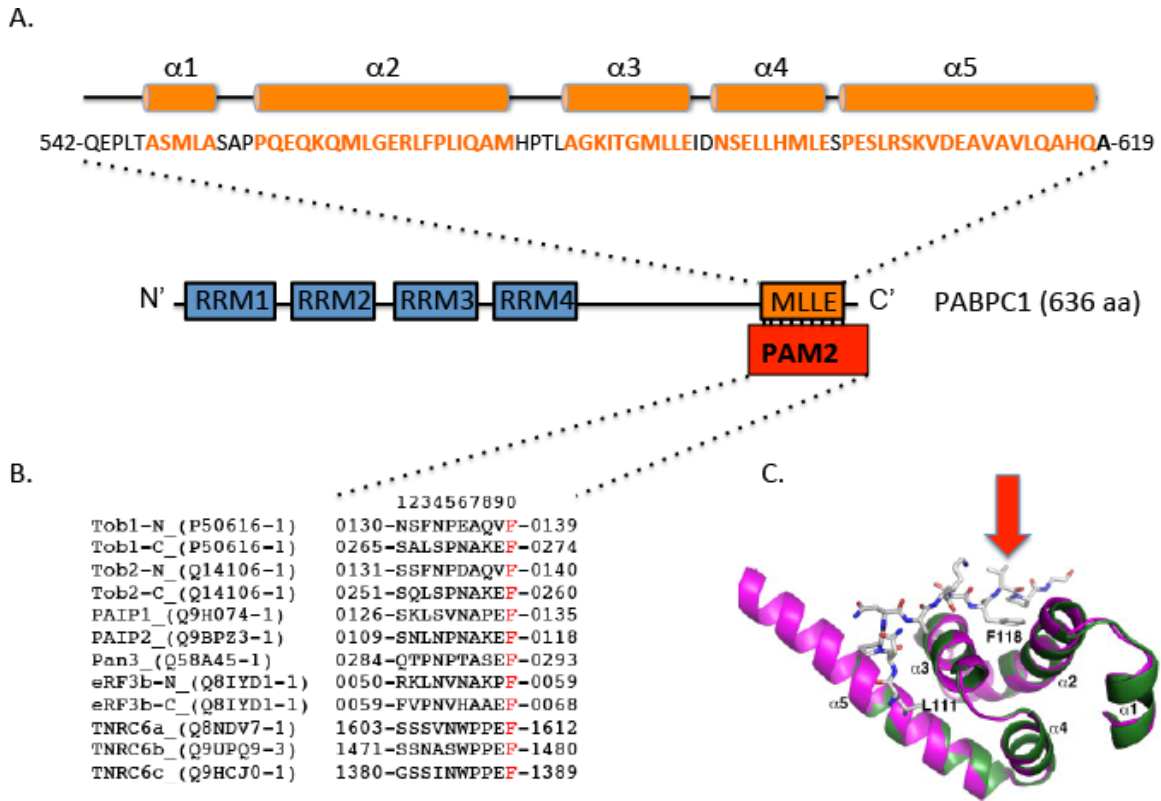


Figure 1.4 Structure and interaction of PABP C-terminal domain MLLE structure with PAM2 motif. MLLE domain at the C-terminal end is consisted of five α -helices (A). MLLE domain is subjected to mediate the interaction of PABP with PAM2 motif of containing proteins. The alignment of well-known PAM2 motifs from human PAM2 motif-containing proteins (B) displays the signature conserved amino acid phenylalanine (red F). Numbers are assigned based on phenylalanine. The crystal structure of MLLE domain interacting with PAM2 motif from Paip2 protein is shown (C). Ribbons represent α -helices 1 to 5 while sticks represent PAM2 motif. Aromatic ring of F118 (red thick arrow) fitting into the grooves created by α 2- and α 3-helices is an indispensable amino acid for the interaction (crystal structure is adapted with permission license No. 3850620841706 from Kozlov, G., Menade, M., Rosenauer, A., Nguyen, L., and Gehring, K. Molecular determinants of PAM2 recognition by the MLLE domain of poly(A)-binding protein. *Journal of molecular biology* 2010 **397**, 397-407).

After decades of X-ray crystallography (32) and atomic force microscope (33) studies, it is now known that those PABPs docking on the mRNA poly(A) tail are in the same directional arrangement and are oligomerized (31) through the C-terminal domain of one PABP to neighboring PABP at yet undetermined sites. In this configuration, although there are several cytoplasmic PABPs docking on the mRNA poly(A) tail, only the very last one at 3' end is thought to have an exposed MLLE motif available for

communication (34) with regulatory proteins (PAM2 motif-containing proteins) and 60S ribosomal subunit (Figure 1.5).

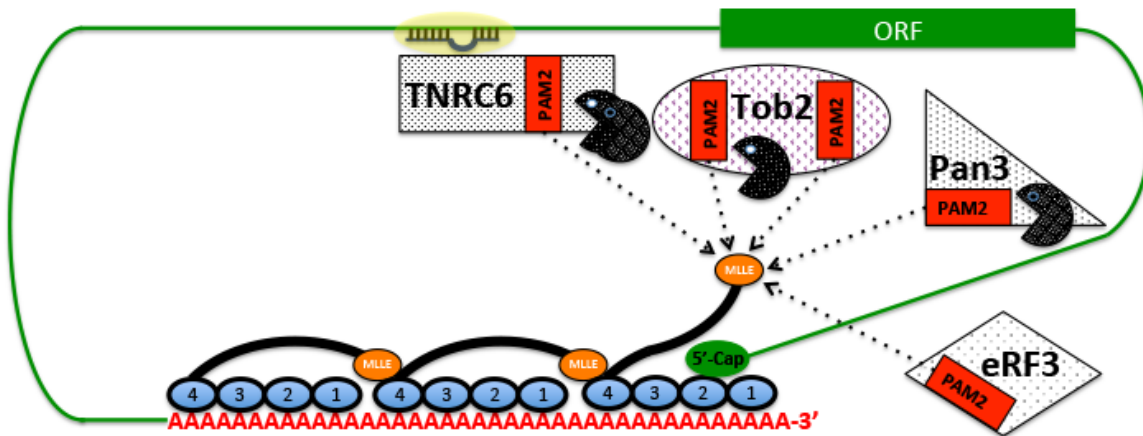


Figure 1.5 Current model: MLE domain of last PABP on poly (A) tail determines which PAM2 motif-containing proteins to interact with. 5' cap (green oval) of mature mRNA (green line) interacts with PABP RRM motif (blue oval) through eIF4E and eIF4G forming a closed loop structure facilitating translation. All three harboring PABPs are arranged in the same direction on the poly (A) tail. MLE domain of each PABP is oligomerized with neighboring PABP except the last PABP on the very 3' end of the tail. This oligomerization is believed to introduce a sterically block preventing 5'Cap structure to interact with all but the last PABP. All PAM2 motifs (red box) of containing proteins are regulated to interact with the only MLE domain on the last PABP at the end of the poly(A) tail. Through PABP interactions, Pan3, Tob2, and TNRC6 (interacting with miRNA-Ago2 on the other end of this protein) bring nucleases to the end of the tail to enhance the poly(A) nuclease processivity.

1.4 PAM2 motif-containing proteins

The PABP-interacting motif (PAM) was first identified in PABP-interacting protein 1 (Paip1) and PABP-interacting protein 2 (Paip2) proteins (35). The PAM1 motif is an acidic region comprising ~25 amino acids and PAM2 motif is consisted of 12 conserved amino acids that interact with the PABP N-terminal RNA-binding motif 2 and PABP C-terminal MLLE motif (36), respectively. In the alignment of the PAM2 motifs from all eukaryotic proteins, three highly conserved amino acids are identified. Among them, phenylalanine at position 10 is strictly conserved without exception (Figure 1.4 B). This phenylalanine is not only a signature feature of the PAM2 motif, but also plays an indispensable role in MLLE motif interaction (37,38). The aromatic ring of phenylalanine sterically fits into the groove created by the second and third α -helices of the MLLE motif (39). Several PAM2 motif-containing proteins have been well studied. For example, by interacting with PABP, 1) Paip1 can enhance the translation efficiency by interacting with eIF4A to stabilize circularized mRNA (40); 2) Paip2 can reduce translation efficiency by competing with the interaction of PABP and eIF4G, causing destabilized circular mRNA (41); 3) Eukaryotic release factor 3 (eRF3, a GTPase) can facilitate the coupling of deadenylation to translation termination by cooperating with eRF1 to support GTP-dependent translation termination, while providing access point on the poly(A) tail for deadenylases to work (42,43); 4) Trinucleotide Repeat-Containing Gene 6 (Tnrc6, a multifunctional scaffold protein in miRNA-mediated gene silencing) can repress translation by enhancing deadenylation and reducing the PABP-eIF4G interaction. This leads to diminished translation efficiency, and recruitment of deadenylase complexes to the end of the poly(A) tail, respectively (44); 5) Pan3 (Poly(A) specific ribonuclease subunit) can promote deadenylation by recruiting the deadenylase Pan2 to the end of

the poly(A) tail (17,45); 6) Transducer of ErbB2 (Tob) can enhance deadenylation by recruiting the deadenylase Caf1 to the end of the poly(A) tail (37,38,45).

1.5 Intrinsically disordered region

Analyzing the crystal structure of the well-studied PAM2 motif-containing proteins reveals a phenomenon that PAM2 motifs are all located in unstructured regions. This observation led us to investigate the amino acid composition surrounding PAM2 motifs by conducting bioinformatics analysis. As will be shown in this dissertation, the PAM2 motifs are embedded in a special region named Intrinsically Disordered Region (IDR) (45). IDR is a region composed of low amino acid complexity with a high proportion of hydrophilic polar uncharged amino acids (e.g., serine, threonine, and glutamine) and a low proportion of hydrophobic amino acids (46-48), which will become the core elements during globular domain formation. The high flexibility of the IDR region is an important feature contributing to protein functionality. Due to its constrained properties, the IDR can easily present an adjacent motif for interaction or post-translational modification, or the IDR itself can serve as a molecular recognition region controlling proteins interaction. Furthermore, a coupling of binding and folding is observed in a majority of the IDRs, which therefore constantly undergo a transition state between unstable (unfolded) and stable (folded) structure (48). Binding of target protein enables IDR to form a secondary or tertiary structure, which can further enhance the function of IDR-containing proteins. The majority of IDR-containing proteins are shown to have promiscuity in terms of target interactions. Therefore, the IDR can serve as a hub for transducing signals coming from upstream molecules. For example, tumor suppressor gene P53 can interact with more than ten targets through its IDR to exert functions (47). That explains well why many deregulated IDR-containing proteins have been associated with pathogenesis.

Functions of IDR have been discovered to impact on many cellular events, such as regulation of transcription and translation, post-translational modification (49), signal transduction, protein complex assembly, as well as RNA folding (50). Many PAM2 motif-containing IDR proteins compete for interaction with the MLLE domain of the last PABP on mRNA poly(A) tail to form messenger ribonucleoproteins (mRNPs) based on the model that only the last PABP of each transcript is available for PAM2 motif interaction (34). Judging from the observation that the majority of RNA binding proteins in interactome have IDRs (51), structural flexibility of IDR surrounding PAM2 motif is plausible to play a critical role in mRNPs remodeling. Therefore, it is interesting to investigate the functional role of IDR in PAM2 motif-containing proteins.

1.6 Post-translational modification-phosphorylation

Due to their structure flexibility and promiscuous interactive characteristics, intrinsically disordered regions are known for their tendency to be post-translationally modified. Nascent peptides/proteins are modified with all sorts of moieties through generally enzymatic covalent-linked reactions. Among them, phosphorylation is the most common and prevalent event. The human kinome accounts for ~2% of genome, which is one of largest gene families in eukaryotes (52). In estimation of kinase substrates, one-third of proteins in eukaryotic cells are phosphorylated in at least on one site. This modification is known to regulate a vast range of cellular functions (e.g., cell proliferation, differentiation, and program-controlled cell deaths at the cellular level; metabolism, DNA replication/repair, and transcription/translation at the molecular level).

Those functional impacts are most often attributed to phosphorylation-induced protein conformational change. For example, a phosphorylated site can simply become a docking site for target proteins. This interaction can facilitate protein shuttling between

the nucleus and the cytoplasm. In another scenario, a phosphorylated site can promote conformational change to either reveal or hinder the other modifiable site subjected for another kinase to act with. This interaction can enable the protein's function to be induced or inhibited. In some cases, phosphorylation itself simply provides a negative charge as a repulsion/attraction force to regulate proteins' interaction. Due to the reversible feature of phosphorylation i.e., phosphatases work oppositely on the same amino acid to remove phosphate group, the effect of phosphorylation can be fine-tuned accordingly to adapt the cell for different needs.

The intrinsically disordered region is structurally highly flexible, and its composition is enriched in polar/uncharged amino acid (i.e. serine and threonine). These properties make it an easily accessed region for post-translational modification and also a favored region for phosphorylation.

1.7 Significance of this study

This study provides insights into the mechanism of PAM2 motif-containing proteins-mediated mRNA deadenylation. PAM2 motif-containing proteins are mediators bringing enzymes to mRNA poly(A) tails. By interacting with a PABP through the PAM2 motif and interacting with nucleases through other motifs, a PAM2-containing protein enhances the processivity of nucleases on digestion of mRNA poly(A) tail. This interaction plays critical roles in the cell; however, little is known about the regulation between PAM2 motif and PABP interaction.

Based on the analysis of intrinsically disordered region in PAM2 motif-containing proteins and predicted potential phosphorylation site in the same proteins, an interesting feature is uncovered: PAM2 motifs, required for PABP interaction, are not only embedded in the intrinsically disordered region but also adjacent to a cluster of potential

phosphorylation sites. Therefore, phosphorylation in the intrinsically disordered region of a PAM2 motif-containing protein may regulate the interaction between PAM2 motif and MLL domain of PABP, leading to change in deadenylation rates.

To test the hypothesis, the work described in Chapter 3 examines whether induction or reduction of phosphorylation status of PAM2 motif-containing proteins by Calyculin A or phosphatase, respectively, regulates their interaction with PABP but not the interaction with nucleases away from PAM2 motif. I found that, in general, the less the phosphorylation of PAM2 motif-containing proteins, the more PABPs it can pull down, and vice versa. The work in Chapter 3 also tested the idea that potential phosphorylation sites in PAM2 motif-containing proteins diminish the Tob2 and Pan3 functions in deadenylation enhancement and the TNRC6c function in gene silencing. My findings open up a new direction for RNA researchers to investigate the role of phosphorylation in all PAM2 motif-containing proteins-mediated biological functions.

The work described in Chapter 4 examines our hypothesis further by pinpointing the real phosphorylated sites and the kinases involved. Mass spectrometry results indicate that c-JUN N-terminal kinase (JNK) can induce phosphorylation of multiple sites in the intrinsically disordered region of Tob2, supporting our finding that the higher the Tob2 phosphorylation induced by JNK1, the less PABP the Tob2 can pull down. This phenomenon confirms the hypothesis proposed in Chapter 3. On the way to identify the most critical phosphorylation site induced by JNK1, one serine inside second PAM2 motif (S245) was found to play a pivotal role in Tob2 functions. The phosphorylation at S254 significantly enhances the Tob2 ability to interact with PABP and may link to enhancing the deadenylation rates of global mRNA.

The effect of Tob2 S254D on PABP interaction is through synergism of the two PAM2 motifs. When S254 is in non-phosphorylation status, only first PAM2 motif is

interacting with PABP. Phosphorylation at S254 not only enables both PAM2 motifs to greatly associate with PABP, but also gives the second PAM2 motifs more affinity toward the PABP than the first one. Based on these observations, a model for the regulation of deadenylation by changing the phosphorylation status of Tob2 was proposed (see Chapter 4).

Chapter 2

Materials and methods

2.1 Plasmids construction

The plasmids myc-PABPC1, HA-Pan3, HA-Tnrc6, λ N-HA-LacZ, Tob2-V5, MS2-Tob2-V5, Paip1-V5, and Caf1-V5 were constructed previously (16,37,38,44,54). Constitutive-activated JNK plasmid Flag-MKK7B2-JNK1a1 (Addgene plasmid # 19726) was a gift from Dr. Roger Davis. In-Fusion approach was used to clone Tob2-V5 (WT, S254A, S254D) into pLVX-tight-puro tetracycline-inducible lentivirus expression vector (Clontech) using the In-Fusion kit (Clontech) according to the manufacturer's protocol. The extra 15 nucleotides sequence that matched to both ends of BamHI and EcoRI cut lentivirus vector were synthesized after 3' end of the primers that flanked the complete Tob2-V5. PCR amplified Tob2-V5 carrying homologous sequence recombined with enzyme-linearized vector.

(Below is an excerpt from “phosphorylation at intrinsically disordered regions of PAM2 motif-containing proteins modulates their interactions with PABPC1 and influences mRNA fate. KAI-LIEH HUANG, AMANDA B. CHADEE, CHYI-YING A. CHEN, YUEQIANG ZHANG, and ANN-BIN SHYU *RNA*. 2013 Mar;19(3):295-305. doi: 10.1261/rna.037317.112.”)

To generate pcDNA6-eRF3b-V5, mRNA from human testis was reverse-transcribed into cDNA. The gene was then amplified using specific primers (5' - TGG AATTCTGCAGATACCATGGATTCGGGCAGCA GC-3' and 5' - GCCACTGTGCTGGATTGTCCTTCTCTGGGACC AAT-3') and subcloned into the EcoRV-linearized pcDNA6-V5 vector. To construct phosphomimetic (PM, Ser/Thr → Asp/Glu) mutants and nonphospho (NP, Ser/Thr → Ala) mutants of Tob2, Pan3, and Tnrc6c, minigene fragments spanning the targeted area of proteins with multiple mutations (Figure 3.5) were synthesized by IDT and Invitrogen. The In-fusion kit (Clontech) was used to replace the targeted regions in wild-type expression

constructs with the minigenes, following the manufacturer's manual. DNA sequencing was performed to confirm all the desired mutations and in-frame fusions.

2.2 PCR-based site-directed mutagenesis

PCR reaction was carried out to create plasmids bearing the mutation. 25 ng of template plasmid is added into total volume of 50µl reaction containing 10uM forward and reverse primers (sequence are listed below), 10mM dNTP, 5 units of Pfu DNA polymerase, and 1X reaction buffer. A negative control reaction, replacing Pfu with water, was set side by side. Amplification is set first at 95°C for 1min, second at 18 cycles of 95°C for 30sec, 55°C for 60sec, and 68°C for 1min/1kb long plasmid, third at 68°C for 10min, and last at 12°C forever. This was followed by 40 units DpnI (NEB) direct treatment in 37°C for 4hr, to eliminate the template plasmid, and 1µl was taken from the reaction for transformation using TOP 10 high efficient competent cells (Invitrogen). The difference of growing colonies between the experiment and the control has to be 10X higher to assure successful following check-up. Selected colonies were subjected to size diagnosis by restriction enzymes, DNA sequencing, and protein over-expression in cells to confirm identity.

Tob2 F260A F	5'-CCCAATGCCAAGGAGGCCGTGTACAACGGTGGT-3'
Tob2 F260A R	5'-ACCACCGTTGTACACGGCCTCCTTGGCATTGGG-3'
Tob2 F140A F	5'-CCTGACGCCCAGGTGGCCGTGCCCATTGGCAGC-3'
Tob2 F140A R	5'-GCTGCCAATGGGCACGGCCACCTGGGCGTCAGG-3'
Tob2 S254A F	5'-CCTCAGTCCCAGCTCGCACCCAATGCCAAGGAG-3'
Tob2 S254A R	5'-CTCCTTGGCATTGGGTGCGAGCTGGGACTGAGG-3'
Tob2 S254D F	5'-CCTCAGTCCCAGCTCGATCCCAATGCCAAGGAG-3'
Tob2 S254D R	5'-CTCCTTGGCATTGGGATCGAGCTGGGACTGAGG-3'

Tob2 S222A F	5'-CCTCGCATGGCCCGCGCACCCACCAACAGCCTG-3'
Tob2 S222A R	5'-CAGGCTGTTGGTGGGTGCGCGGGGCCATGCGAGG-3'
Tob2 S222D F	5'-CCTCGCATGGCCCGCGACCCACCAACAGCCTG-3'
Tob2 S222D R	5'-CAGGCTGTTGGTGGGTGCGCGGGGCCATGCGAGG-3'
Tob2 S117A F	5'-CTGTACCTGGATGACGCCGAGGGTTGCGGTGCC-3'
Tob2 S117A R	5'-GGCACCGCAACCCTCGGCGTCATCCAGGTACAG-3'
Tob2 S117D F	5'-CTGTACCTGGATGACGACGAGGGTTGCGGTGCC-3'
Tob2 S117D R	5'-GGCACCGCAACCCTCGTCGTCATCCAGGTACAG-3'
Tob2 S119A F	5'-GGGGGCGGGGCAGCAGCCGGTGGGGGTGTAGCC-3'
Tob2 S119A R	5'-GGCTACACCCCCACCGGCTGCTGCCCCGCCCCC-3'
Tob2 S119D F	5'-GGGGGCGGGGCAGCAGACGGTGGGGGTGTAGCC-3'
Tob2 S119D R	5'-GGCTACACCCCCACCGTCTGCTGCCCCGCCCCC-3'
Tob2 T224A S226A F	5'-ATGGCCCGCTCACCCGCCAACGCCCTGCTGAAGCACAAG-3'
Tob2 T224A S226A R	5'-CTTGTGCTTCAGCAGGGCGTTGGCGGGTGAGCGGGCCAT-3'
Tob2 T224E S226D F	5'-ATGGCCCGCTCACCCGAGAACGACCTGCTGAAGCACAAG-3'
Tob2 T224E S226D R	5'-CTTGTGCTTCAGCAGGTCGTTCTCGGGTGAGCGGGCCAT-3'
Tob2 S232A F	5'-CTGCTGAAGCACAAGGCCCTCTCTCTGTCTATG-3'
Tob2 S232A R	5'-CATAGACAGAGAGAGGGCCTTGTGCTTCAGCAG-3'
Tob2 S232D F	5'-CTGCTGAAGCACAAGGACCTCTCTCTGTCTATG-3'
Tob2 S232D R	5'-CATAGACAGAGAGAGGTCCTTGTGCTTCAGCAG-3'
Tob2 T244A F	5'-TCACTGAACTTCATCGCCGCCAACCCGGCCCCT-3'
Tob2 T244A R	5'-AGGGGCCGGGTGGCGGCGATGAAGTTCAGTGA-3'
Tob2 T244E F	5'-TCACTGAACTTCATCGAGGCCAACCCGGCCCCT-3'
Tob2 T244E R	5'-AGGGGCCGGGTGGCCTCGATGAAGTTCAGTGA-3'
Tob2 S251A F	5'-AACCCGGCCCCTCAGGCCAGCTCTACCCAAT-3'

Tob2 S251A R	5'-ATTGGGTGAGAGCTGGGCCTGAGGGGCCGGGTT-3'
Tob2 S251D F	5'-AACCCGGCCCCCTCAGGACCAGCTCTCACCCAAT-3'
Tob2 S251D R	5'-ATTGGGTGAGAGCTGGTCCTGAGGGGCCGGGTT-3'

2.3 Cell culture, transfection, and protein induction

U2OS and 293T cells are cultured in DMEM high glucose (Invitrogen) containing 10% fetal bovine serum (Invitrogen) and 1x penicillin/streptomycin/glutamine (Gibco). NIH3T3 and B2A2 cells (Shyu et al. 1998) are cultured in the DMEM high glucose containing 10% calf serum (Invitrogen) and 1x penicillin/streptomycin/glutamine (Invitrogen). 500ng/ml tetracycline (Sigma) and 200 ng/ml of doxycycline (Sigma) are added in culture medium for maintaining B2A2 cell and stable cloned Tob2-V5 inducible U2OS cell, respectively. 5% CO₂ is provided in 37°C incubator for cells to grow.

Transfection is performed in reverse fashion. Briefly, Opti-MEM I Reduced Serum Medium (Invitrogen) is used to dilute plasmids and Lipofectamine 2000 (Invitrogen) in separate tubes. The ratio of plasmid to Lipofectamine 2000 is kept at 1µg to 3µl. Each 10cm dish of cells is transfected with 18µg of plasmids DNA including 6µg Tob2 expression plasmid and 12µg carrier plasmid. After 5min RT incubation of dilution, diluted plasmids are mixed with diluted Lipofectamine 2000 thoroughly, and kept another 20min for complexes to form. In the meanwhile, cells number that will make 60% confluence of dish once attached are seeded. Mixture is directly added into the just seeded cells. Cells are ready for analysis after 1-day incubation.

To screen the kinases, Tob2-overexpressed cells are pretreated with various kinase inhibitors U0126 (Selleckchem), SB203580 (Selleckchem), SP600125 (Selleckchem), LY294002 (Selleckchem), SB216763 (Selleckchem), Rapamycin

(Selleckchem), SL0101 (Calbiochem), and Akt inhibitor IV (Calbiochem) before Calyculin A (Cell Signaling) treatment.

To measure the kinetics of default deadenylation, transcriptional pulse strategy was used by delivering reporter gene plasmid under the control of inducible promoter into mammalian cell and allowing a short period of time for transcription before harvest RNA in time course to monitor shortening of mRNA poly(A) tail and decaying of mRNA body (13). To induce cells to express transient transfected β -globin reporter gene and stable cloned Tob2-V5 genes, cells were grown in the reduced 50ng/ml tetracycline or Doxycycline-containing medium, one night before induction. On the day of induction, cells were washed twice with RT PBS followed by another two washes with the culture medium containing tetracycline-free FBS (Clontech) and 1x penicillin/streptomycin/glutamine. Cells were grown in the culture medium used for wash for specific times, 24hr for co-IP, Northern blot, and poly (A) size distribution assays; 10hr for pulse-chasing bromouridine metabolic RNA labeling assay.

2.4 Stable cell lines establishment

To establish tetracycline-controlled transactivator (tTA) expressing stable U2OS cell line and following Tob2-V5 Tet-off inducible U2OS cell line, lentivirus system, Lenti-X Tet-off Advanced Inducible Expression System (Clontech), was adopted to produce the viruses carrying gene of interest. Briefly, for tTA-U2OS cell establishment, 1.5×10^7 293T cells were reverse transfected with 24 μ g in total pLVX-Tet-off advance (Clontech), psPAX2 (a gift from Dr. Didier Trono, Addgene plasmid # 12260), and pMD2.G (a gift from Dr. Didier Trono, Addgene plasmid # 12259) plasmids in the ratio of 3 : 2 : 1 in 10cm dish using Lipofectamine 2000. Change to fresh medium 8hr after transfection.

Virus-containing medium was harvested 3 times after 32, 48, and 56 hr of transfection by collecting the medium in 50ml tube and replacing fresh medium back.

Cell debris was removed immediately by spinning at 500g for 10min in 4°C. The virus-containing medium was kept at a temperature of 4°C while waiting for later time point virus medium. Concentration of virus particles was necessary to enhance transduction efficiency by mixing 3 part of virus medium with 1 part of Lenti-X concentrator (Clontech) prior overnight 4°C incubation to spin down virus pellet by centrifuge the tube for 45min in 4°C. The virus pellet was resuspended with 1/40th of original volume of medium containing polybrene (Santa Cruz) at final concentration of 10µg/ml. U2OS cells seeded in 12-well plate were infected by replacing growth medium with virus medium for a day. The infected cell population were expanded for a period of 10 days while doing selection by adding 400µg/ml G418 (ThermoFisher) and 50ng/ml Doxycycline (Sigma). In order to pick single colony, cells were split and 50 of the cells were seeded in 10cm dish following another 10 days to let single cells grow into visible colonies. Cloning cylinders (Corning) combined with vacuum grease (Corning) and trypsin was used to collect single colonies. From the 48 picked colonies, U2OS clone29 were selected depending on the inducibility test.

U2OS clone29 cell is used as a parental cell for establishing of Tob2-V5 inducible stable cell lines. In brief, lentivirus is produced by transient transfection of lentivirus expression vector pLVX-tight-puro (Clontech) carrying Tob2-V5 gene and packaging plasmids into 293T. The harvested virus-containing medium was concentrated before adding onto the cell culture. After 1 day of transduction, a selection culture medium (10% FBS, 1x penicillin/streptomycin/glutamine, 400µg/ml G418, 200ng/ml Doxycycline, 5µg/ml puromycin) was used for total 48hr of incubation to kill non-infected cells. Parental U2OS clone29 cell was grown side by side during the

selection period to serve as negative control. Puromycin and G418 were removed from medium for continuing cell culture after the selection period.

2.5 Proliferation assay

CyQUANT Cell Proliferation Kit (Invitrogen) was used to detect the amount of DNA in each well of plate to represent the cell number in that well. Briefly, 1×10^3 cells were seeded in each of 96-well black-well clear-flat-bottom plate (Corning) supplied with 100 μ l of medium. Harvest plates were used each day for the course of 5 days by pouring out the medium and draining the remaining on paper towels before freezing the plates in -80°C waiting for all time points of plates were collected. The plates were thawed in RT under low light environment, adding 200 μ l 1X cell lysis buffer containing CyQUANT GR dye working solution into each well and incubated for 5 min with shaking before measuring the fluorescent on the Infinite 200 PRO plate reader (Tecan) with 480nm excitations and 520nm emissions.

2.6 Cell cycle analysis

A 10cm dish of ~50% confluent cells ($2\sim3 \times 10^6$) were harvested by trypsinization, followed by neutralization with cold medium in 15ml tube. The cells were washed twice with 10ml cold PBS, and resuspend in 0.5ml PBS. To fix the cells, the tube was vortexed gently while adding 5ml of cold 75% EtOH drop by drop into the tube. This was incubated in 4°C overnight, and then moved to -20°C for temporary storage to wait for all time course samples to be collected. Propidium iodide (Invitrogen) was used to stain the chromosomes. In brief, cells were spun down at 600g for 5min prior to the two cold PBS washes. All supernatants were carefully removed and cells were resuspended in 400 μ l PI staining solution (40 μ g/ml propidium iodide, 200 μ g/ml RNase A and 0.1%

Triton X-100 in 1X PBS). This was incubated in 37°C for 30min for RNase A to work. During the incubation, the tubes were agitated every 10min to assure homogeneous penetration of RNase A into cells. The tubes were kept on ice while transferring cells into filtered-top flow cytometry tubes (BD Biosciences). The fluorescent intensity in each cell was detected on the BD FACSCalibur and followed by data analysis using FlowJo software. Watson cell cycle model was applied to each analysis result to avoid phase distribution assignment bias.

2.7 Co-immunoprecipitation and western blot

One 10cm dish of cells ($\sim 5 \times 10^6$) was washed twice with cold PBS on ice before scraping down into 1.5ml tube with 1ml of cold PBS. The cells were spun down and lysed in 900 μ l of co-IP lysis buffer (50mM Tris pH7.4, 150mM NaCl, 0.4% NP-40, 1mM EGTA, and 10% glycerol) with protease and phosphatase inhibitors (2mM sodium orthovanadate, 2mM sodium pyrophosphate, 10mM sodium fluoride, 1mM phenylmethylsulfonyl fluoride, 1x complete Protease inhibitor from Roche, 1x phosphatase inhibitor cocktail 3 from Sigma). RNase A (Sigma) 200 μ g was added into each tube and incubated in 4°C with rotation for 1hr to digest RNA. After removing the debris with 12,000g 15min spinning, the supernatant was collected and the concentration with BCA reagent (Bio-Rad) was measured. The concentration of each sample was adjusted to the same with cold lysis buffer. An equal volume of lysate was subjected for co-IP. One-tenths of the volume was saved for input protein level examination. To pull down V5-tagged protein, an anti-V5 agarose affinity beads (Sigma) was used. Briefly, 50 μ l 50% slurry beads were washed three times with cold lysis buffer for each dish of cells. All wash buffers were discarded before adding lysate and incubated at 4°C with rotation for 2hr. The beads were spun down with 500g for 3min,

and the supernatant was removed. The beads were then washed with 1ml cold lysis buffer for 3min. The washing process was repeated for a total of five times. The buffer above the beads was removed as much as possible by using 31G needle attached to the suction. The beads were boiled in 50µl 1x Laemmli Sample Buffer (Bio-Rad) for 5min to release and denature co-immunoprecipitated proteins. In order to obtain well-resolved Tob2 phosphorylation pattern, 7.5% polyacrylamide denature gel was prepared. Two-thirds of the samples were running at 80V till the bromophenol blue dye front disappeared. Proteins in the gel were transferred to PVDF membrane (Millipore) using a semi-dry system running at 20V for 20min. The membrane was first soaked in blocking buffer (5% non-fat milk in 1xPBS with 0.1% tween-20) for 1hr, then changed to the blocking buffer containing diluted antibody in the following ratios: 1:2000 for rabbit anti-PABP (RRM4) antibody (a gift from Dr. Richard E. Lloyd); 1:2000 for rabbit anti-Caf1 antibody (16); 1:2500 for mouse anti-V5-HRP conjugated antibody (Invitrogen); 1:2000 for rabbit anti-Flag antibody (Sigma); 1:1000 for rabbit anti-JNK antibody and for rabbit anti-phospho-JNK (Thr183/Tyr185) antibody (Cell Signaling); 1:1000 for rabbit anti-GAPDH-HRP conjugated antibody (Santa Cruz). After overnight incubation with gentle shaking in 4°C followed by three times 5min wash in PBST, the membrane was now either ready for signal development if primary antibody had HRP conjugated or ready for secondary antibody detection. The ratio 1:5000 was applied to dilute HRP-conjugated anti-mouse or anti-rabbit secondary antibodies (Bethyl) in blocking buffer. After 1hr incubation with the secondary antibody followed by three times 5min wash, the membrane was ready for signal development. SuperSignal West Pico chemiluminescent solution (Thermo) was applied on the membrane and stood for 5min before exposure. Signals were captured by GeneGnome (Syngene) and quantified by GeneSnap (Syngene) software.

2.8 RNA preparation and RNA-immunoprecipitation

Cytoplasmic RNA was extracted from cell using RNeasy Mini Kit (Qiagen) and following the manufacturer's manual. In brief, cell pellet collected from 10cm dish of cells was lysed with 180µl RLN buffer (50mM Tris pH8.0, 1.5mM MgCl₂, 140mM NaCl, 0.5% NP-40, 1X complete EDTA-free Protease Inhibitor from Roche, and 1X phosphatase inhibitor cocktail 3 from Sigma). Debris was removed by spinning at 500g for 5min before collecting cytoplasmic fraction. The collected 170µl of the solution was mixed with 600µl RLT/b-ME with vigorous vortexing. RNA was precipitated by adding 430µl 100% RT EtOH. The mixture was passed through the mini column and the column was washed with RW1 buffer. To ensure pure RNA extraction with DNA contamination, on-column DNase I (Qiagen) treatment was carried out for 1hr in RT. The column was washed with RW1 buffer again followed by several times of washes with RPE wash buffer. The column was dried by centrifugation and RNA was eluted with ddH₂O to make concentration around 1µg/µl empirically. The concentration was measured using NANODROP LITE (Thermo).

For RNA-immunoprecipitation, samples were first adjusted to the same concentration with ddH₂O. Equal amount of RNA was used as input for precipitation. In order to have 1µg of bromouridine-labeled RNA, about 100µg of total RNA was required to start with. To prepare the beads for 100µg RNA pull down, 150µl Dynabeads Protein G (Invitrogen) was first washed with cold WASH/IP buffer (0.1% BSA and 0.02% Triton X-100 in 1X PBS) 3 times. The beads were restored to their original volume with WASH/IP buffer before adding 12µg mouse anti-BrdU clone 3D4 antibody (BD Biosciences). The mixture was rotated in 4°C overnight followed by washing it 4 times with cold WASH/IP buffer. The antibody-conjugated beads were resuspended to the

volume that was equal to the volume of input RNA with WASH/IP buffer in order to control the concentration of RNA and keep it consistent 0.5µg/µl between samples and experiments. RNase out (Invitrogen) was added into the resuspended beads to have final concentration of 1 unit/µl. Total RNA was added onto the beads and incubated on rotator in 4°C for 4hr. This was washed 5 times thoroughly with cold WASH/IP buffer, and the beads were moved to a new tube during the last wash. The bromouridine-labeled RNA was eluted from the beads using RNeasy Mini Kit (Qiagen) RNA clean-up manufacture's protocol. To obtain accurate pull down RNA concentration, Quant-iT RiboGreen RNA Assay Kit (Thermo) was used.

2.9 Sample preparation for RNA sequencing

Confluent cells at ~70% were prepared in a dish ready on the day of labeling. Half of the medium was collected from the dish, and 200mM bromouridine (Sigma) stock was added into the medium to make a final 10mM concentration. The rest of the medium was collected from the dish for later uridine chasing purpose. Working bromouridine medium was added back to the dish, and incubated at 37°C with 5% CO₂ for 2hr. Meanwhile, 2M uridine stock was added into the other half of medium to make a final 20mM concentration. Right after 2hr incubation, bromouridine-containing medium was replaced with uridine-containing medium, and the cell was harvested using trypsin method in the time course manner. Cell pellet was washed twice with cold-PBS before RNA extraction. Removal of rRNA contamination was conducted using Ribo-Zero Gold beads. Cleaned-up RNA was fragmented into average 155bp by heating. Double strand blunt end cDNA was synthesized and repaired. Adenosine was added to 3' end of each cDNA followed by ligation with barcoded adaptor. cDNA pool went through 15 cycles of amplification to enrich those DNA fragment that have adaptors at both ends. Library

validation was running on Agilent DNA 1000 chip (Agilent) to confirm the size of library was around 260bp. RNA sequencing was conducted (LC Sciences, Houston TX) on Illumina Hi-Seq 2000 with 2 x 100bp paired-end sequencing run.

2.10 Northern blot

To detect changes of size and amount of specific RNA (ranged around 500bp), 8µg of total cytoplasmic RNA was subjected to electrophoresis on 1.4% agarose gel (1X MOPS buffer, 7.5% formaldehyde solution, and 0.2µg/ml EtBr). Briefly, RNA sample was first dried in Speedvac concentrator followed by dissolution in denature buffer (134µl deionized formamide, 40µl 37% formaldehyde solution, 18µl 20X MPOS, and H₂O to 250µl total volume). Denature was carried out for 15min in 65°C water bath and chilled on ice. 4X loading dye (50% sucrose and 0.2% bromophenol blue) was mixed with sample before running on the gel overnight with consistent 60V. The gel was washed thoroughly in H₂O and 10X SSC buffer before transferring the RNA onto GeneScreen membrane (PerkinElmer) for blotting. RNA was fixed on the membrane with 120,000uJ UV, and the membrane was blocked with ULTRAhyb hybridization buffer (Thermo) for 2hr in 42°C oven. Gene specific isotope-labeled probe was generated using Rediprime II random primer labeling system (Amersham). To detect β-globin, 25 ng of probe was mixed with 5µl of 6,000 Ci/mmol [α-³²P]-dCTP (Perkin-Elmer) in the reaction, and incubated for 1hr at 37°C. To remove free [α-³²P]-dCTP, the probe was purified through illustra MicroSpin G-25 column (GE Healthcare). After TCA precipitation, scintillation counter calculation, and heat denaturation, 1x10⁵ cpm/ml probe was added into hybridization reaction for overnight incubation at 42°C. The membrane was washed thoroughly with three buffers several times (2X SSC/0.1%SDS, 0.1XSSC/1%SDS, and 0.1XSSC) in order before exposure. To generate poly(A)- RNA for negative control use

purpose, total RNA was mixed with oligo (dT)_{12~18} primer followed by RNase H treatment. Decay profile was plotted using ImageJ (NIH) software. All experiments were repeated at least twice with reproducible results.

2.11 Poly (A) tail distribution assay

To measure tail length of total mRNA population, 3' end of each tail has to be labeled with isotope before digestion of the non-poly (A) part of mRNA with RNases. Resolving this pure tail sample provides the information of tail length distribution of whole mRNA population. Briefly, 3µg of total RNA was subjected to 3' end tail labeling with [α -³²P]-dATP in the reaction containing 1X poly (A) polymerase buffer, 600 units poly (A) polymerase (Affymetrix), 20 units RNase inhibitor, and 10uCi [α -³²P]-dATP. DNA ladder (Invitrogen) was labeled with the same isotope in the reaction (1X terminal transferase buffer, 0.8 units/µl terminal transferase, 0.25mM CoCl₂, 1.5µg DNA ladder, and 10uCi [α -³²P]-dATP) side by side. This was incubated in 37°C water bath for 1hr before removal of free isotope following RNeasy Mini Kit (Qiagen) RNA clean-up manufacture's protocol. 20 ng RNase A (Sigma) and 100 units of RNase T1 (Sigma) were mixed in the 20µl digestion buffer (62.5mM Tris pH7.4, 250mM KCl, 12.5mM EDTA pH8, and 2µg/µl yeast RNA), and added into eluted 30µl RNA for exactly 30min in 37°C incubation. 2X stop buffer (200mM Tris pH7.4, 25mM EDTA pH8, 2% SDS, 0.8µg/µl proteinase K, and 0.2µg/µl Glycogen) was added followed by another 30min in 37°C incubation. After phenol/chloroform extraction, EtOH precipitation, TCA precipitation, and scintillation counter calculation, equal amounts of 20,000cpm isotope-labeled RNA samples were denatured in 2X formamide loading dye (Deionized formamide, 10mM EDTA pH8, 1mg/ml bromophenol blue, and 1mg/ml xylene) and loaded onto denaturing 8% polyacrylamide (Acrylamide:Bis=19:1) urea (7M) gel. The gel was dried with Gel

Drying Kit (Promega) overnight, and exposed. The profile of poly (A) tail distribution was plotted using ImageJ (NIH) software.

2.12 Sample preparation for Mass spectrometry

To reach lowest non-specific background signal, co-immunoprecipitation method was modified accordingly for this analysis. In brief, cells were lysed in special co-IP lysis buffer (50mM Tris pH7.4, 150mM NaCl, 1% NP-40, 1mM EGTA, 10% glycerol, and 2% BSA) with protease and phosphatase inhibitors (2mM sodium orthovanadate, 2mM sodium pyrophosphate, 10mM sodium fluoride, 1mM phenylmethylsulfonyl fluoride, 1x complete Protease inhibitor from Roche, 1x phosphatase inhibitor cocktail 3 from Sigma). RNA was digested with RNase A (Sigma) before centrifugation to remove cellular debris. The concentration of lysate was then adjusted to 0.5µg/µl to avoid the chance of non-specific binding. The lysate was ready for pull down after pre-cleaning with non-relevant anti-HA agarose beads (sigma). Anti-V5 agarose beads (Sigma) were pre-blocked with the special co-IP lysis buffer overnight before adding into lysate. After thorough washes, Tob2-V5 was eluted with V5 peptide elution buffer (0.4mg/ml V5 peptide from Sigma, 25mM Tris pH7.4, 100mM NaCl, and 0.05% Triton X-100). The eluted solution was then concentrated by passing through 10 KD cut-off centrifugal filter column (Amicon). Silver staining (Bio-Rad) was performed to ensure specificity by comparing the gels between Tob2-V5 and Vector –expressing cell lysate. Gel bands were analyzed by microcapillary LC/MS/MS (Taplin Mass Spectrometry Facility, Harvard Medical School).

2.13 Renilla and firefly dual luciferase assay

(An excerpt from “Phosphorylation at intrinsically disordered regions of PAM2 motif-containing proteins modulates their interactions with PABPC1 and influences

mRNA fate. KAI-LIEH HUANG, AMANDA B. CHADEE, CHYI-YING A. CHEN, YUEQIANG ZHANG, and ANN-BIN SHYU *RNA*. 2013 Mar;19(3):295-305. doi: 10.1261/rna.037317.112.”)

U2OS cells were transiently transfected using Lipofectamine 2000 (Invitrogen) according to the manufacturer's instructions. Briefly, 0.6×10^6 of U2OS cells were seeded in six-well plates before addition of 20 ng of the reporter plasmid (psi-check2 or psi-check2-4xboxB) and 3 ug of pcDNA- λ N-HA-lacZ, pcDNA- λ N-HA-TNRC6C (WT or mutant). Cells were harvested 42 h after transfection, and samples were analyzed simultaneously for firefly and Renilla luciferase activities using the Dual-Glo Luciferase Assay System (Promega) according to the manufacturer's instructions. The relative levels of Renilla luciferase activity were normalized by dividing each reporter's Renilla luciferase activity by its firefly luciferase control.

Chapter 3

Phosphorylation of intrinsically disordered region of PAM2 motif-containing proteins modulates their interaction with PABP and influences mRNA fate

This chapter is reprinted with permission from

Huang, K. L., Chadee, A. B., Chen, C. Y., Zhang, Y., and Shyu, A. B.

Phosphorylation at intrinsically disordered regions of PAM2 motif-containing proteins
modulates their interactions with PABPC1 and influences mRNA fate.

RNA. 2013 Mar; 19(3): 295–305.

doi: 10.1261/rna.037317.112.

Introduction

Mammalian cytoplasmic poly(A)-binding protein (PABP) C1 is a highly conserved and abundant RNA-binding protein that binds to the 3' poly(A) tails of mRNAs and has several roles in controlling the cytoplasmic fate of mRNA(24,55). In the cytoplasm, PABPC1 proteins in complex with mRNA 3' poly(A) tails facilitate formation of the “closed-loop” structure of the mRNA-ribonucleoprotein particle (mRNP) (56). This closed-loop mRNP structure helps enhance translation initiation and termination, promote recycling of ribosomes, and influence the stability of the mRNA (19,57-59). In these cytoplasmic processes, PABPC1 serves as a binding scaffold for other proteins involved in translation regulation and mRNA turnover. The recent discovery that interactions of GW182/Tnrc6 proteins with PABPC1 are critical for miRNA-mediated gene silencing (60) further highlights the importance of studying the actions of interactions between PABPC1 and its partners for understanding the post-transcriptional control of gene expression.

Among mammalian PABPC1-interacting proteins, at least 16 contain the motif of ~12 amino acids termed the PABP-interacting Motif 2 (PAM2) (36,60). Structural data show that the PAM2 motif binds to the highly conserved MLLE domain in the C-terminal region of PABPC1 (30,42,61). Among the PAM2- containing proteins are several well-studied translation and mRNA decay factors, including PAIP1 (35), PAIP2 (62), Tnrc6 (63), Eukaryotic peptide chain release factor 3 (eRF3) (31), PABP-dependent poly(A) nuclease subunit 3 (Pan3) (64), and transducer of erbB-2 proteins (Tob) (65). The number of PAM2- containing proteins and their varied roles in mRNA metabolism suggest several important questions. For example, how does the cell regulate interactions between PABPC1 and its binding partners to respond to different biological

processes? What molecular mechanism controls association and dissociation between PABPC1 and individual binding partners?

In view of the observation that PAM2 motifs appear to occur outside globular protein domains (36), we hypothesized that PAM2 motifs primarily reside in intrinsically disordered or unstructured regions (IDRs). IDRs can retain significant regions of disorder under physiological conditions, even when positioned near one or more structured domains (46,47,66). Interestingly, a recent study of mRNA interactomes found that proteins associated with mRNAs are highly enriched in IDRs compared to the human proteome overall (51). The dynamic nature of IDRs combines structural flexibility with a high functional density and multiple interaction interfaces (48,50,67). The major functions currently ascribed to disordered regions are protein–protein binding, protein–DNA/RNA binding, and substrate–ligand binding. Therefore, this region serves as a good target for posttranslational modification-phosphorylation (48,50,67).

Reversible protein phosphorylation provides a key regulatory mechanism for a plethora of signal transduction processes in eukaryotic cells (68-70). Most phosphorylation occurs at serine or threonine residues (71,72). One characteristic feature of disordered segments is an enrichment in polar, uncharged amino acids such as serine and threonine (49). It has also been noted that the amino acid composition, sequence complexity, hydrophobicity, and charge of regions adjacent to phosphorylation sites resemble those of IDRs (49,73). Based on these observations, IDRs are predicted to be “hotspots” for protein phosphorylation(49).

We have conducted a bioinformatics analysis of thirteen human PAM2-containing proteins and found that, with the exception of eRF3b, the PAM2 motif is embedded in an extended IDR and is close to a cluster or clusters of potential Ser/Thr phosphorylation sites. We hypothesized that reversible phosphorylation of these Ser/Thr clusters is

required for modulating interactions between the PAM2-containing protein and PABPC1, thereby controlling mRNA fate. To test this hypothesis, in this study we used complementary approaches to change the phosphorylation states of three representative PAM2-containing proteins and determine the corresponding functional consequences. The experimental results not only support our hypothesis but also provide a new framework for designing future studies to investigate how the many distinct mRNA functions involving PABPC1 and its PAM2-containing interacting partners may be regulated and coordinated in eukaryotic cells.

Results

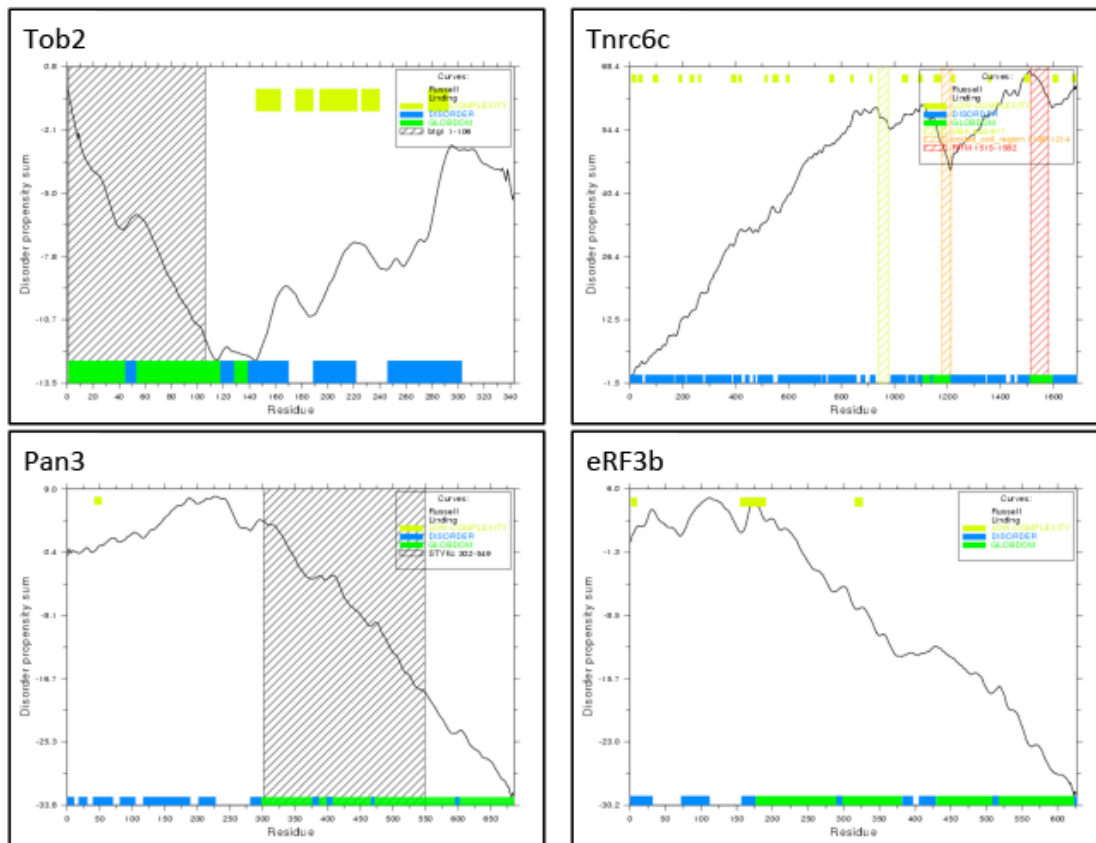
3.1 PAM2 motifs are generally embedded within intrinsically disordered regions. As PAM2 motifs in general occur in protein regions that seem not to assume any known structure (36), we used two online tools, “PONDR” and “Globplot,” to identify candidate IDRs within 13 human MLLE domain-interacting, or PAM2-containing, proteins (Table 3.1). PONDR analysis predicts regions that are not rigid (including random coils, partially unstructured regions, and molten globules) based on local amino acid composition, flexibility, and hydropathy (74,75). The Globplot predicts regions with a high propensity for globularity on the Russell/ Linding scale (propensities for secondary structures and random coils) (76). Analyses done by PONDR predict that all PAM2-containing proteins examined have an extensive IDR, with eRF3b predicted to be ~25% IDR and the others predicted to be >32% IDR (Table 3.1). Moreover, the PAM2 motifs in these proteins reside within the predicted IDRs (see representative examples schematically shown in Figure 3.2).

Protein	Cellular function	Amino acid length	PAM2 motif	% Disorder
Pan3 (PAN3_HUMAN, Q58A45)	mRNA decay. Recruits Pan2 deadenylase.	687	86-102	36
Tob1 (TOB1_HUMAN, P50616)	Anti-proliferative. Recruits Caf1 deadenylase. Inhibits cell cycle progression.	345	127-144;263-278	34
Tob2 (TOB2_HUMAN, Q14106)	Anti-proliferative. Recruits Caf1 deadenylase. Inhibits cell cycle progression.	344	128-145; 248-264	32
eRF3b (ERF3B_HUMAN, Q81YD1)	Translation termination. Interacts with eRF1.	628	47-64	15 - 25*
TNRC6a (TNRC6A_HUMAN, Q8NDV7)	miRNA-mediated gene silencing. Interacts with Ago proteins and recruits Pan2-3 and Caf1-Ccr4 deadenylases.	1962	1605-1622	65
TNRC6b (TNRC6B_HUMAN, Q9UPQ9)	miRNA-mediated gene silencing. Interacts with Ago proteins and recruits Pan2-3 and Caf1-Ccr4 deadenylases.	1833	1362-1381	62
TNRC6c (TNRC6C_HUMAN, Q9HCJ0)	miRNA-mediated gene silencing. Interacts with Ago proteins and recruits Pan2-3 and Caf1-Ccr4 deadenylases.	1690	1382-1399	75
PAIP1 (PAIP1_HUMAN, Q9H074)	Coactivator in translation initiation and mRNA decay.	479	123-140	45
PAIP2 (PAIP2_HUMAN, Q9BPZ3)	Repressor in transition initiation.	127	107-123	55
Ataxin-2 (ATX2_HUMAN, Q99700)	Unknown	1313	908-925	77
HELZ (HELZ_HUMAN, P42694)	Unknown. Helicase with Zinc finger domain.	1942	1095-1112	36
USP10 (UBP10_HUMAN, Q14694)	Deubiquitinating enzyme. Regulator of p53/TP53 stability.	798	81-93	45
TPRD (TPR_HUMAN, P53804)	Unknown	2363	1202-1219	76

Table 3.1 Survey of 13 human proteins known or predicted to interact with PABPC1 through the PAM2 motif, which is generally embedded within intrinsically disordered region (IDR). PONDR and/or Globplot predictions identified several segments of IDRs throughout the proteins analyzed. PAM2 motifs were identified from Pfam searches or previously published work (36,60). (*: Several predicted IDRs of eRF3b are scattered within the extensive region of structured domains at C-terminal half; these scattered IDRs are not taken into account for calculating its % disorder. In addition, eRF3b has extensive low-complexity regions around PAM2 motif; when these regions are excluded, its % of disorder drops to 15.) This survey was initiated by Amanda B Chadee and edited by Chyi-Ying A. Chen and Ann-Bin Shyu.

Four of the PAM2-containing proteins analyzed by PONDR (Tob2, Pan3, eRF3b, and Tnrc6c, a paralog of Tnrc6 or GW182) are relatively well-characterized, with known cellular functions. We thus focused on these four proteins to perform additional analysis using Globplot. The results of this analysis (Figure 3.1 A) corroborated the PONDR results (Figure 3.1 B) and also highlight regions of low complexity (i.e., sequences with overrepresentation of a few particular residues), a feature of many proteins containing IDRs (76). The predicted disordered regions with embedded PAM2 motifs and structured regions of the four proteins are schematized in (Figure 3.2)

A



B

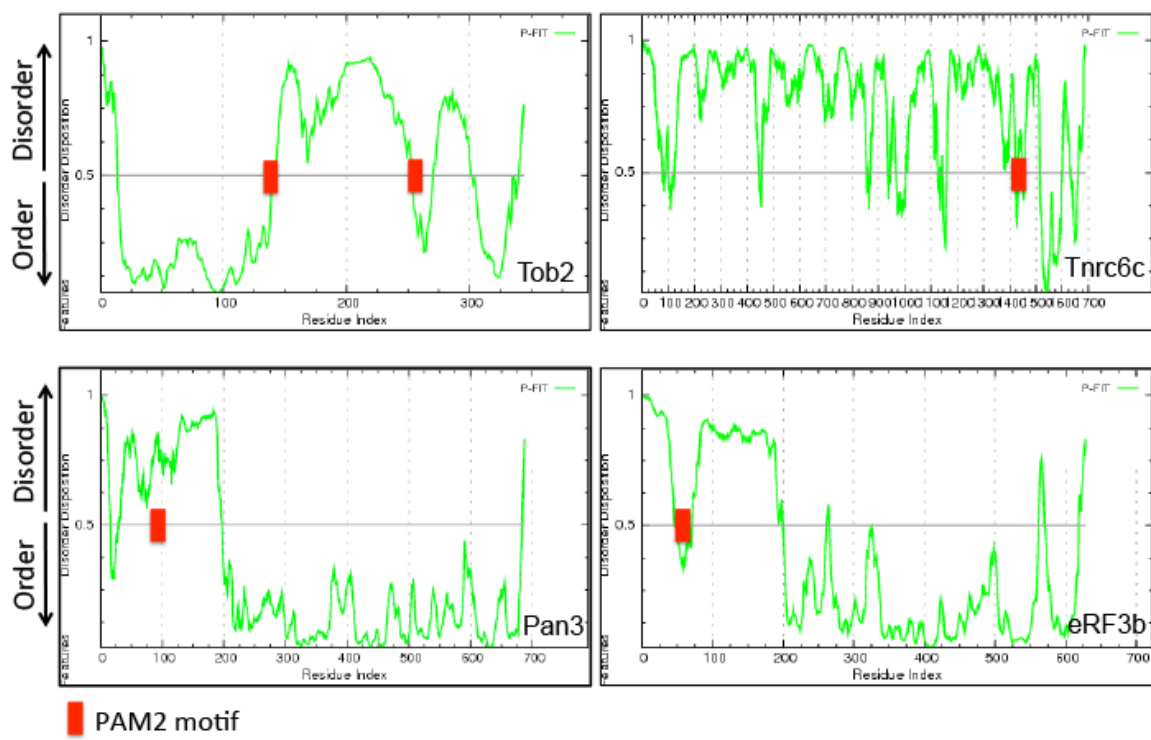


Figure 3.1 PAM2 motif-containing proteins contain extensive regions of intrinsic disorder. Human Tob2, Pan3, Tnrc6c and eRF3b protein sequences were analyzed for intrinsically disordered or unstructured regions (IDR) by Globplot (A) or PONDER (B) predictor. The websites are listed in the text. Note that in panel a, blue boxes at the bottom of each plot depict the predicted IDRs for each protein while structured domains were shown as green boxes. In panel b, green lines above 0.5 are considered IDRs by PONDR. Also indicated is the position of PAM2 motif in each protein analyzed (red box). This analysis was initiated by Amanda B Chadee and edited by Chyi-Ying A. Chen and Ann-Bin Shyu.

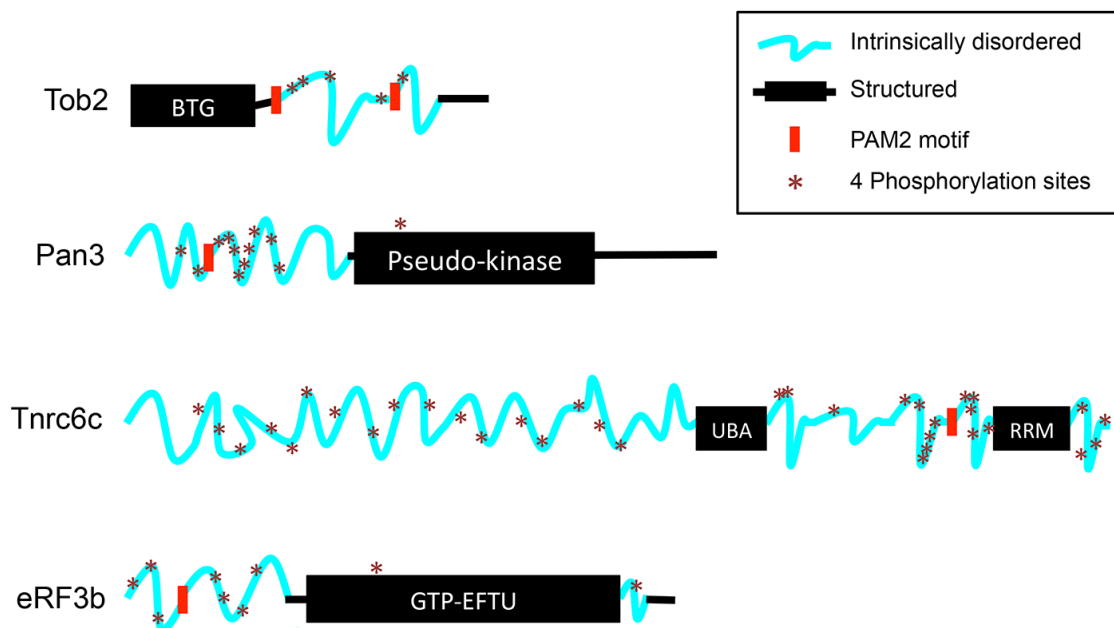


Figure 3.2 Diagram of four representative PAM2-containing PABPC1-interacting proteins showing PAM2 motifs (red blocks), IDRs (blue wavy lines), clusters of potential phosphorylation sites (asterisks; each asterisk denotes four Ser/Thr sites within a span of 10–20 aa), and structured regions (black rectangles and lines). Human Tob2 ([Q14106](#)), Pan3 ([Q58A45](#)), TNRC6c ([Q9HCJ0](#)), and eRF3b ([Q8IYD1](#)) amino acid sequences were analyzed by DISPHOS (DISorder-enhanced PHOSphorylation predictor; <http://www.ist.temple.edu/DISPHOS>).

3.2 PAM2 motifs in IDRs are generally located next to a cluster of phosphorylation sites. We used several web-based protein phosphorylation algorithms to predict the sites and extent of potential phosphorylation in the IDRs of the PAM2-containing proteins listed in Table 3.1. The tools we used included DISPHOS (DISorder-

enhanced PHOSphorylation predictor, <http://www.ist.temple.edu/DISPPOS>), Scansite (locates motifs associated with protein kinase phosphorylation; http://scansite.mit.edu/motifscan_seq.phtml), PhosphoNET (a repository of known and predicted information on human phosphorylation sites and their evolutionary conservation; <http://www.phosphonet.ca>), and NetPhos 2.0 Server (<http://www.cbs.dtu.dk/services/NetPhos>). These algorithms predicted that the IDRs in the PAM2-containing proteins are also the segments that contain clusters of potential phosphorylation sites. It is striking that, in all cases except eRF3b, there is at least one cluster of phosphorylation sites very close to PAM2 motifs (see representative examples schematically shown in Figure 3.2). These bioinformatics results suggest that PAM2-containing proteins have the potential to be hyper-phosphorylated by kinases at clusters within their IDRs. Based on this, we suspected that the interaction of a PAM2 motif with the MLLE domain of PABPC1 could be modulated via variable phosphorylation at these serine/threonine clusters. This regulatory scheme could form the basis by which cells differentially and selectively control the interaction of PABPC1 with distinct PAM2-containing partners during mRNA turnover, translation, and gene silencing.

3.3 Phosphorylation of Tob2 and its ability to interact with PABPC1. To test whether the interaction of a PAM2 motif with the MLLE domain of PABPC1 is modulated by the degree of phosphorylation, we first determined whether the extent of Tob2 phosphorylation affects its association with PABPC1. Tob2 is a known phosphoprotein that can simultaneously interact with Caf1 deadenylase via its structured N-terminal BTG domain and with PABPC1 via the two PAM2 motifs in the C-terminal IDRs (37,77-79). Point mutations that change the highly conserved phenylalanines to alanines in each of the two PAM2 motifs (Tob2-FF mutant) (37) abolish Tob2's ability to interact with

PABPC1. Ectopically expressed Tob2, either wild-type (WT) or FF mutant, displays three distinct bands by Western blot analysis, and in vitro alkaline phosphatase (AP) pretreatment collapsed the three bands into one major band (Figure 3.3 A, upper left), indicating that Tob2 proteins can be phosphorylated to different extents. As a control, we showed that AP pretreatment of TTP, an ARE-binding protein known to be highly phosphorylated (80,81), effectively removed its phosphates. It is worth noting that the relative mobilities and intensities of the three bands for Tob2-FF differ from those for WT Tob2, suggesting a link between its phosphorylation state and its ability to interact with PABPC1.

Co-immunoprecipitation (co-IP) experiments were then performed to see whether phosphate removal from Tob2 affects its interaction with PABPC1. To rule out the possibility that co-precipitation of the proteins is due to their association with RNA, the co-IP experiments were performed in the presence of RNase A. Ectopically expressed Tob2-V5 was pulled down and divided into two equal parts, one with AP treatment and one with mock treatment. Both samples were then incubated with lysate from myc-PABPC1- expressing cells. The results showed that phosphatase-treated Tob2 pulled down more myc-tagged PABPC1 than mock-treated Tob2 that remains phosphorylated (Figure 3.3 A, upper right).

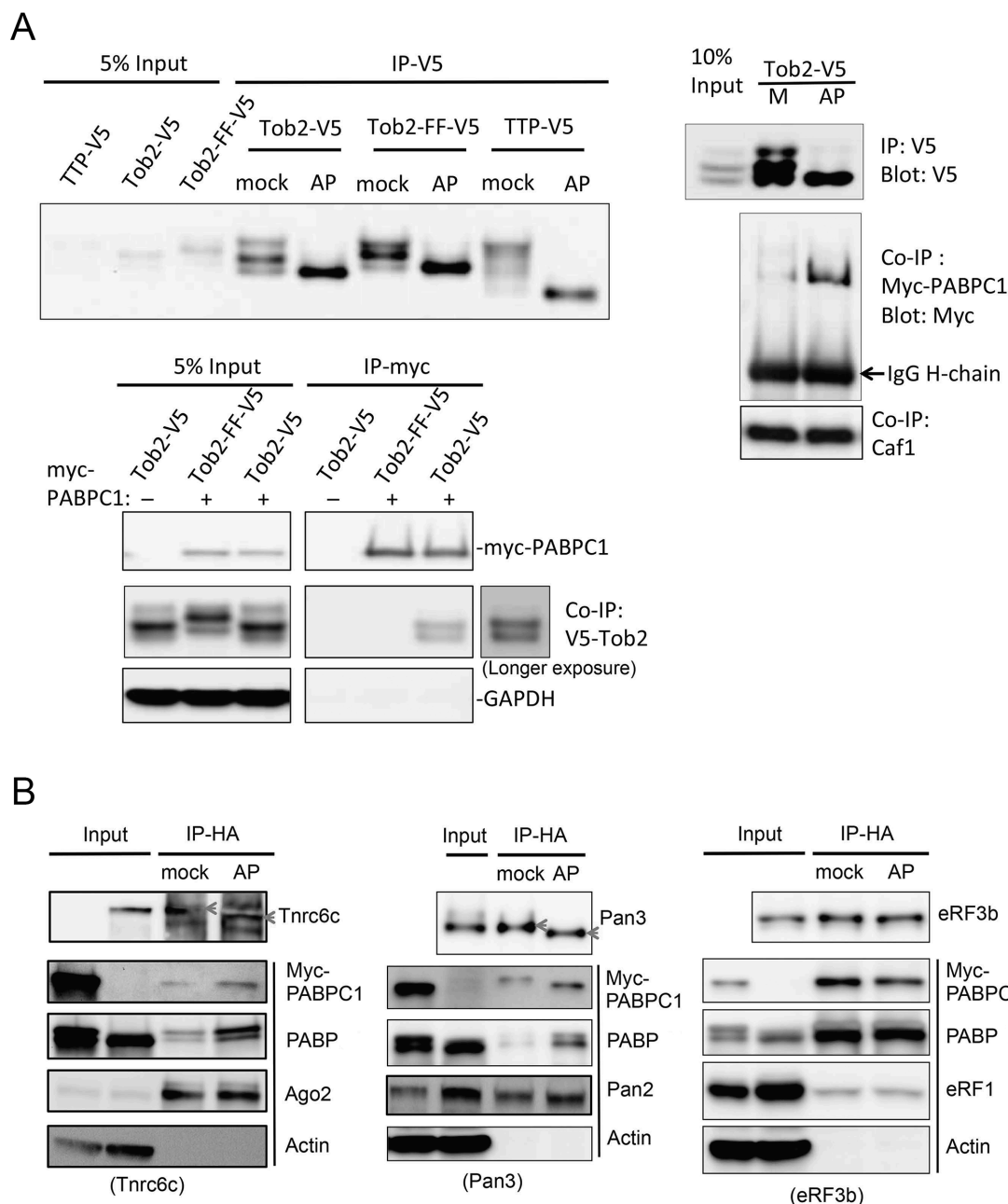


Figure 3.3 Effects of alkaline phosphatase treatment on phosphorylation of four PAM2-containing proteins and their interactions with PABPC1. (A) *Upper left*: Alkaline phosphatase (AP) or control (mock) treatment of immunoprecipitated Tob2-V5, Tob2-FF-V5, and TTP-V5 leads to a collapse of multiple higher bands into one band in SDS-PAGE. TTP, a highly phosphorylated protein, was used as a positive control for phosphatase treatment. *Upper right*: Western blot analysis showing that phosphatase-treated Tob2-V5 pulls down much more myc-PABPC1 than does mock-treated Tob2-V5, whereas both pull down an equal amount of Caf1. *Lower left*: Western blot analysis showing that myc-PABPC1 selectively pulled down the bottom two bands, corresponding to less-phosphorylated forms of Tob2-V5 and did not pull down Tob2-FF-V5 or GAPDH. (B) Effects of alkaline phosphatase treatment on phosphorylation of Tnrc6c (*left*), Pan3 (*middle*), or eRF3 (*right*) and their interactions with PABPC1 or other partners. Actin

served as a negative control. Gray arrowheads denote migration change of HA-Tnrc6c or Pan3 bands following AP treatment. Cell extracts for IP experiments were prepared from NIH3T3 cells that were transiently transfected with the plasmids encoding the proteins indicated.

In contrast, there was no difference in the amount of Caf1 pull-down via the structured N-terminal domain of Tob2 (Figure 3.3 A, upper right). Together, these observations suggest that the extent of phosphorylation of Tob2 is inversely proportional to the strength of its interaction with PABPC1. To corroborate this result, a complementary co-IP experiment in which cells were co-transfected with myc-PABPC1 and Tob2-V5 was conducted. The result (Figure 3.3 A, lower left) showed that myc-PABPC1 selectively pulls down the two less phosphorylated bands of WT Tob2. The control experiment showed that myc-PABPC1 did not pull down the Tob2-FF mutant, which lacks the ability to interact with PABPC1 (37). Collectively, we conclude that, while the two PAM2 motifs of Tob2 are essential for eliciting its interaction with PABPC1, the extent of Tob2 phosphorylation modulates the strength of this interaction.

3.4 Removal of phosphates from Pan3 and Tnrc6c enhances their interaction with PABPC1. We next tested whether removal of phosphates from three other PAM2-containing proteins (Pan3, Tnrc6c, and eRF3b) also enhances their interaction with PABPC1. Among the three proteins, Tnrc6c is predicted to have the highest proportion of IDR and potential phosphorylation sites, and eRF3b is predicted to have the least (Figure 3.2). The results of the co-IP experiments showed that phosphatase-treated Tnrc6c pulled down appreciably more PABPC1 than the mock-treated one (Figure 3.3 B, left). As expected, phosphatase treatment resulted in a clear increase of HA-Tnrc6c migration on SDS-PAGE, indicative of removal of an appreciable amount of phosphates from this protein. In contrast, there was no obvious difference in

the amount of co-immunoprecipitated Ago2 following phosphatase treatment. Ago2 serves as an internal control giving that Ago2 interacts with N-terminal region of Tnrc6c, which is away from the PAM2 motif located close to C-terminal region, and Ago2-Tnrc6c interaction is not affected by the phosphorylation adjacent to the PAM2 motif.

Similarly, phosphatase treatment increased the migration of HA-Pan3 and increased the amount of co-immunoprecipitated PABPC1 (Figure 3.3 B, middle), whereas there was only a marginal increase in the amount of Pan2 deadenylase pull-down after phosphatase treatment. Pan2 serves as internal control in the same fashion as Ago2 in these experiments. In contrast to Tnrc6c and Pan3, HA-eRF3b did not show any apparent change in its SDS-PAGE migration after phosphatase treatment (Figure 3.3 B, right), consistent with the prediction that this protein has fewer phosphorylation sites in its IDR compared to other PAM2-containing proteins (Figure 3.2). Moreover, phosphatase treatment did not change the amount of PABPC1 or eRF1 pulled down by HA-eRF3b. It is worth noting that eRF3b co-immunoprecipitates much more PABPC1 than Tob2, Pan3, or Tnrc6c does (Figure 3.3), suggesting that eRF3b has stronger intrinsic PABPC1-binding than the other three proteins. Together, these results support the notion that the extent of phosphorylation of PAM2-containing proteins modulates the strength of their interactions with PABPC1.

3.5 Effects of increased phosphorylation of Tob2 and Pan3 on their interactions with PABPC1. We then used a complementary approach to test whether increasing phosphorylation of the PAM2-containing proteins affects their interaction with PABPC1. Cells transfected with Tob2 were first treated with increasing amounts of Calyculin A, a potent inhibitor of the Ser/Thr phosphatase activities (82) of two major mammalian phosphatases, PP1 and PP2A (83). The Calyculin A treatment resulted in

significantly increased phosphorylation of Tob2. This effect appears to be significant for Tob2 as it was not detected with PABPC1, Caf1, or actin (Figure 3.4 A). The results of co-IP experiments using these Calyculin A-treated lysates showed that, when the phosphorylation of Tob2 increased, the amount of PABPC1 (both endogenous and myc-tagged) pulled down by Tob2 decreased (Figure 3.4 A). In contrast, Calyculin A treatment had no effect on the ability of Tob2 to pull down Caf1. Together, these results show that increasing phosphorylation of Tob2 compromised its interaction with PABPC1.

We then tested the effect of Calyculin A treatment on Pan3, Tnrc6, and eRF3b. The results showed that Calyculin A treatment increased the phosphorylation of Pan3 and also diminished the amount of PABPC1 pulled down by Pan3 (Figure 3.4 B, upper left). On the other hand, Tnrc6 exhibited only a modest change in SDS-PAGE mobility after Calyculin A treatment (Figure 3.4 B, upper right), suggesting that little increase in phosphorylation occurred. As expected, eRF3b showed no migration change (Figure 3.4 B, lower left), indicating that Calyculin A did not elicit an increase in phosphorylation of eRF3b. The results of co-IP/Western experiments showed that the amounts of PABPC1 pulled down by Tnrc6c and eRF3b were not affected by Calyculin A treatment (Figure 3.4 B, upper right and lower left). Thus, the extent of change in phosphorylation of PAM2-containing proteins correlated with the degree of change in their interaction with PABPC1. Calyculin A did not change the electrophoretic migration of PABPC1 (Figure 3.4) or other interacting partners of Pan3, Tnrc6, and eRF3 (Pan2, Ago2, and eRF1, respectively) (Figure 3.4 B), confirming that phosphorylation of these proteins was minor if any by Calyculin A. The control experiments showed that Calyculin A treatment did not change the amount of Pan2, Ago2, or eRF1 pulled down by Pan3, Tnrc6c, or eRF3b, respectively (Figure 3.4 B). Thus, results from the two complementary approaches of decreasing and increasing phosphorylation (Figures 3.3, 3.4) support our hypothesis that

phosphorylation at the Ser/Thr clusters in their IDRs can modulate the interaction of PAM2-containing proteins with PABPC1.

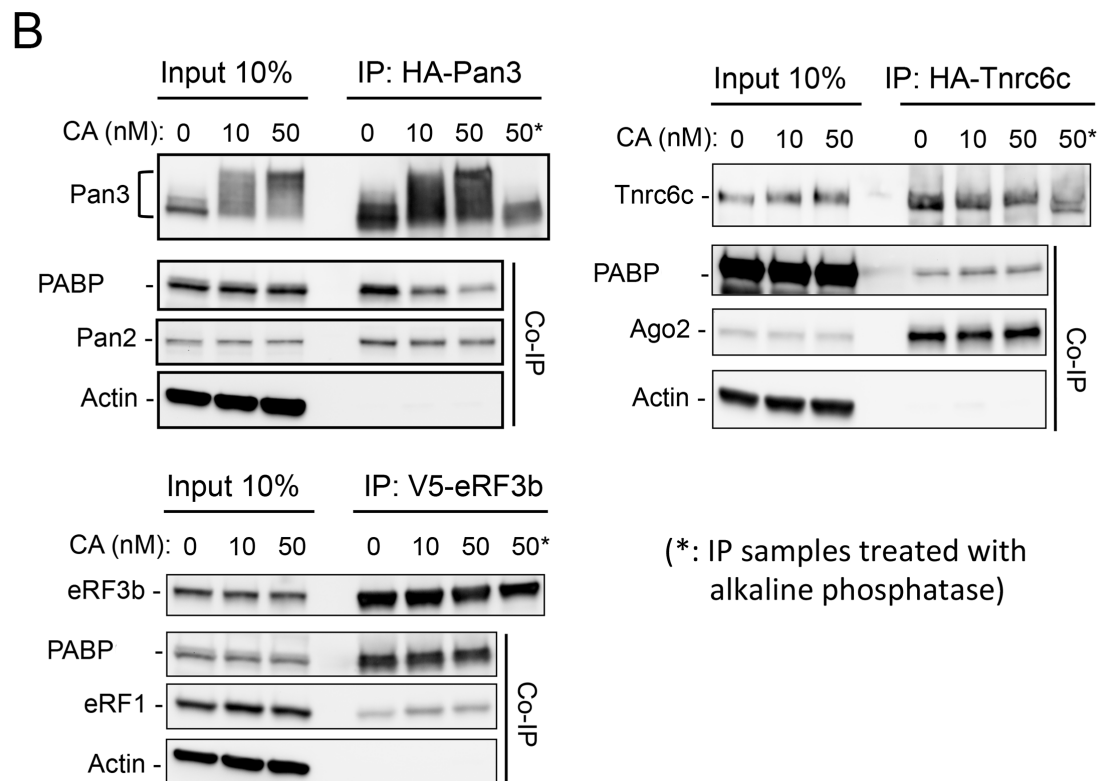
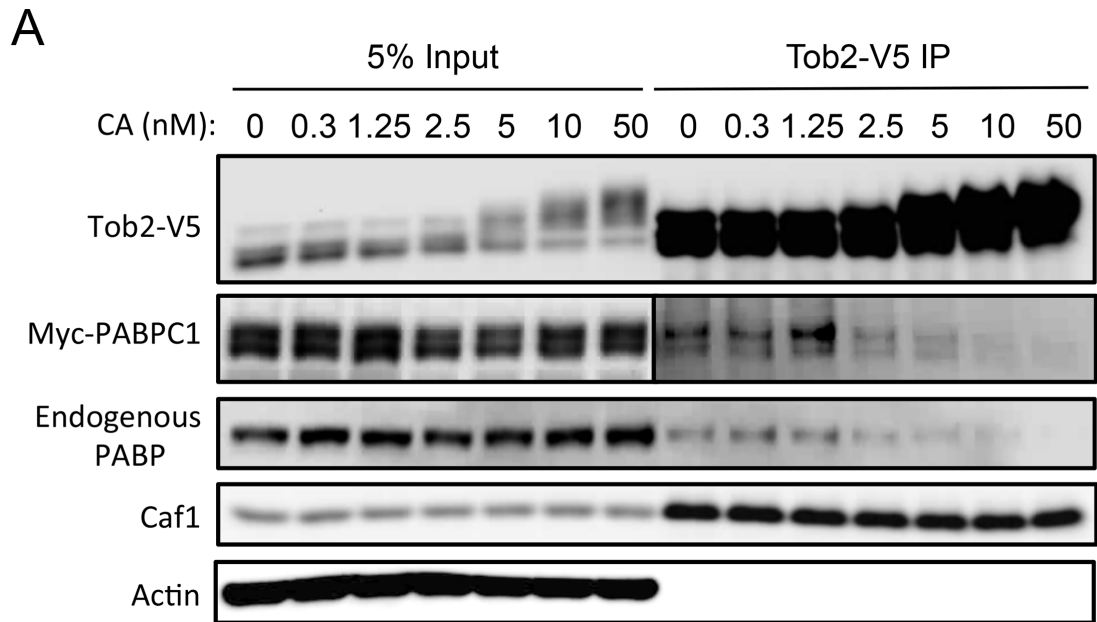
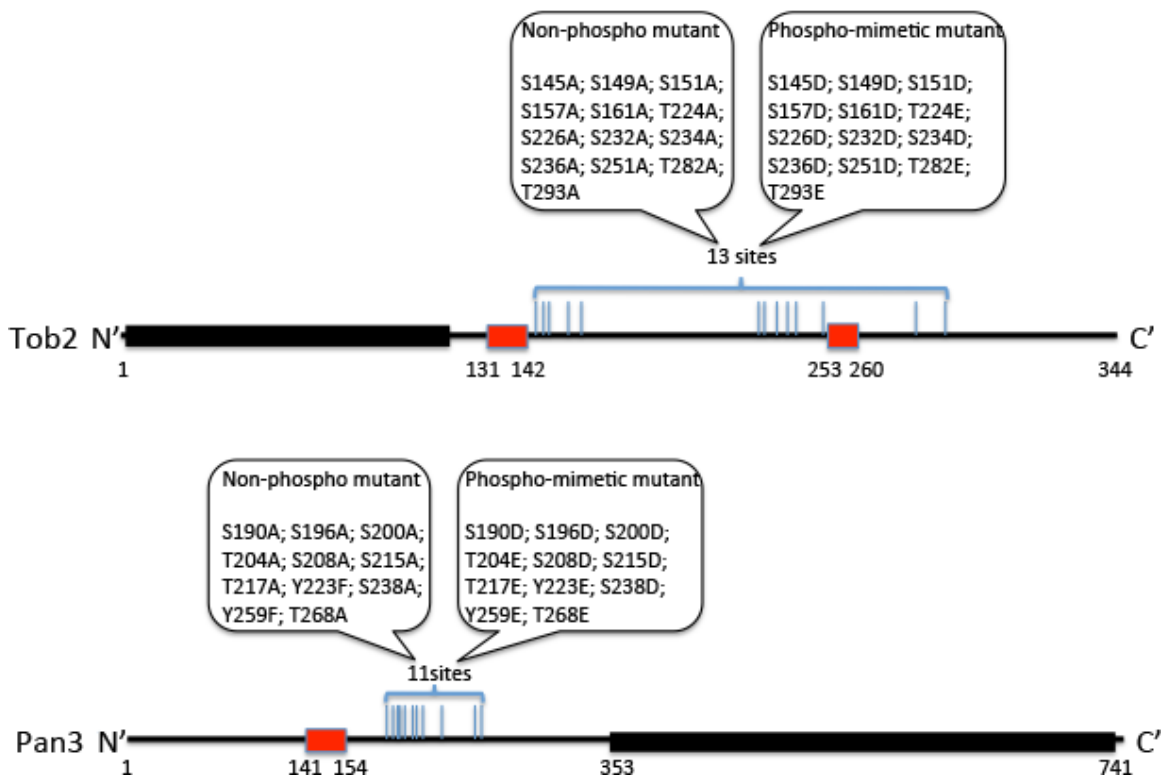


Figure 3.4 Effects of Calyculin A treatment on phosphorylation of PAM2-containing proteins and their interactions with PABPC1. (A) Western blot analysis showing that Tob2-V5 undergoes dosage-dependent increases in phosphorylation after Calyculin A (CA) treatment. Myc-PABPC1, endogenous PABP, Caf1, and actin did not show discernable changes in migration. Immunoprecipitated Tob2-V5 from CA-treated cell lysates pulled down less myc-PABPC1 and endogenous PABP as the CA concentration increased, whereas no such change was observed for co-IP of Caf1. (B) Co-IP and Western blotting experiments showing the effects of CA treatment of Pan3 (*upper left*), Tnrc6c (*upper right*), and eRF3 (*lower left*) on their interactions with endogenous PABP and other partners. Asterisks denote IP samples that were further treated with alkaline phosphatase and served as unphosphorylated controls. Note that eRF3 did not show any discernable change in its migration. Cell extracts for IP experiments were prepared from NIH3T3 cells that were transiently transfected with the plasmids encoding the proteins indicated.

3.6 Phosphomimetic mutations in the IDRs of Tob2, Pan3, and Tnrc6c

diminish their interactions with PABPC1. To further test our hypothesis, we created phosphomimetic mutants of Tob2, Pan3, and Tnrc6c. We targeted the Ser/ Thr residues within IDRs that are predicted to be phosphorylation sites and are near the PAM2 motif in each of the three proteins (Figures 3.2 & 3.5). The Ser/Thr residues were changed either to alanines to create nonphosphorylatable (NP) mutants or to Asp/Glu residues to create phosphomimetic (PM) mutants. Western blot analysis showed a discernable difference in the apparent molecular weights between the respective NP and PM mutants, as expected with different levels of phosphorylation in wild type proteins (Figure 3.6 A). The results of co-IP experiments (Figure 3.6 A) showed that, in all three proteins, the PM mutants pulled down much less PABPC1 than did the corresponding WT proteins, indicating a diminished interaction of PM mutants with PABPC1. On the other hand, the amounts of PABPC1 pulled down by the NP mutants of Pan3 and Tnrc6c were similar to those pulled down by the corresponding WT proteins (Figure 3.6 A, left and right). The Tob2 NP mutant pulled down less PABPC1 than did WT Tob2 (Figure 3.6 A, middle). It is unclear whether some of phosphorylation sites might be important for Tob2-PABP interaction instead of destabilizing the interaction. However, in

all cases the NP mutant pulled down more PABPC1 than did the corresponding PM mutant (Figure 3.6 A). Moreover, neither PM nor NP mutations affected the amount of Caf1 pulled down by Tob2, Pan2 pulled down by Pan3, or Ago2 pulled down by Tnrc6c (Figure 3.6 A). Collectively, these results further support the notion that phosphorylation in the IDRs near PAM2 motifs specifically compromises the interaction of PAM2-containing proteins with PABPC1.



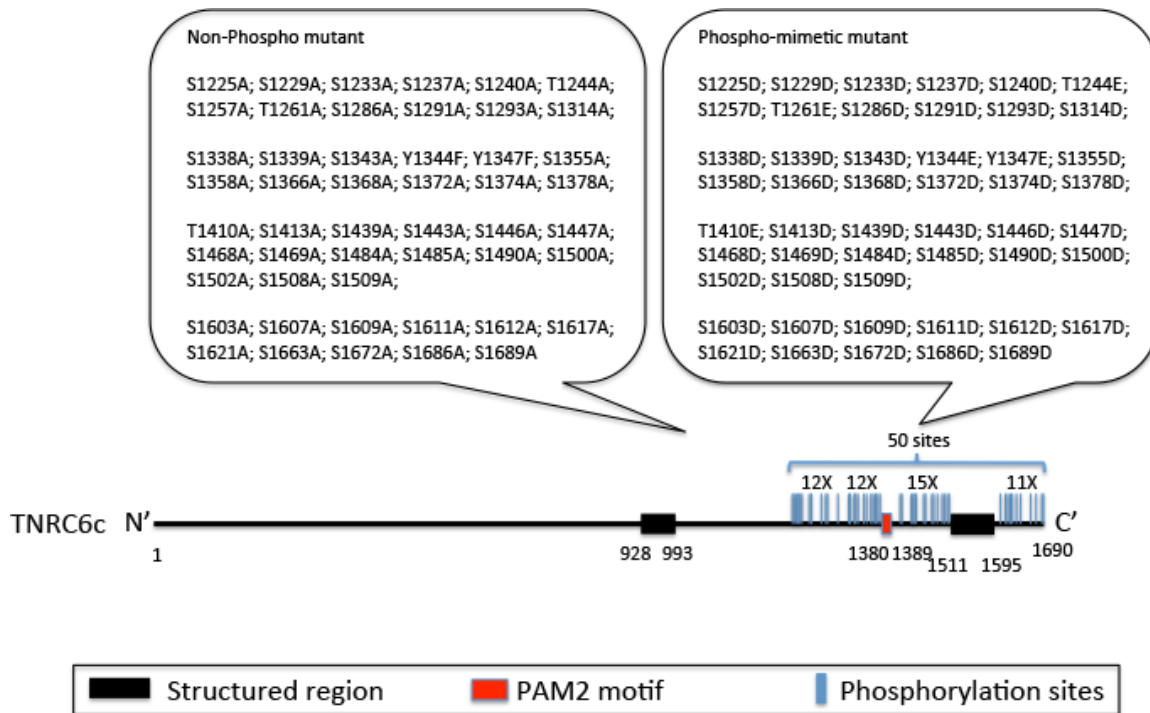


Figure 3.5 Diagram shows the mutation sites introduced into protein Tob2, Pan3, and Tnrc6c. Non-phospho mutant is created by changing serine (S) and threonine (T) to alanine (A). Phospho-mimetic mutant is created by changing serine (S) and threonine (T) to aspartic acid (D) and glutamic acid (E), respectively. Note that the cluster of potential phosphorylation sites shown above for Pan3 includes two tyrosine residues that were also mutated to phenylalanines or glutamates in the respective NP or PM mutant of Pan3.

3.7 Phosphomimetic mutations alter Tob2, Pan3, and Tnrc6c functions.

Pan3 and Tob2 act as positive regulators of Pan2 and Caf1 deadenylases, respectively, in a PABPC1-dependent manner. To test the functional significance of the effect of PM mutations on the interactions of Pan3 and Tob2 with PABPC1 (Figure 3.6 A, left and middle), cell-based poly (A) size-distribution assay was carried out to determine whether the PM mutations alter the deadenylation-enhancing function of the proteins (Figure 3.6 B). Total cytoplasmic mRNA was extracted, and the poly(A) tails were labeled at the 3' end with α -[32P] 3' - deoxyadenosine (cordycepin) (84), followed by digestion with RNases T1 and A to remove the mRNA bodies. The resulting poly(A) tail samples were

then analyzed by denaturing gel electrophoresis. The results showed that WT Pan3 and Tob2 enhance the Pan2 and Caf1 activities, respectively, resulting in accumulation of mRNAs with shorter poly (A) tails (Figure 3.6 B). The NP mutants of Pan3 and Tob2 remained capable of enhancing deadenylation mediated by Pan2 and Caf1, respectively, resulting in poly(A) size-distribution patterns similar to those caused by WT Pan3 or Tob2 (Figure 3.6 B). In contrast, Pan3 PM and Tob2 PM mutants, which exhibit diminished interactions with PABPC1, did not enhance Pan2- or Caf1-mediated deadenylation; the poly(A) tail size distributions were similar to those observed in the absence of Pan3 or Tob2 (Figure 3.6 B). Together, results from this functional assay showed that PM mutations near the PAM2 motif in IDRs of Pan3 and Tob2 have a functional consequence, namely, decreasing the ability of Pan3 and Tob2 to promote deadenylation mediated by Pan2 and Caf1, respectively.

To test whether PM or NP mutations in the silencing domain of Tnrc6c affect its function in miRNA-mediated gene silencing, we used an RNA-tethering approach combined with a dual luciferase assay. λ N-peptide (λ N), a high-affinity ligand for the boxB RNA stem-loop, was fused to HA-Tnrc6c and its PM and NP mutants. Each fusion protein vector was co-transfected with the vector encoding Renilla luciferase (RL) mRNA that carried four boxB sites in the 3' UTR (44,85). The results of the dual luciferase assay showed that WT Tnrc6c effectively repressed RL activity (Figure 3.6 C; compare to negative control that co-expressed with λ N-HA-lacZ). The overall RL activity with ectopic expression of the Tnrc6c PM mutant was higher than that with the Tnrc6c WT or the NP mutant (Figure 3.6 C, left), indicating that the PM mutation most impaired the gene silencing function of Tnrc6c. These results led us to conclude that both NP and PM mutations in the IDR around the PAM2 motif in Tnrc6c compromise its silencing function, with the PM mutation having a larger impact than the NP mutation. The observation that

both PM and NP mutations of Tnrc6c compromise silencing suggests that this silencing function requires reversible Tnrc6c phosphorylation.

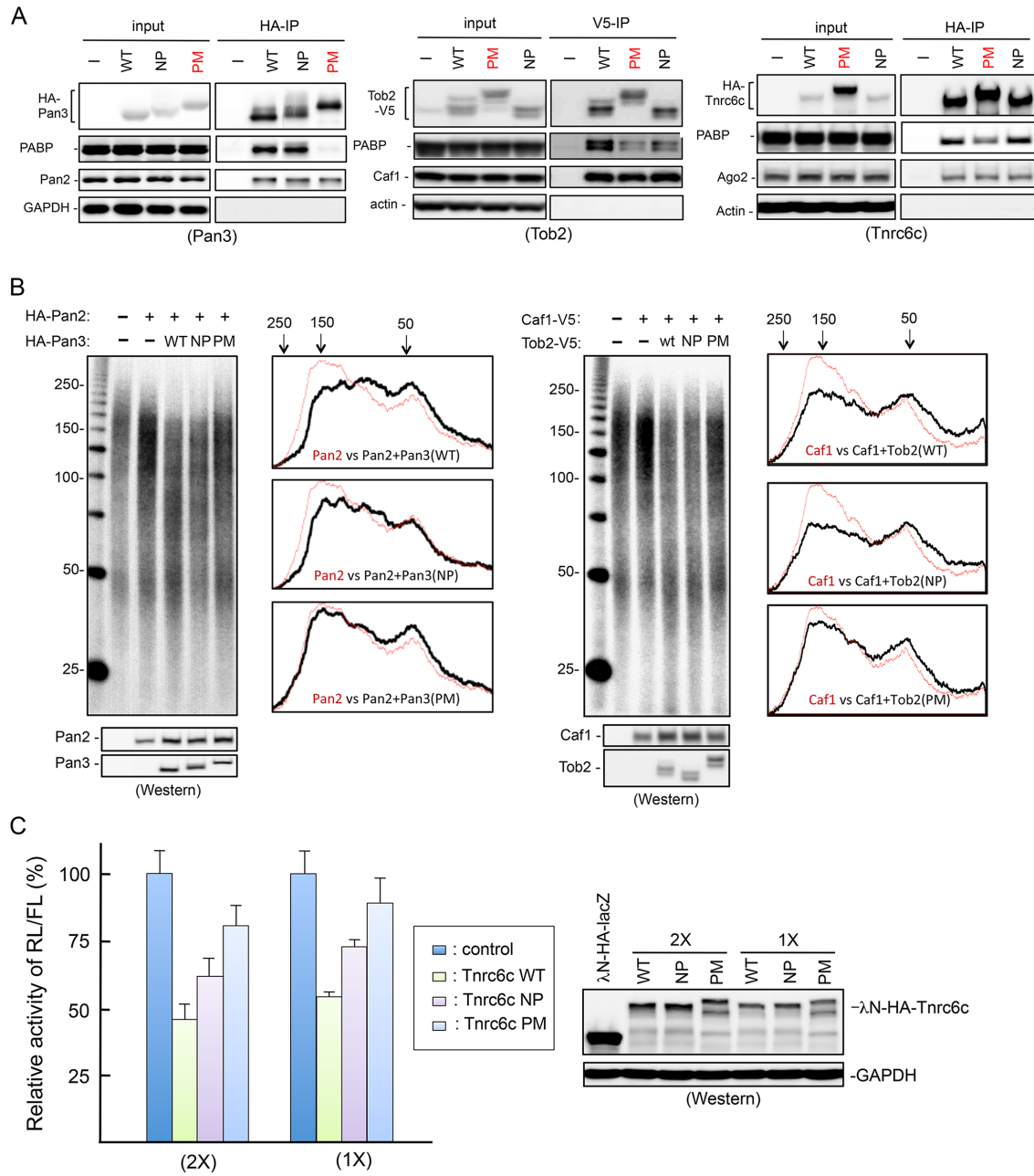


Figure 3.6 Functional impacts of phosphomimetic (PM) and nonphosphorylatable (NP) mutations on Tob2, Pan3, and Tnrc6. (A) Co-IP and Western blotting experiments showing effects of nonphosphorylatable (NP) and phosphomimetic (PM) mutations of Pan3 (*left*), Tob2 (*middle*), and Tnrc6c (*right*) on their interactions with PABPC1 or other partners. GAPDH served as a control for nonspecific co-IP. (B) Functional effects of NP and PM mutations of Pan3 (*left*) and Tob2 (*right*). Poly(A) size-distribution profile

analysis for Pan3 and Tob2 was performed as described in Materials and Methods. Cells were transiently transfected with the plasmids encoding the proteins indicated. Western blot analysis assesses protein expression levels. (C) Results of dual luciferase assays showing the gene silencing actions of WT Tnrc6c and its NP and PM mutants. Histograms (*left*) show the relative changes of *Renilla* luciferase (RL) activity detected in extracts from cells that were transiently co-transfected with a plasmid coding for firefly luciferase (FL) mRNA and RL mRNA that contain four boxB sites in the 3' UTR, and a plasmid coding for λ N-HA-Tnrc6c (WT or mutant). The RL/FL activity observed in the extract expressing λ N-HA-lacZ was set at 100%. All data represent the normalized mean \pm standard errors ($n = 3$). Western blot analysis (*right*) was used to assess the expression levels of the recombinant proteins. Pan3 panels in figure (A) was performed by Amanda B Chadee. Figure (C) was performed by Yueqiang Zhang.

Discussion

This study focuses on the PAM2-motif containing partners of PABPC1 in mammalian cells. Bioinformatics and structural analyses revealed that thirteen human PAM2-motif containing proteins exhibit similar structural features: (1) They contain IDRs; (2) PAM2 motifs are embedded within the IDRs; and (3) the PAM2 motifs are near one or more clusters of potential phosphorylation sites (Figure 3.2; Table 3.1). Based on these observations, we hypothesized that protein phosphorylation at these Ser/Thr clusters may modulate the interactions between PABPC1 and the PAM2-containing proteins. The results of experiments with four of these PAM2- containing proteins (Tob2, Pan3, Tnrc6c, and eRF3b) support our hypothesis. We thus propose that in the process of interaction between PABP and PAM2 motif-containing proteins, reversible phosphorylation at the IDRs near the PAM2 motifs serves to modulate the interaction. This mechanism may represent a general means to regulate the functions of the various PAM2-containing proteins in eukaryotes.

The results of the present study support our model. Tob2, Pan3, and Tnrc6c all can undergo appreciable degrees of reversible phosphorylation. Among the PAM2-containing proteins tested here, eRF3b is the least phosphorylated and Tnrc6c is the

most phosphorylated, while Tob2 and Pan3 appear moderately phosphorylated. Two complementary approaches showed that the degree of phosphorylation of these PAM2-containing proteins correlates inversely with their ability to interact with PABPC1. First, dephosphorylation by alkaline phosphatase treatment greatly enhances the ability of Tob2, Pan3, and Tnrc6c proteins to bind to PABPC1 (Figure 3.3). The PABPC1 binding of eRF3b, whose electrophoretic mobility is not affected by phosphatase treatment, is not altered by the phosphatase treatment (Figure 3.3 B, right). It is worth noting that eRF3b is the least phosphorylated of the four proteins and binds more PABPC1 than the other three proteins (Figure 3.3). Second, Calyculin A treatment, which greatly increased phosphorylation of Tob2 and Pan3, decreased their association with PABPC1 (Figure 3.4 A & B, upper left). On the other hand, Calyculin A did not change the apparent phosphorylation state of eRF3b or alter its interaction with PABPC1 (Figure 3.4 B, lower left). Calyculin A treatment also did not greatly increase the phosphorylation or decrease the PABPC1 binding of Tnrc6 (which is predicted to be already highly phosphorylated) (Figure 3.4 B, upper right).

The amounts of PABPC1 pulled down by Tnrc6 in the co-IP experiments presented here seem lower than those reported in previous studies (86-88). It is worth noting that the earlier studies did not use full-length Tnrc6 paralogs for the co-IP experiments. Instead, the earlier experiments used nonphosphorylated recombinant Tnrc6, the Tnrc6 silencing domain alone (86,88), or a GFP-Tnrc6 fusion (87) that could affect phosphorylation and expression of Tnrc6. It is plausible that, in the present study, Tnrc6 has more phosphorylation and, thus, lower PABPC1 binding. Our finding that Tnrc6c pulled down more PABPC1 after phosphatase treatment (Figure 3.3 B, left) supports this notion.

Functional assays showed that PM mutations of Tob2, Pan3, and Tnrc6c that diminish their interactions with PABPC1 (Figure 3.6 A) impair their biological functions to a greater degree than do NP mutants in the same proteins (Figure 3.6 B & C). Pan3 PM and Tob2 PM mutants were less effective in enhancing the Pan2 and Caf1 deadenylases' activities in mammalian cells, respectively (Figure 3.6 B). Similarly, the PM mutant of Tnrc6c exhibited a decreased gene silencing effect (Figure 3.6 C). It should be noted that the functional impairment seen in PM mutants could have other explanations, e.g., fortuitous alteration of protein conformation or folding as a result of introducing a number of Asp/Glu residues. Moreover, as some NP mutants showed moderately decreased functionality, overly persistent binding of a PAM2 motif-containing protein to PABPC1 could also hinder the cellular function. Thus, the results here suggest that the cellular functions of PAM2-containing proteins require their binding to PABPC1 to be both specific and reversible.

Tnrc6c, Pan3, and Tob2 are all positive regulators for mRNA decay, with Tnrc6c being specific for miRNA targets (37,89-91). Moreover, all three proteins participate in mRNA decay by promoting deadenylation (13,17). Previously, we showed that mRNA deadenylation is biphasic, with Pan2-Pan3 and Ccr4-Caf1 involved in the first and second phases, respectively (16). Through simultaneous interactions with PABPC1 and Pan2, Pan3 recruits Pan2 deadenylase directly to the 3' poly(A)-PABPC1 complex to initiate the first phase of deadenylation (16,89). Tob2 enhances the second phase of deadenylation by recruiting the Ccr4- Caf1 complex directly to the 3' poly(A)-PABPC1 complex (37,77,89). Interestingly, Tnrc6c is an integral part of a miRNA-RISC complex on miRNA-targeted mRNAs, a complex that recruits Pan2-Pan3 and Caf1-Ccr4 deadenylases to the mRNAs without involving PABPC1 (11,92,93). This raises the question of the functional significance of the interaction between Tnrc6 and PABPC1. A

recent study (94) shed new light on this issue by showing that PABPC1, through its interaction with Tnrc6, helps binding of the miRISC complex on the target mRNA during the early phase of silencing. Subsequently, during the silencing phase, when deadenylases are recruited, the interaction between PABPC1 and Tnrc6 weakens, allowing deadenylation to proceed. In light of this observation, we proposed that during anchoring of miRISC, a less-phosphorylated state of Tnrc6 allows stronger interaction with PABPC1, whereas during the silencing phase, increasing phosphorylation of Tnrc6 lessens its interaction with PABPC1 and allows deadenylation. One important implication of the results in the present study is that a global change in miRNA-mediated gene silencing can be accomplished through signal-dependent, reversible phosphorylation of Tnrc6 proteins.

In summary, our finding that PAM2-containing proteins generally contain IDRs and are subject to dynamic phosphorylation provides a framework for understanding how interactions of various PAM2-containing proteins with PABPC1 are regulated to coordinate PABPC1's multiple roles in mRNA turnover and translation. It is worth noting that the linker between the four RNA-recognition motifs (RRMs) and the MLLE domain in PABPC1 is also intrinsically disordered according to our analyses using PONDR and Globplot. Moreover, a recent study (95) reported that PABPC1 is subjected to extensive post-translational methylation and acetylation, some of which was suggested to impact the interactions between PABPC1 and PAM2-containing proteins. It will be interesting to learn if reversible phosphorylation at the IDR in PABPC1 has a role in its interactions with PAM2-containing proteins. Our findings open up new avenues to decipher the kinase/phosphatase signaling pathways that modulate the interactions between PABPC1 and PAM2-containing proteins. Given that most of the RNA-binding proteins in the mRNA interactome have IDRs (51), the mechanism reported here may represent a

general new paradigm in which reversible phosphorylation of intrinsically disordered mRNA-binding proteins helps remodel mRNPs from their biogenesis in the nucleus to their turnover in the cytoplasm.

Chapter 4

Phosphorylation regulates Tob2 function on global mRNA deadenylation

Introduction

Phosphorylation in eukaryotic cells is well appreciated and involves signal transduction and every aspect of cellular processes to control from proteins interaction and activation to metabolism, transcription, translation, and cell proliferation etc. from prokaryotes to eukaryotes cell (52,96,97). Deadenylation, a process for cells to remove poly adenosine (A) tail from 3' end of mature mRNAs and to control mRNA fate, is demonstrated recently to be regulated by this post translational modification (45). The majority of eukaryotic mRNAs have a poly(A) tail added at its 3' end immediately after being transcribed from DNA (6). The tail length described in yeast and mammals is around 100 and 250 nucleotides, respectively (17,98). Right after the tail is synthesized, poly(A) binding proteins (PABPs) instantly harbor on it homogeneously with an average of 25 adenosines per molecule (24). The poly(A) tail-PABPs complex determines every aspect of mRNA's lifespan, starting from maturation, splicing, nuclear exportation, localization, translation initiation, translation termination, microRNA-mediated gene silencing, and degradation (2) (Figure 1.1).

PABP is known for its roles in the tail complex as a scaffold protein for various regulatory proteins to join the tail complex and to control the mRNA functions through adjusting either the structure of messenger ribonucleoprotein (mRNP) or the length of poly(A) tail (24). A regulatory protein, eIF4G, creates a closed-loop mRNA structure to benefit translation efficiency through interaction between the mRNA 5' cap structure and PABP (40); two deadenylases Pan2 and Caf1 are recruited to 3' end of mRNA to shorten the poly(A) tail by interacting with PABP-binding regulatory proteins Pan3 and Tob2, respectively (17). The PABP family includes five paralogs in human, four located in cytoplasm and one in nucleus (24). All PABPs contain RRM motifs in the N-terminal

region for RNA-binding, but only three cytoplasmic forms have a unique motif, MLLE, located near the end of C-terminal region for interaction with PABP-interacting motif-2 (PAM2) found in various regulatory proteins (Figure 1.3). Within these three PABPs, one is testis-specific and another one is inducible form, PABPC1 is the only abundant form of PABP in cytoplasm to function through interacting with PAM2 motif-containing proteins. The importance of this interaction can be highlighted by Tnrc6-PABP, which is required for microRNA-mediated gene silencing(44,61,88).

The current model indicates that only the last PABP at the end of poly (A) tail has its MLLE domain exposed for interaction with regulatory proteins (34) (Figure 1.5). Therefore, the mechanism for the MLLE domain to selectively interact with a PAM2 motif-containing protein but not others, and what the impacts these interactions have on mRNA fate, are still unclear. This chapter describes work using poly (A) tail-PABP-Tob2 interaction as a model to study how the mRNP remodeling is regulated by multi-layer phosphorylation events leading to adjustment of global deadenylation rate.

Tob2, a protein ubiquitously expressed in all tissues (65,99), belongs to the BTG/TOB (B-cell translocation gene/transducer of ERBB2) protein family. This family of proteins is known for its roles in embryonic development, cell cycle progression, anti-proliferation, apoptosis, and as a tumor suppressor gene (100-102). All of the six family members have a highly conserved BTG domain at their N-terminus. In the subfamily of Tob, the BTG domains of Tob1 and Tob2 share 96% similarity in amino acid sequence (82% identical in amino acid) and are shown to interact with MAP kinases (Erk2 and JNK2) in Tob1 (103,104) and with Caf1 deadenylase in both Tob proteins (37,38). Since the BTG domains from Tob1 and Tob2 are highly conserved, it is plausible that Tob2

can also interact with Erk2 and JNK2. Distinctively at C-terminal end, Tob proteins have a long stretch of unstructured region in the C-terminal domain sharing lower (73%) similarity in amino acid sequence (47% identical in amino acid) (101). Besides, both Tob proteins have two separated PAM2 motifs embedded inside IDR for PABP interaction, a unique feature among all PAM2 motif-containing proteins. How these two motifs intramolecularly communicate with each other in terms of PABP interaction is an intriguing question.

Tob1/2 proteins are discovered to be able to enhance mRNA deadenylation through direct interaction with Caf1 through BTG domain and interaction with PABP through its two PAM2 motifs (37). The deadenylation promoting function of Tob2 was linked to its anti-proliferation function (38,105). Our recent study further demonstrated that the C-terminal region of Tob2 is highly intrinsically disordered and potentially multiple-phosphorylated (45). These potential multiple-phosphorylation sites in the intrinsically disordered regions of PAM2 motif-containing proteins Tob2, Pan3, and Tnrc6 can diminish their interaction with PABP and regulate their functions on mRNA fate upon phosphorylation (45). In mammals, Tob1 has been shown to be phosphorylated at three sites by MAP kinases Erk1/2 in intrinsically disordered region (103) to alter their anti-proliferation function. However, there are many more sites capable of being phosphorylated. It is still unclear as to how these multiple phosphorylation sites cooperate with each other in modulating the Tob2 function of promoting mRNA deadenylation and anti-proliferation, and what are the signal pathways involved to control mRNA fate through post-translational modification of Tob2 protein. Furthermore, the underlying mechanism by which Tob2 regulated the anti-proliferation function is linked to its ability to promote deadenylation remains elusive.

This chapter describes results supporting multi-layers of phosphorylation-regulated mechanism of Tob2 in mRNP remodeling and mRNA deadenylation, in which phosphorylation induced by different stimuli can crosstalk at intrinsically disordered region of Tob2 to control global mRNA stability through synergism of two PAM2 motifs.

Results

4.1 c-Jun N-terminal kinase can trigger Tob2 hyper-phosphorylation and weaken Tob2-PABP interaction

In our previous study, hyper-phosphorylated Tob2 induced by Calyculin A treatment was shown to weaken its ability to interact with PABP and reduce its functional impact on promoting mRNA deadenylation (45). To further dissect the underlying mechanism, it was imperative to first identify the kinase responsible for Tob2 hyper-phosphorylation. Taking advantage of the reversible property of inducing hypo-phosphorylation and hyper-phosphorylation of Tob2, Tob2-expressing cells were pre-treated with several major kinase inhibitors prior to a phosphatase inhibitor, Calyculin A treatment. An initial test showed that c-JUN N-terminal kinase inhibitor, SP600125, is a candidate that has the potential to diminish hyper-phosphorylated Tob2 induced by Calyculin A, suggesting that Calyculin A-induced hyper-phosphorylated Tob2 may be mainly through JNK pathway. Hyper-phosphorylation of Tob2 only affects its interaction with PABP, but has no effect on its interaction with Caf1(45). We then tested the effects of over-expression with an increasing amount of constitutive-activated JNK1 (CA-JNK1) plasmid on Tob2 phosphorylation. Co-IP western result showed that the hyper-phosphorylated Tob2 band became stronger when the ectopic expressed CA-JNK1 increased (Figure 4.1). In addition, it also showed that the more Tob2 is hyper-phosphorylated, the less it can pull down endogenous PABP (Fig 4.1).

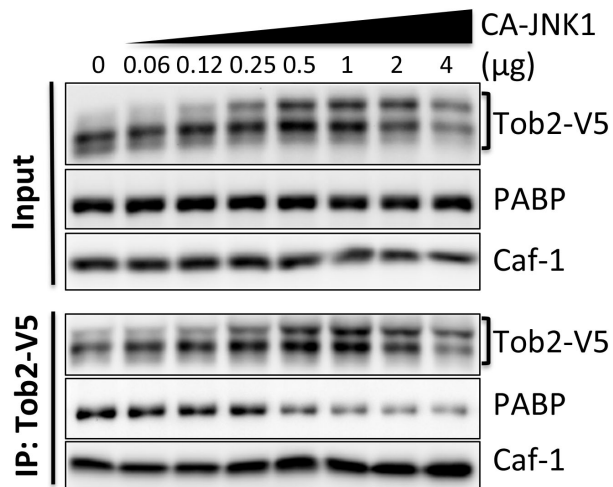


Figure 4.1 Co-expressing constitutive activated JNK1 and Tob2 in U2OS cells induces Tob2 hyper-phosphorylation. The more Tob2 is hyper-phosphorylated by increasing JNK1 expression level, the less PABP is co-immunoprecipitated with it.

Since Tob2 has been shown to be an anti-proliferation factor inhibiting G1 through S phase of cell cycle (65,106), as an effort to find out the physiological conditions that trigger change of Tob2 phosphorylation pattern, we tested whether arresting cell cycle in G1/S phase or synchronizing cells in specific phase can induce Tob2 phosphorylation pattern change. As exposing cells to UV irradiation is known to induce cell cycle G1 checkpoint arrest, I treated cells with increased dose of UV and examined whether the treatment can trigger change of Tob2 phosphorylation status and lead to a change in the PABP affinity (Figure 4.2 A). The results show that the phosphorylation status of Tob2 is correlated with the dose of UV treatment, and the more Tob2 is phosphorylated the less it can pull down PABP. When Nocodazole (Noc) was used to synchronize Tob2-expressing cells in Mitosis phase and subsequently

removed, reduction of Tob2 phosphorylation was observed and more PABP was pulled down (Figure 4.2 B).

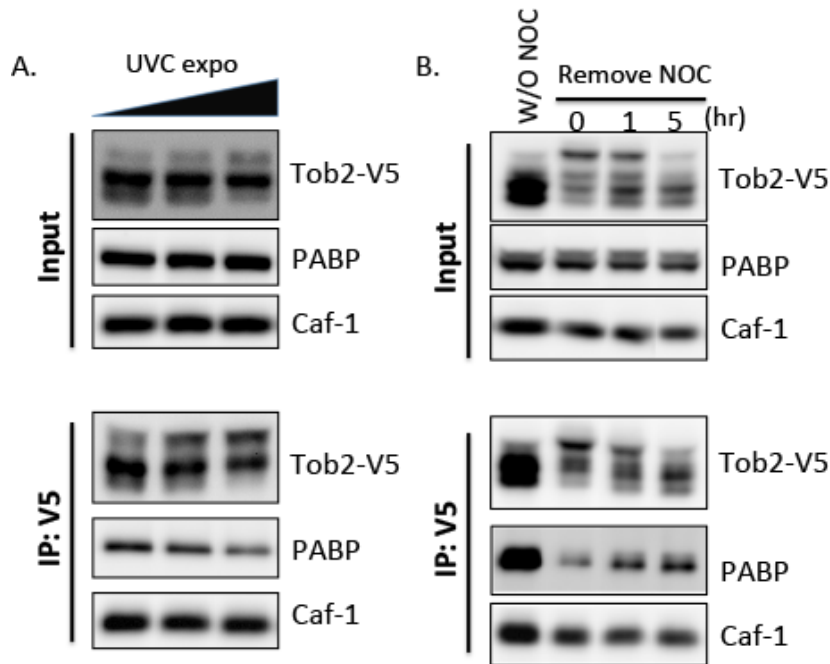


Figure 4.2 Tob2 hyper-phosphorylation can be triggered by UV or Nocodazole. Tob2 overexpressed cells were (A) exposed to 25 J/m² and 250 J/m² of UVC, or (B) treated with 100ng/ml Nocodazole (NOC) for 18 hours. A Co-IP western was run to check Tob2 phosphorylation pattern and PABP interaction.

These observations are consistent with the notion that activating JNK1 can induce hyper-phosphorylation of Tob2 and lower binding affinity of Tob2 with PABP.

4.2 Identification of JNK1-induced hyper-phosphorylation sites for Tob2-PABP interaction

To elucidate the steady-state Tob2 phosphorylation sites and JNK-induced hyper-phosphorylation sites, we pursued Mass Spectrometry analysis using ectopic expressed Tob2 protein samples isolated from U2OS cells co-transfected with either vector alone or CA-JNK1 (Fig 4.3 A). The comparison between these two Tob2 forms allowed us to identify phosphorylation sites that appeared only when CA-JNK1 was over-

expressed. Mass Spectrometry analysis results (Fig 4.3 B) not only confirmed that Tob2 has more phosphorylated sites when CA-JNK was co-expressed, but also revealed two important features of Tob2 phosphorylation pattern: i) The Majority of phosphorylation sites are located inside the intrinsically disorder region (light blue box), which is in accordance with the prediction (45) that this region is prone to post-translational modifications; ii) JNK-induced phosphorylation sites on Tob2 are adjacent to PAM2 motif, which also confirms our previous hypothesis (45) that the interaction between PAM2 motifs and PABP are controlled by a cluster of phosphorylation sites located near PAM2 motif.

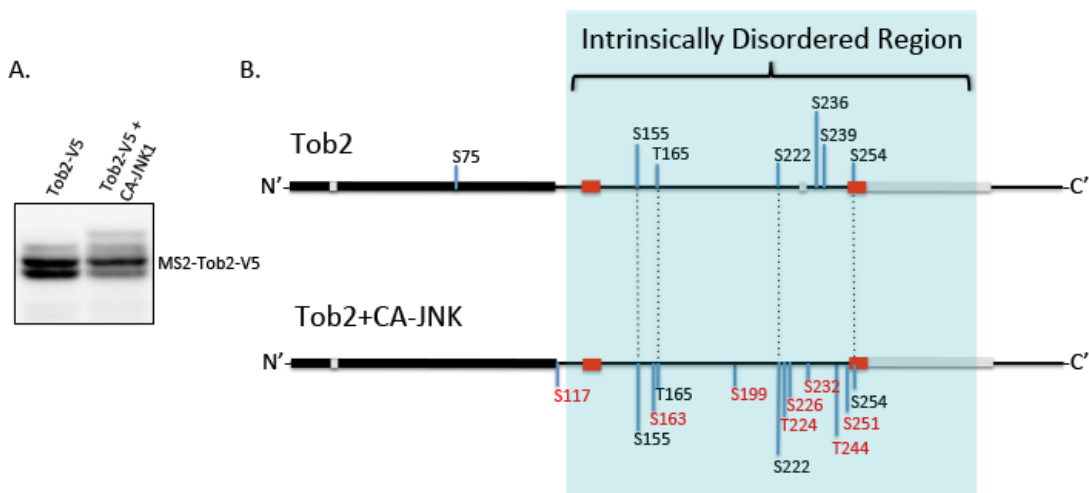


Figure 4.3 Identify JNK1-induced hyper-phosphorylation sites by Mass Spectrometry. (A) Western blot result shows steady-state Tob2 phosphorylation pattern and JNK1-induced hyper-phosphorylation pattern after co-transfection in U2OS cell. (B) Mass Spectrometry detects common and differential Tob2 phosphorylation sites between non-induced and induced JNK1. Numbers indicate the confident phosphorylation sites detected. Red numbers indicate the sites induced by JNK1 over-expression. Gray box indicates none-detectable sites. Solid red boxes are PAM2 motifs. Light blue box highlights the region of intrinsically disorder region.

To test the role of these sites in Tob2-PABP interaction, I performed Tob2 mutagenesis assay to create mutants that carry only a single mutation on one of the common phosphorylation sites or one of the sites that was induced by CA-JNK1 kinase.

Co-IP western was performed to check whether any of the single site mutation would change Tob2 phosphorylation pattern and thus alter Tob2-PABP1 interaction. The results showed that the single JNK-induced phosphorylation site mutation at serine 254, which is located right inside second PAM2 motif, dramatically affects the Tob2 phosphorylation pattern and Tob2-PABP interaction (Figure 4.4). When Tob2 serine 254 was mutated to alanine to mimic non-phosphorylation form, the middle and top bands disappeared. This suggests that serine 254 is a phosphorylation site critical for subsequent phosphorylation elsewhere. Interestingly, opposite from Chapter 3 where Tob2 with less phosphorylation pulled down more PABP, the phospho-resistant mutant Tob2 S254A can barely pull down PABP while phospho-mimetic mutant Tob2 S254D can dramatically enhance Tob2-PABP interaction. Because the serine 254 is in the second PAM2 motif and is not in the intrinsically disordered region, these results support a model illustrating two layers of regulation by phosphorylation inside and outside of the PAM2 motif (see discussion of this chapter).

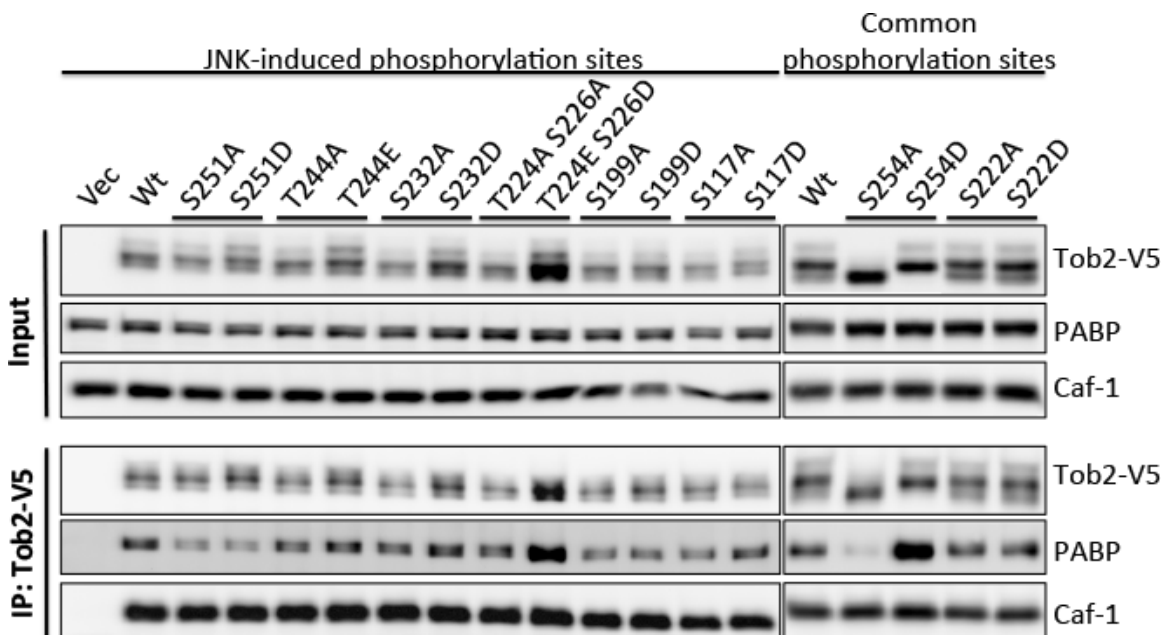


Figure 4.4 Mutagenesis study to evaluate the impact of JNK1-induced phosphorylation sites and common highly confident sites on PABP interaction. U2OS cells were overexpressed with individual mutant for 24 hours before subjected to co-IP western. The phospho-mimetic (S→D) and –resistant (S→A) mutations of common phosphorylation site serine 254 not only have distinct phosphorylation pattern but also have a dramatically opposite ability to interact with PABP. With S254 changed to A, the hyper-phosphorylation band was no longer visible, suggesting a priming effect.

Since the Tob2 S254 phosphorylation in the conserved PAM2 motif region plays a critical role in PABP interaction, it was interesting to learn whether other PAM2 motif-containing proteins have the same feature in PAM2 motif. Alignment of known human PAM2 motif-containing proteins revealed that three of them contain a serine at position 4 of the PAM2 motif (Figure 4.5) as in Tob2. Serine 254 of Tob2 is also reported to be phosphorylated in vivo in previous studies (107-109), and this study demonstrates its impact on the PAM2 motif interaction with PABP.

		PAM2 motif	
		1234567890	
Tob1-N_ (P50616-1)	0120-NGCELDKEIKNSFNPEAQV	F	FMPISDPAS-0147
Tob1-C_ (P50616-1)	0255-PPQQQQQKTSAL	S	SPNAKEFIFPNMQGQ-0282
Tob2-N_ (Q14106-1)	0121-GAPELDKEIKSSFNPDAQV	F	FVPIGSQDS-0148
Tob2-C_ (Q14106-1)	0241-NFITANPAPQSQL	S	SPNAKEFVYNGGGSP-0268
PAIP1_ (Q9H074-1)	0116-PQVVVAPVLM SKL	S	VNAPEFYPSGYSSS-0143
PAIP2_ (Q9BPZ3-1)	0099-GSSLEDLVVKSNI	N	NPNAKEFVPGVKYGN-0126
Pan3_ (Q58A45-1)	0274-WWNRVTENNLQ	T	ENPTASEFIPKGGSTS-0301
eRF3b-N_ (Q8IYD1-1)	0040-QREPLSSAFSRKL	N	VNAKPFVPNVHAAE-0067
eRF3b-C_ (Q8IYD1-1)	0049-SRKLNVNAKPFV	V	ENVHAAEFVPSFLRGP-0076
USP10_ (Q14694-1)	0071-LPRTPSYSISSTI	N	PQAPEFILGCTASK-0098
HELZ_ (P42694-1)	1088-QLEALELKKT	Y	VINPLAPEFIPRALRLQ-1115
TPRD_ (P53804-1)	1195-SKAGEYVRVKLQ	L	INPAAREFKPDVKS KP-1222
Ataxin2_ (Q99700-1)	0902-KKDAAEQVRKSTI	N	PNNAKEFNPRSF SQP-0929
TNRC6a_ (Q8NDV7-1)	1593-GWPRAKSPNGSSS	V	NWPPEFRPGEPWKG-1620
TNRC6b_ (Q9UPQ9-3)	1461-SPPTNKIGSKSSN	A	SWPPEFQPGVPWKG-1488
TNRC6c_ (Q9HCJ0-1)	1370-AKSDSDKISNGSS	I	NWPPEFHPGVPWKG-1397

Figure 4.5 Alignment of known PAM2 motifs from Homo sapiens. The canonical motif sequence is in yellow background with number labeled. Only three proteins carry serine at position 4 of PAM2 motifs marked in Red. The conserved phenylalanine is marked in blue in all PAM2 motifs

4.3 S254 phosphorylation of Tob2 enhances mRNA deadenylation in vivo

To study the functional impact of serine 254 of Tob2 in terms of deadenylation, I performed Northern blotting analysis to measure the deadenylation rates of β -globulin reporter gene under the influence of vector, Tob2 WT, Tob2 S254A, or Tob2 S254D in U2OS Tet-off cells (Figure 4.6 A). The overexpressed Tob2 proteins were checked by western blot to confirm success of transfection (Figure 4.6 B). Profiles of each band were plotted, and overlapped with the profile of vector alone for better comparison of the Tob2 effect on deadenylation (Figure 4.6 C). The results show that Tob2 WT alone can accelerate deadenylation. Phospho-mimetic mutant Tob2 S254D dramatically enhances the acceleration while phospho-resistant mutant S254A slightly slows down the acceleration of deadenylation speed. In order to further examine the impact of phosphorylation at Tob2 S254, I performed poly(A) tail distribution assay to monitor the global endogenous mRNA deadenylation under the influence of Tob2. Vector or one of the Tob2 constructs (WT, S254A, & S254D) was transfected into cells, and the length of total mRNA poly(A) tail was examined to check the effect on deadenylation (Figure 4.7 A). The profiles of each lane were plotted and overlapped with vector alone profile (Figure 4.7 B). Tob2 S254D mutant makes the pool of mRNA tail shorter than that of Tob2 WT or S254A.

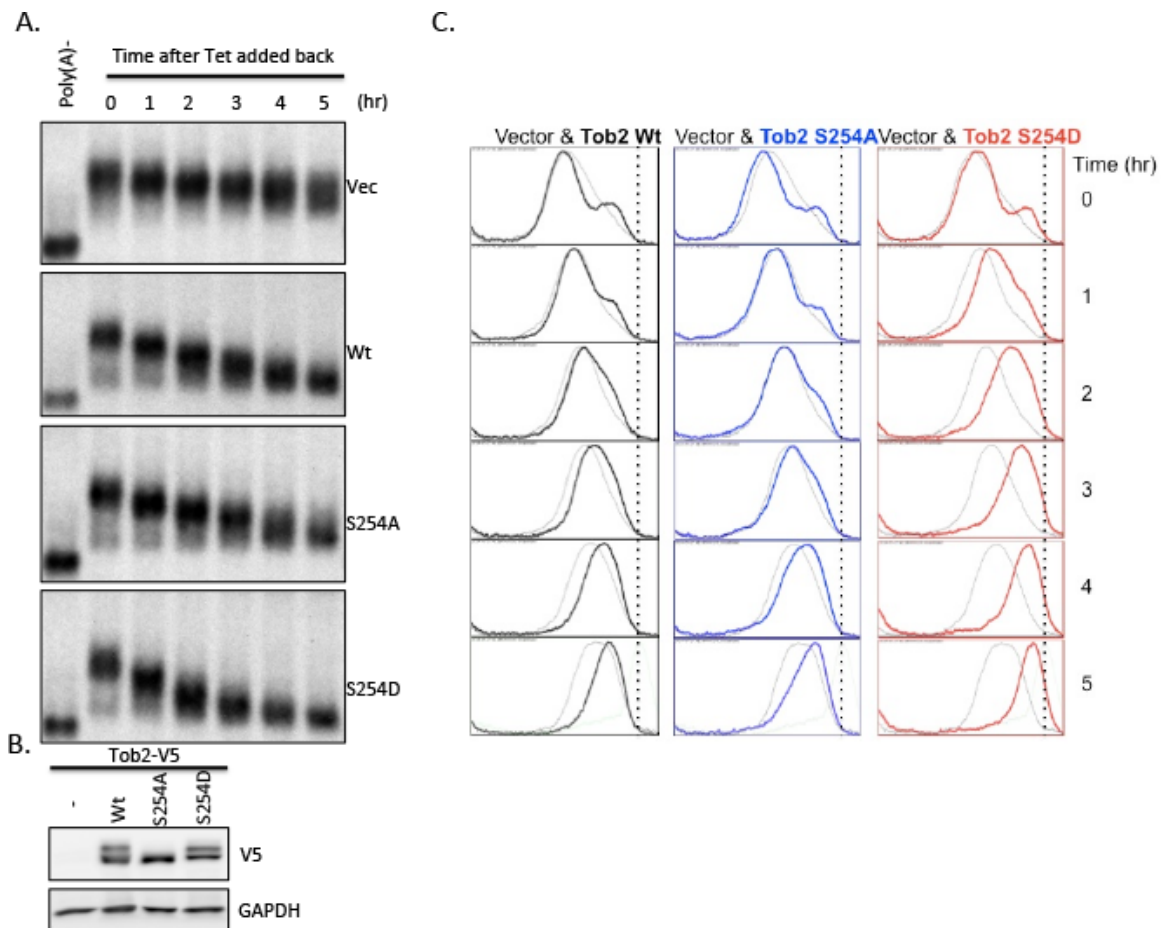


Figure 4.6 Tob2 serine 254 phospho-mimetic mutation enhances Tob2 function in promoting β -globin reporter mRNA deadenylation. B2A2 cells (NIH3T3 Tet-off stable cell line) were transfected with reporter gene β -globin together with vector or Tob2 plasmids. Transcriptional pulse-chase experiment was carried out and the cells were harvested in time course. (A) Northern blot results show that phospho-mimetic S254D mutant enhances β -globin mRNA reporter deadenylation kinetics comparing to wild type Tob2. The poly(A)⁻ lane serves as a base line control representing β -globin mRNA without poly(A) tail. (B) Western blot to check Tob2 wild type and mutants' protein expression. (C) The profile of each band was plotted and superimposed to the same time point of vector expressing cell. The black dot line indicates the position of mRNA without poly(A) tail.

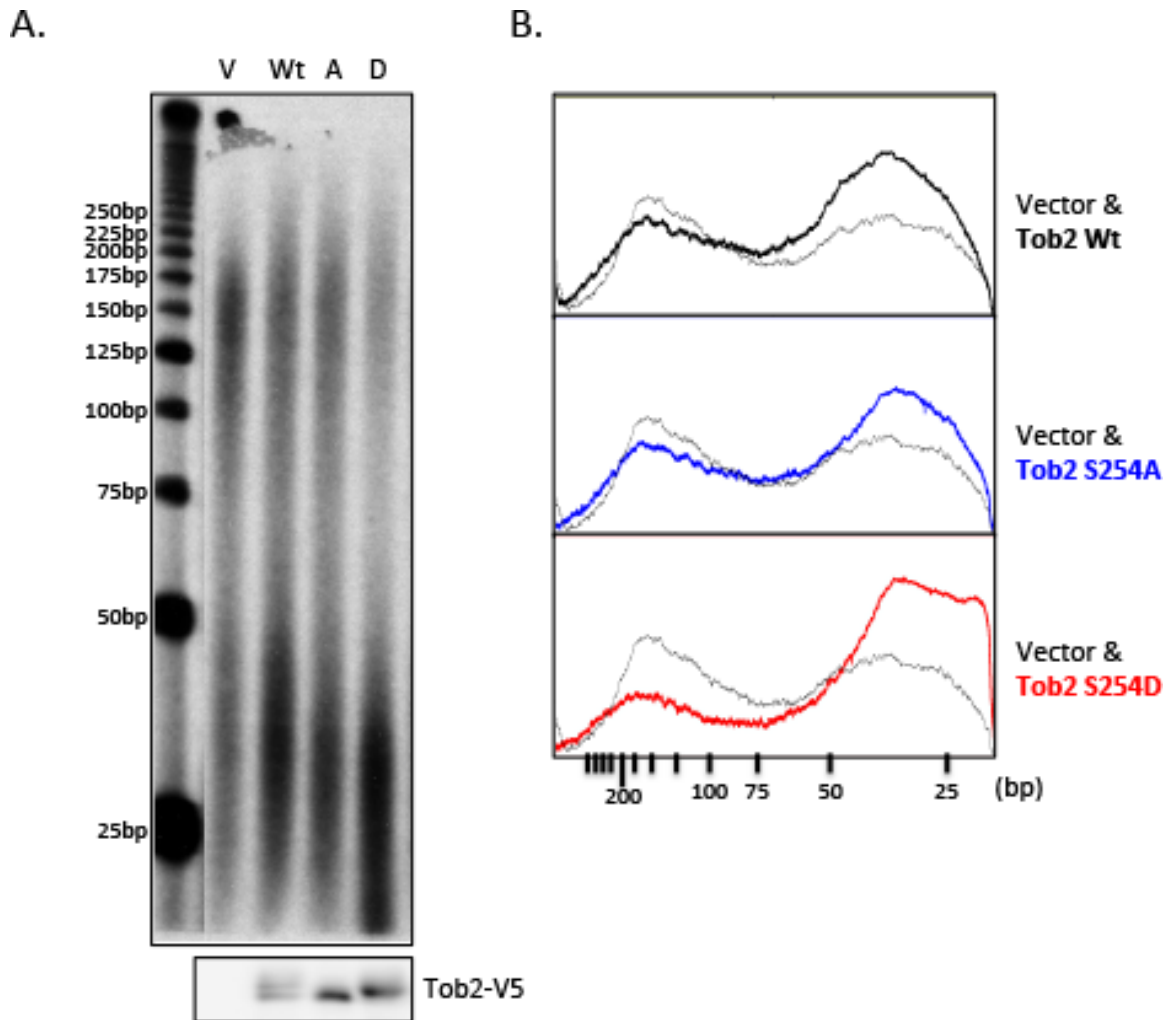


Figure 4.7 Tob2 serine 254 phospho-mimetic mutation enhances Tob2 function in promoting global mRNA deadenylation. U2OS cells were transfected with vector or Tob2-Wt, -S254A, or -S254D plasmids for 24 hours before total RNA was extracted. (A) Global poly(A) size distribution assay result shows that Tob2 S254D mutant can further promote deadenylation as compared to Tob2 wild type. The panel on the bottom is western blot to check ectopic Tob2 protein expression. (B) Poly(A) size distribution profile of each lane is plotted and superimposed to the profile of vector alone. V: vector; Wt: wild type; A: S254A; D: S254D

Together, the results show that Tob2 phospho-mimetic mutation S254D can enhance the deadenylation kinetics of reporter mRNA as well as the shortening of global mRNA poly (A) tail as compared to wild type Tob2. Phospho-resistant mutation may reduce Tob2 effect on promoting mRNA deadenylation.

4.4 Multiple phosphorylation outside PAM2 motif of Tob2 reduces PABP

interaction

Since JNK kinase can induce hyper-phosphorylation of Tob2 leading to reduction of Tob2-PABP interaction, we then tested whether this also occurs in the case of Tob2 with serine 254 phosphorylated. Co-IP western results showed that CA-JNK1 can induce hyper-phosphorylation and moderate level of phosphorylation on Tob2 S254D and S254A mutants, respectively. In the meanwhile, the interaction ability of Tob2 WT and S254 mutants to PABP are all diminished in different extent (Fig 4.8).

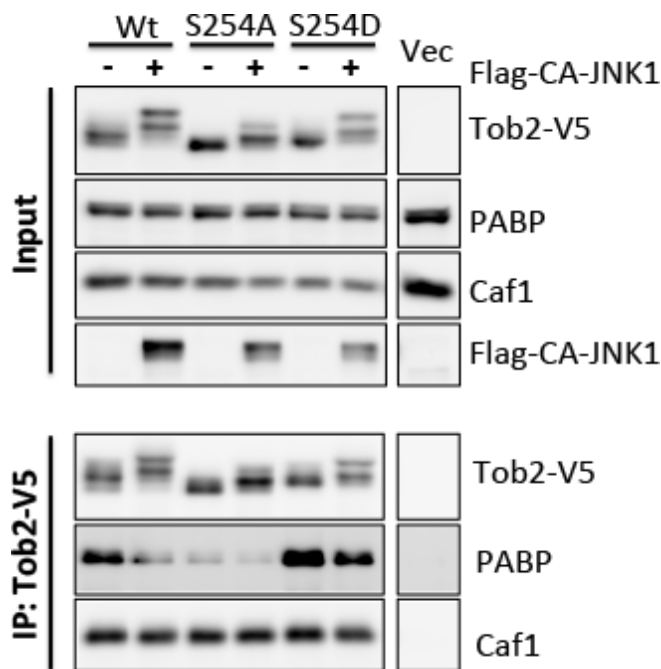


Figure 4.8 JNK reduces Tob2-PABP interaction regardless of S254 status. Tob2 WT, S254A, or S254D mutants were co-transfected with either vector alone or CA-JNK1 for 24 hours. Harvested protein lysates were subjected to co-IP western. The results show that constitutive-activated JNK1 kinase not only targets wild type Tob2 but also S254 mutants in terms of phosphorylation induction. Hyper-phosphorylated Tob2 S254D also shows weakened PABP interaction as hyper-phosphorylated wild type Tob2 does.

This result suggests that when JNK is activated, the ability of Tob2-S254D to interact with PABP is also reduced.

4.5 PAM2 motifs of Tob2 work synergistically to interact with PABP

To check if there's functional intra-molecule cross-talk between the two PAM2 motifs, the interactions between PABP and Tob2 carrying different PAM2 mutations, were tested by Co-IP western (Figure 4.9). The results show that mutation of either PAM2 motif (F140A, loss of first PAM2 function; F260A, loss of second PAM2 motif function) causes dramatic reduction of PABP interaction. When both PAM2 motifs are mutated (Tob2 FF), Tob2 no longer pulls down any PABP. The amount of PABP pulled down by individual PAM2 motif is much less than that pulled down by two intact PAM2 motifs in WT Tob2, suggesting a synergistic and indispensable role of two PAM2 motifs for Tob2-PABP interaction. Mutating serine 254 to alanine reduces PABP interaction to a level similar to that of knocking down individual PAM2 motif. When Tob2 serine 254 is not phosphorylated, second PAM2 motif alone does not function. Together, these observations suggest a regulatory role of S254 in controlling the synergism of Tob2 PAM2 motifs in terms of their interactions with PABP (Figure 4.9).

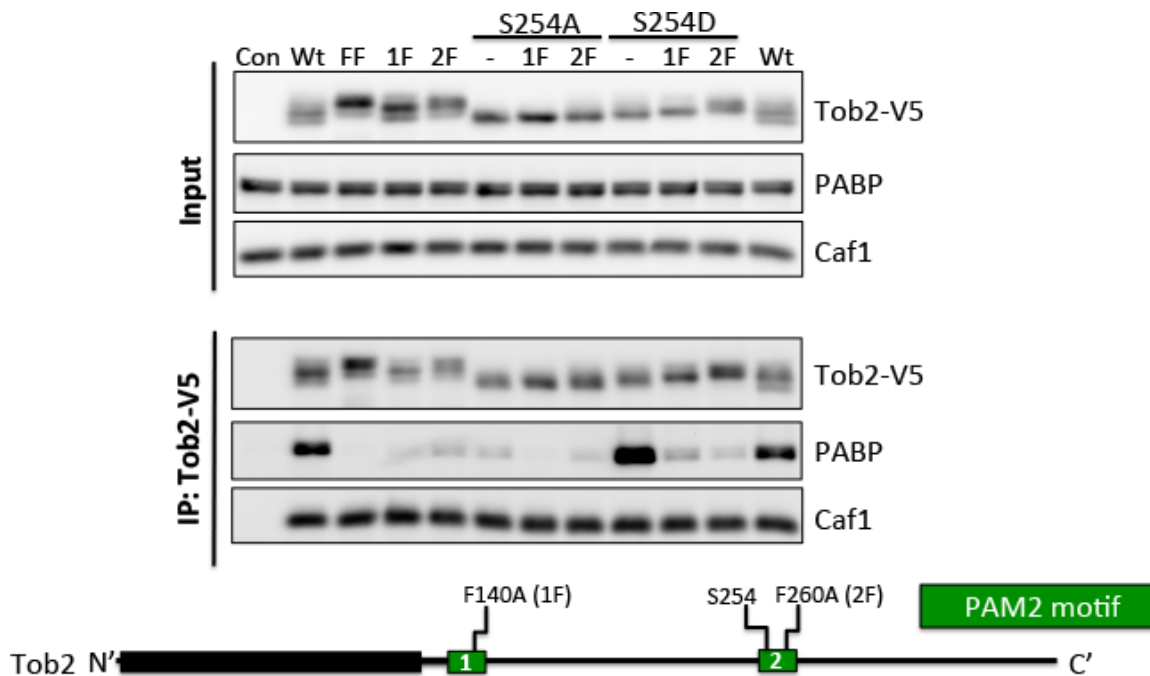


Figure 4.9 The synergism of Tob2 individual PAM2 motifs with PABP interaction. Mutagenesis was practiced to create Tob2 mutants carrying either F140A (1F), F260A (2F), or both (FF) on top of Tob2 WT, S254A, or S254D mutation. U2OS cells were transfected with these plasmids for 24 hours before co-IP western to detect PABP interaction ability of each mutant. Co-IP result shows FF mutant with both PAM2 motifs being knocked out lost PABP interaction, and knocking out first (F140A) or second (F260A) PAM2 motif in Tob2 wild type or either S254 mutant drastically reduces PABP interaction.

4.6 Establishment of Tob2 inducible cell line

Tob2 is known for its role as an anti-proliferation protein. Overexpression of Tob2, results in cell cycle arrest and decrease of cell growth rate (65,106). In order to study the function of Tob2 on mRNA deadenylation with minimal changes in cell physiology beforehand, an inducible system is required. Tetracycline-controlled gene activation was developed to meet timely expression of gene of interest by simply adding (Tet-on) or removing (Tet-off) the antibiotic tetracycline from the culture medium(110). This system enables researchers to study the functions of tumor suppressor genes. To set up this transcriptional pulsing machinery in cells, cells were required to stably express tetracycline-controlled transcription activator (tTA). In Tet-off system, tTA will

bind to Tet-responsive element in the absence of tetracycline, and therefore, brings it transcriptional activation function to the promoter of gene of interest to activate transcription (Figure 4.10 A). To have a tTA-expressing stable cell line, lentivirus system is adopted to help insertion of promoter-tTA sequences into the chromosome. Since binding of tTA to each TRE upstream of a gene contributes to the transcription activation of the gene, having more tTA would enable the cell to reach higher levels of induction. To address this notion while establishing cell lines, cells were infected by lentivirus either once or twice. The expression of tTA is confirmed by western blot (Figure 4.10 B). More infection times gives higher tTA expression level. HeLa Tet-off cell, which is commercially available and claimed to have optimal induction, serves as a comparison base line.

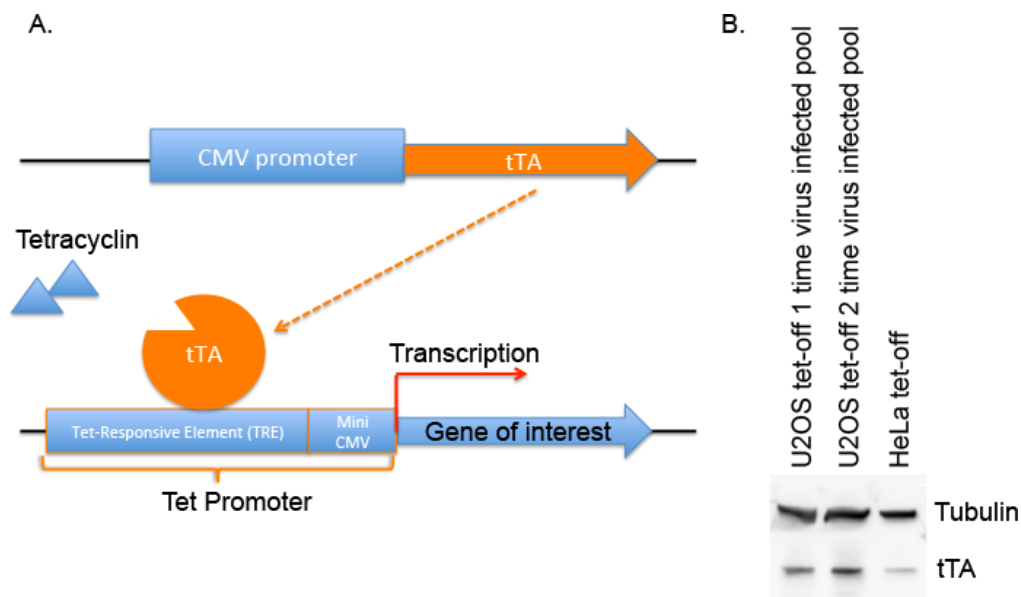
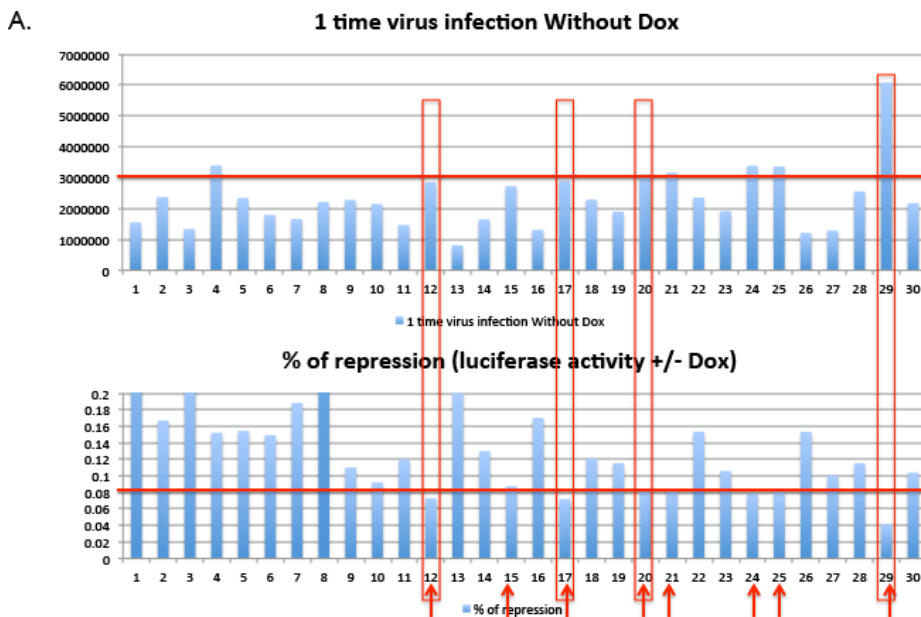


Figure 4.10 Create tTA-expressing U2OS Tet-off stable cell line. To drive transcription of gene of interest under the control of Tet promoter, cell is required to express tetracycline-controlled transcription activator (tTA). In the absence of tetracycline, tTA will bind to Tet promoter and activate transcription (A). Cells, which were infected with lentivirus carrying tTA gene, were checked for tTA expression level (B). HeLa Tet-off cell was commercially purchased and served as positive control.

Since lentivirus introduces tTA gene sequence in a random manner, each cell in pooled population may behave differently due to this random gene insertion. In order to have best induction while keeping cells in as normal as possible in terms of morphology and growth rate comparing to parental cells, a single colony selection was performed. From one-time infected pool of cells, 30 colonies were picked; from two-times infected pool of cells, 56 colonies were picked (Figure 4.11). Gene induction (without tetracycline) and repression (with tetracycline) in each individual colony was tested by delivering luciferase reporter gene under the control of Tet promoter. Cells, which exhibit either higher luciferase activity or higher repression rate (luciferase activity with/without Doxycycline), were first selected. Further narrowing down of candidate cells was achieved by comparing their morphology and growth rate to that of the parental U2OS cells. It is interesting to learn that increased frequency of virus infection resulted in increased morphology and growth changes in cells. Only 2 out of 12 selected cells from two-times virus infected clones exhibited normal shape and growth rate while 4 out of 8 selected cells from one-time virus infected clones had a better rate of success.



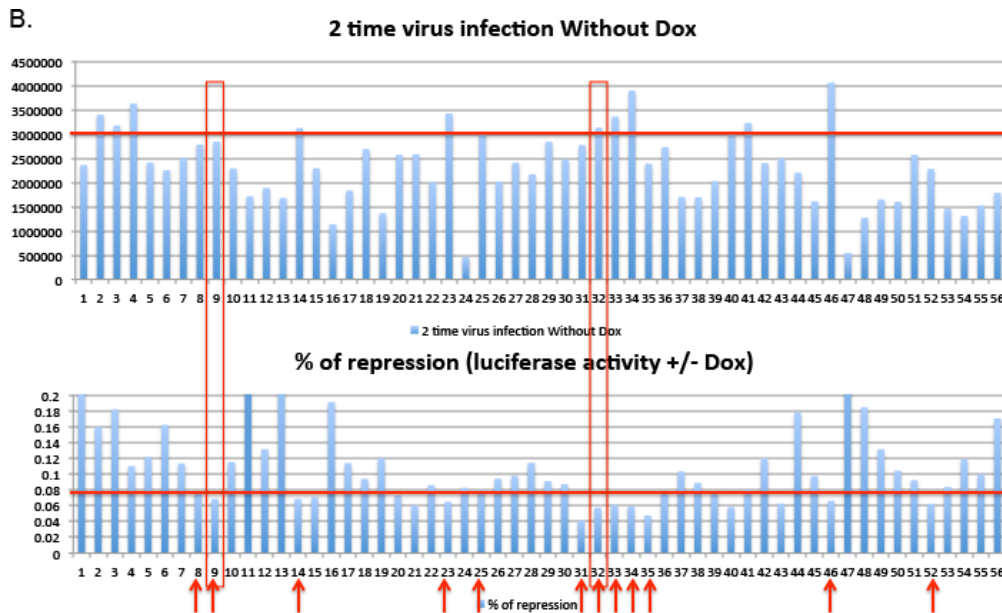


Figure 4.11 Examination of the capability of each stable cell line to induce and to repress luciferase gene in the absence and presence of doxycycline, respectively. (A) Thirty cloned one-time virus infected cells, and (B) fifty-six cloned two-times virus infected cells were transfected with Tet-promoter-controlled luciferase gene plasmid. The luciferase activity was measured. Clones that met the induction and repression threshold (red lines) were picked (red arrow). Cells, which have similar morphology to parental U2OS cell, were further selected (red rectangle). Four out of eight are normal in (A) while two out of twelve are normal in (B).

To select the clone for future mRNA deadenylation study, the same test with different reporter genes was performed on Northern blot system in order to have a more close-to-real readout to select with (Figure 4.12). Within four clones, all gave good strong induction of reporter gene shown in shorter exposure film. Considering the extent of repression shown in longer exposure film, clone 29 gives a superior result having lowest transcriptional leaky signal smear in the presence of doxycycline. Therefore, U2OS Tet-off clone 29 was selected for subsequent experiments.

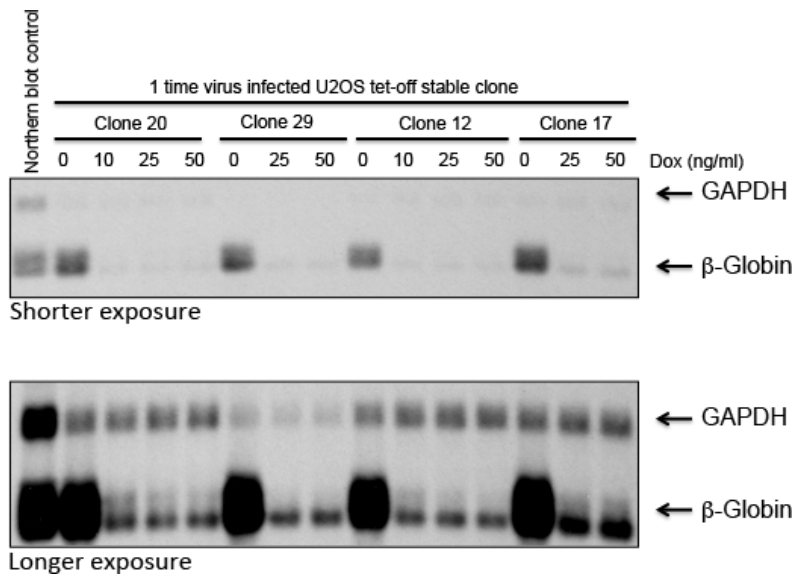


Figure 4.12 Testing the capability of U2OS Tet-off stable cell lines to induce and to repress reporter RNA. Four cloned cells were transfected with Tet-controlled β -globin reporter and internal control GAPDH. Without or with increased amount of doxycycline was applied to cells for 24hr. Northern blot was performed to check RNA level. Upper panel, shorter exposure is for better comparison of robust induction; Lower panel, longer exposure is for better examination of transcriptional leaky from doxycycline repression. All thin bottom bands of β -globin in lanes with Dox treatment were due to no Dox in the first 8hr of transfection.

4.7 Optimization of condition for checking Tob2 S254D effect on deadenylation

To study mRNA decay, transcriptional inhibitor actinomycin D has long been used to shut down RNA polymerase transcription. However, the disadvantages of using it have been found to alter many mRNA half-life(111-114), nucleus-cytoplasm shuttling(115,116), and long non-coding RNAs stability(117,118). More recently, an inhibitor-free method has been developed to metabolically label newly synthesized RNA with 5'-bromo-uridine and other metabolites. This uridine analog is incorporated into RNA transcriptionally and has little cytotoxicity (119). Using this compound to measure mRNA decay, uridine-chasing step is necessary prior to harvesting cell in time course manner. In these most critical labeling steps, optimization of BrU concentration and

duration for labeling is essential to achieve highest incorporation. Thus, a transcriptional pulse-labeling with BrU labeling approach was established in our lab (Figure 4.13).

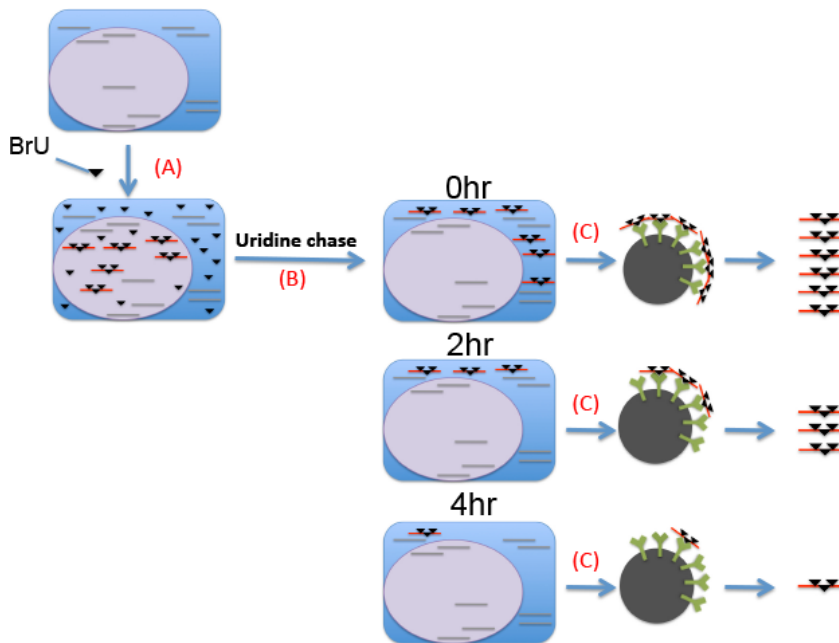


Figure 4.13 Schematic diagram of pulse-chase bromouridine RNA immunoprecipitation. (A) 10mM bromouridine (black triangle) is added into cell culture medium to be incorporated into newly synthesized RNA (red line). (B) After 2 hr labeling, bromouridine was washed away and replaced with uridine for chasing period. Cells were harvested in time-course manner. (C) Total RNA was extracted from each time point sample, and subjected to be immunoprecipitated by anti-BrdU (green symbol) on magnetic beads (gray ball) followed by elution of bromouridine labeled RNA from beads.

Use of established U2OS Tet-off clone 29 inducible cell line with optimized pulse-chase bromouridine RNA Immunoprecipitation, Tob2 effect on promoting deadenylation of newly synthesized RNA can be measured with the smallest disturbance in cells. Tob2 S254D inducible cell line was then established on top of U2OS Tet-off clone 29, using the same lentivirus approach. Unlike single colony selection, a pool of Tob2 inducible

cell was used. To test the effect of Tob2 S254D on endogenous mRNA, Tob2 S254D was induced to express first, followed by BrU metabolic labeling RNA-IP (Figure 4.14).

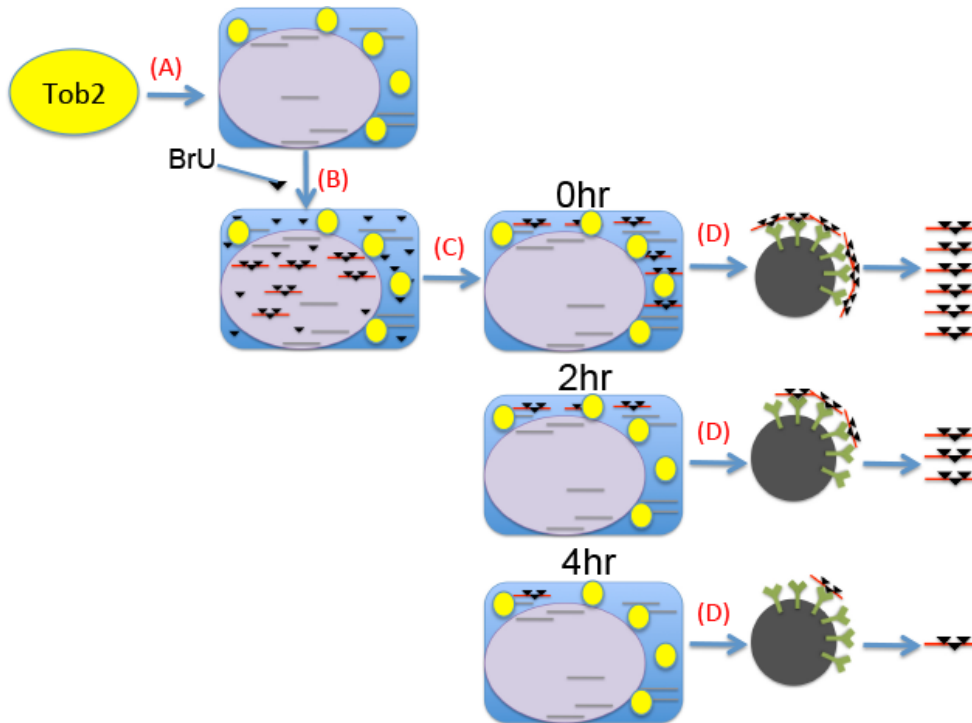


Figure 4.14 Schematic diagram shows the usage of metabolic labeling approach to study the impact of Tob2 on mRNA stability globally. (A) Tob2 (yellow oval) was induced by removing of doxycycline from cell culture medium. When Tob2's function, in terms of promoting deadenylation, reached the highest point, BrU metabolic labeling RNA-IP was performed (B to D).

To check when Tob2 S254D expression and deadenylation function can be readily detected, I carried out a time course experiment after induction of Tob2 S254D. Total RNA extracted from each time point were subjected to poly(A) tail distribution assay (Figure 4.15 A). Without Tob2 S254D, the normal population of mRNA is characterized with two typical groups: one with a longer tail with an average size of around 150 nucleotides and the other one with a shorter tail of around 50 nucleotides. Because Tob2 S254D enhances shortening of poly(A) tail, the ratio changed between

these two groups can be calculated. The preliminary results showed that Tob2 S254D was readily detected in the earliest time point after 6 hours of induction and that the induction quickly reached to top after the 14-hour removal of doxycycline. By profiling and counting the two groups of tails distribution percentage (Figure 4.15 B), Tob2 S254D function reached maximum after 10 hours of induction. Thus, I started the pulse-chase bromouridine labeling before reaching the 10-hour time point, following removal of doxycycline. Total RNA from each time point was subjected to poly(A) size distribution assay to check the effect of Tob2 S254D on deadenylation (Figure 4.16). The reduction of the top peak from 0 hour of chasing time point (equal to 10 hours after induction of Tob2 S254D), indicates that Tob2 S254D indeed exerts its function effectively.

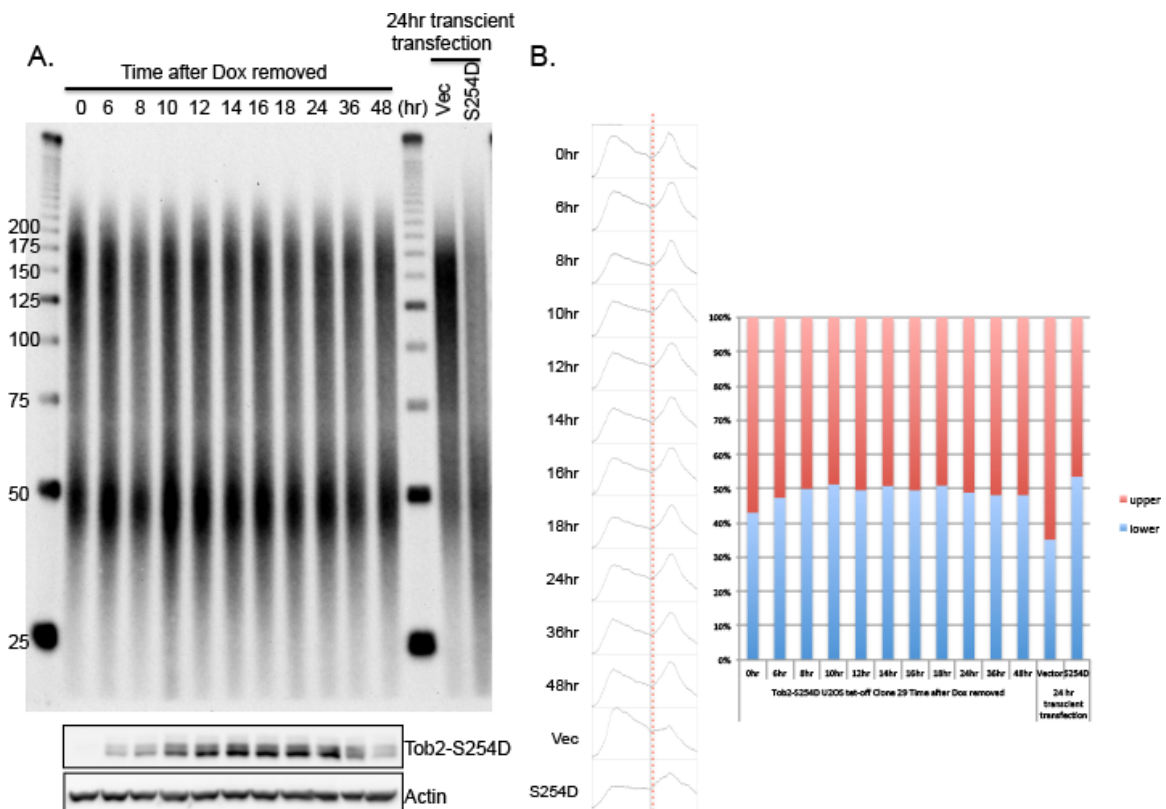


Figure 4.15 Estimation of the earliest time point where induced Tob2 S254D exerts highest function on promoting deadenylation. (A) Doxycycline was removed from U2OS Tet-off Tob2-S254D-expressing cell. RNA were extracted from cells harvested in time-

course manner. An equal amount of CPM of each cordycepin-labeled poly(A) tail sample was subjected to poly(A) tail distribution assay. Two lanes on the right of gel served as positive control. Lower panels, western blot results showing the Tob2-S254D induction status of each time point. (B) Profile of each lane resolved on gel was plotted using Image J software. The two-peak profile of each image was further divided into two parts from the center of the groove at molecular weight around 75bp (red dotted line). Ratio of divided areas of each image was plotted in a bar graph. In each bar, the red colored portion indicates the longer poly(A) tail ranging from 75 to 250 bp; the blue colored portion indicates the shorter poly(A) tail ranging from 75 to 25 bp.

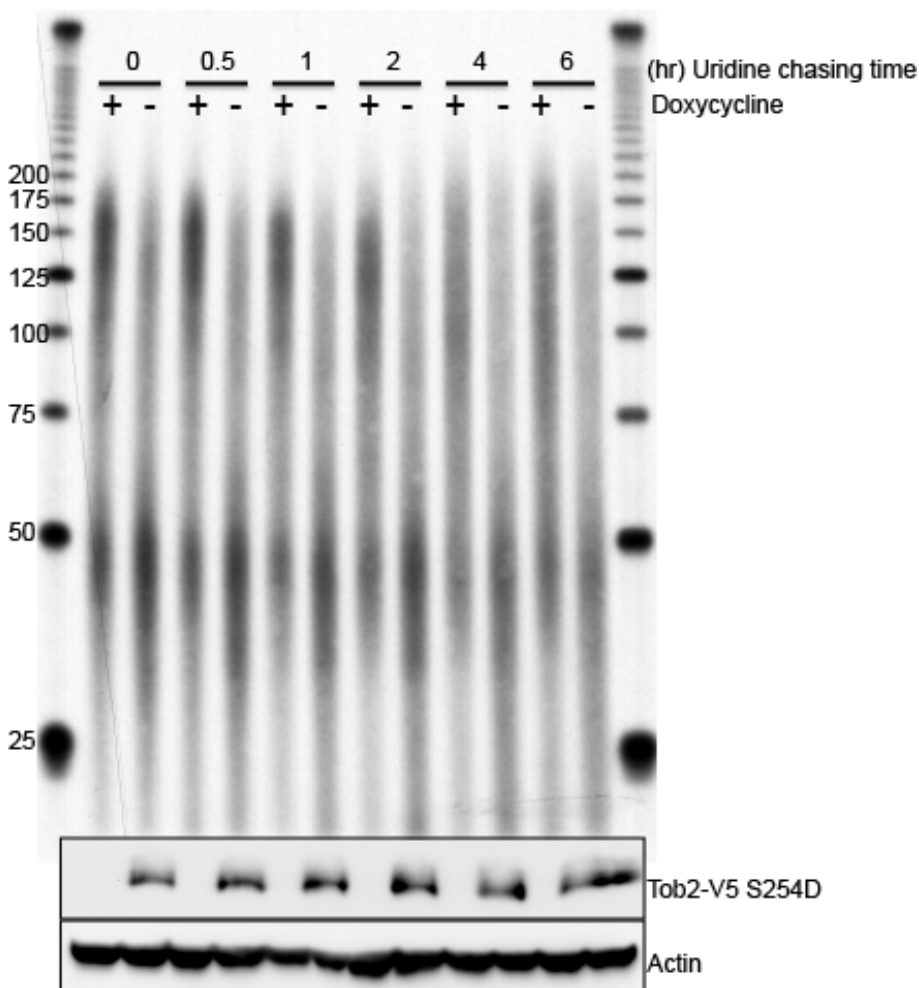


Figure 4.16 Poly(A) size distribution assay checking the effect of Tob2 S254D on global mRNA population. Six time points after removing of bromouridine were selected. Each time point has two sample comparisons: with or without Tob2-S254D induction. The bottom panels are western blot showing the expression level of Tob2 S254D in each

induced time point. The 0 time point on gel is 10 hours after removal of Doxycycline or 2 hours after bromouridine treatment.

4.8 Tob2 anti-proliferation effect is linked to destabilization of cyclin mRNAs

The deadenylation function of Tob2 is required for its anti-proliferation function (38,53). However, it is still uncertain as to how Tob2 regulates cell growth through deadenylation. One early study showed that Tob2 prevents cell cycle progression from G1 to S phase using bromodeoxyuridine-incorporation study to count what percentage of cells is able to go through G1/S check point under microscope(65). However, the microscopic study is limited and lacking the scope to cover all phases of cell cycle. With the successful set up of pulse-chase bromouridine RNA IP deep sequencing system in our lab, newly synthesized RNAs were metabolically labeled with bromouridine following Tob2 S254D induction. Cells were collected at different times during the chase period with uridine. Extracted RNAs were subjected to co-IP with anti-bromouridine antibody before removal of rRNA and cDNA libraries construction according to Illumina's protocol. Preliminary data based on deep sequencing results analyzed with the help from Dr. Jeffrey Chang suggest that Tob2 S254D preferentially destabilizes major cyclin mRNAs.

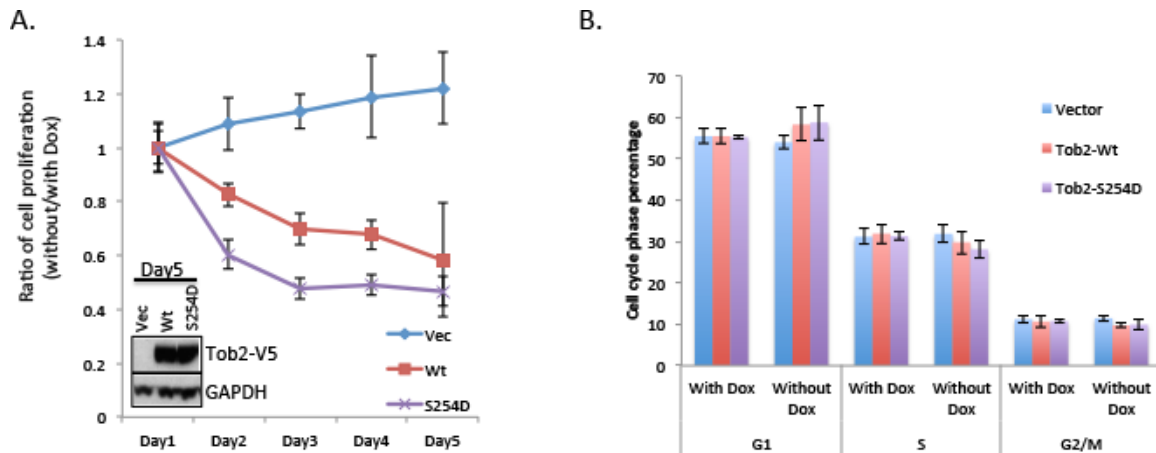


Figure 4.17 Tob2 anti-proliferation effect does not affect cell cycle distribution. (A) The ratio of cell proliferation rate of each Tet-off stable cell line without over with doxycycline over a time course was calculated. The number of cells was calculated based on the amount of DNA. The effect of Tob2-mediated anti-proliferation is further enhanced by S254D mutation. The western blot panels show the expression of Tob2 protein after 5 days' induction. (B) Propidium iodide staining with flow cytometry analysis was performed to check cell cycle distribution after induction of Tob2 genes from 1 to 3 days. The percentage of each phase of 3 days' time point of each cell was averaged and plotted.

The anti-proliferation effect of Tob2 was checked using Tet-off inducible stable cell lines expressing vector, Tob2 WT, or Tob2 S254D gene after removal of doxycycline. By calculating the ratio of amount of DNA from cells without (Tob2 expression induced) and with doxycycline (Tob2 expression suppressed), the effect of vector alone, Tob2 WT, and Tob2 S254D for the period of 5 days' measurement was plotted. Meanwhile, the same batches of cells (from 1, 2, and 3 days after induction) were subjected to cell cycle analysis using flow cytometer. The results confirmed Tob2 WT effect on cell proliferation and also demonstrated that Tob2 S254D mutant can further enhance Tob2 anti-proliferation function (Figure 4.17 A). While cell proliferation rate was significantly slowed down by Tob2 without visible cell death (Figure 4.17 A), the cell cycle phases distribution was not affected by either Tob2 WT or S254D mutant (Figure 4.17 B). Together, the results suggest that arresting cell growth by Tob2 is, at least in part, accomplished through reducing major cyclins by destabilizing their mRNAs.

4.9 CDK1 is likely a major kinase to phosphorylate Tob2 at serine 254

Based on the knowledge of direct interaction of kinase-substrate and the notion that cells would respond to changes to bring homeostasis back by compensation, we reasoned that when Tob2 S254A is overexpressed and interferes with the deadenylation machinery, more kinase(s) specific for this site might dock on this mutant longer. Therefore, co-immunoprecipitation assay was performed (Figure 4.18 A) for subsequent Mass spectrometry analysis to identify proteins that interact with Tob2 WT, S254A, and S254D. The results show that after subtracting nonspecific background binding, 698 proteins were identified to be pulled down by Tob2, 525 by Tob2 S254A, and 550 for Tob2 S254D (Figure 4.18 B). Among all the kinases identified by Mass spec, CDK1 is the top hit (16 total peptides detected) and S254A pulled down significantly more kinases including CDK1 than WT Tob2 or S254D mutant. In addition, several CDK family members were also identified to interact with Tob2 proteins.

Collectively, the results show that phosphorylation is a critical post-translational modification controlling Tob2 functions in terms of PABP interaction and global mRNA deadenylation. These functions can be tuned up or down through phosphorylation of the serine 254 in the second PAM2 motif.

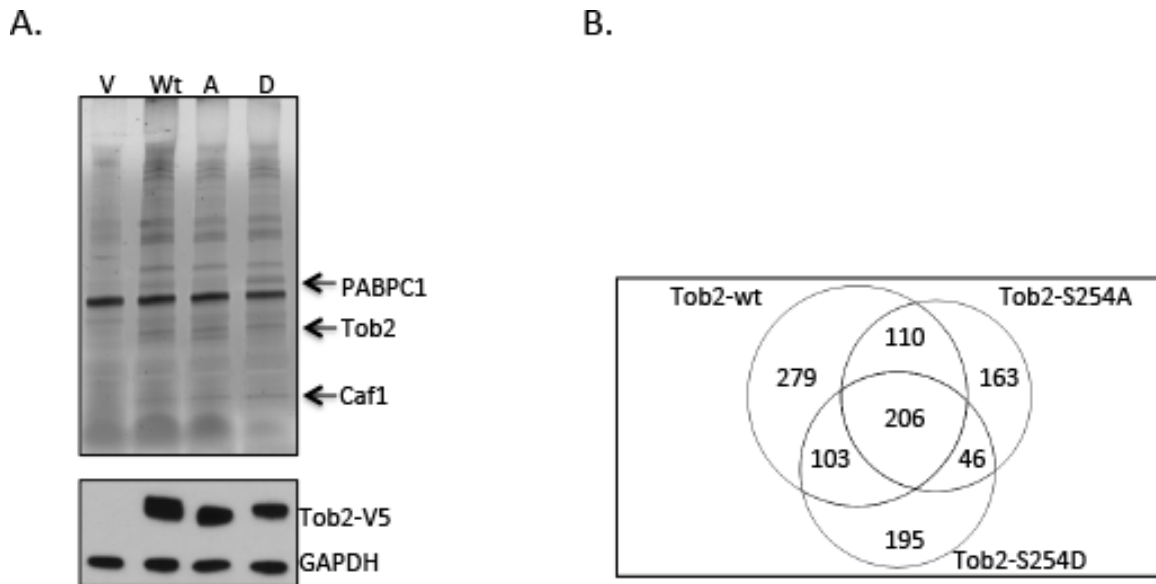


Figure 4.18 Mass Spectrometry analysis to identify unique and overlapping interacting proteins of Tob2 WT and S254 mutants. Tob2-V5 genes were induced for 24 hours before co-immunoprecipitation of using anti-V5 antibody. Co-immunoprecipitated protein complexes were subjected to a Mass Spec analysis. (A) Silver staining gel shows the co-immunoprecipitated proteins complex by vector and Tob2 (WT, S254A, and S254D). The western blot below shows the induction of each gene. (B) Venn diagram shows the number of unique and common proteins co-immunoprecipitated by Tob2 proteins.

Discussion

Poly(A)-binding protein (PABP) has been recognized as the key factor involved in Poly(A) tail mRNP remodeling process to influence mRNA fate. Tob2, among many that can interact with PABP, is known to promote mRNA deadenylation through recruiting nuclease Caf1 to the end of poly(A) tail. However, the mechanism of how cell regulates this function is still unclear. The work described in the previous chapter showed that phosphorylation at the intrinsically disorder region of PAM2-motif containing proteins decreases their interaction with PABP and reduces their function. This chapter describes how we manipulated Tob2 phosphorylation status and identified common and differential phosphorylation sites between steady-state and JNK1-induced hyper-phosphorylated condition. A critical phosphorylation site at serine 254 in the second PAM2 motif was

identified, and it was found that phosphorylation of this site not only enhances PABP interaction but also accelerates global deadenylation *in vivo*.

Based on the crystallography X-ray structure of interacting PAM2 motif from Paip2 and MLLE domain from PABP(39), enhancement of PABP interaction could be achieved by negatively charged (PO_4^{3-}) serine 254 in Tob2 (Figure 4.19). According to the structure, asparagine on 4th position of Paip2 PAM2 motif forms hydrogen bond with glutamic acid in third α -helix of PABP MLLE domain. If in the case of Tob2 where 4th position is a phosphorylated serine, it is possible that negative side chains of both amino acids will repulse each other. Since PAM2 is surrounded by intrinsically disordered peptides with high flexibility on conformation, the electrical repulsion force would possibly push phosphorylated serine to the nearest amino acid with positive charged side chain, which could be histidine 617 or lysine 580. The salt bridge formed then may be the reason why phosphorylated serine can interact with PABP more strongly.

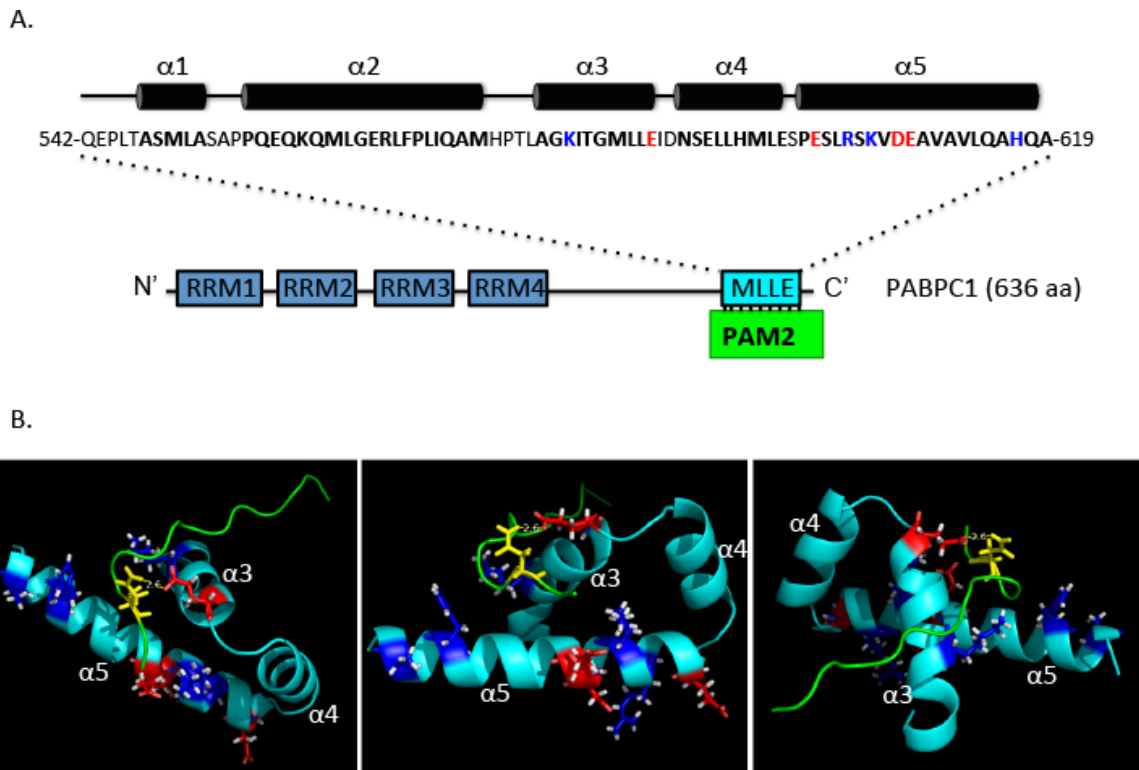


Figure 4.19 From co-crystallized structure of PAM2 (from Paip2)-MLE to hypothesize Tob2 S254 effect on PABP interaction. (A) MLE domain of PABP. Positive charged amino acids (blue) and negative charged amino acids (red) are labeled in α -helix 3 and α -helix 5. (B) The amino acid asparagine at 4th position (yellow) of PAM2 motif (green line) forms hydrogen bond with the glutamic acid (red) in α -helix 3 of MLE domain (cyan). The distance between the two is 2.6Å. α -helix 3~5 are in bright blue.

On the way of searching for the kinase targeting Tob2 serine S254, the peptide sequence around the serine is analyzed. The serine is followed by a proline. This SP motif in the cell is the most popular phosphorylation site for cyclin-dependent kinases (CDK), mitogen-activated protein kinases (MAPK), c-JUN N-terminal protein kinase (JNK), etc. This proline-directed serine phosphorylation controls many fundamental cellular processes including cell proliferation(120). Because of the promiscuous characteristic of the serine, it is difficult to pinpoint the best kinase at present. In different cellular conditions and stages, the interacting kinase may vary.

Consistent with the results described in Chapter 3, additional phosphorylation sites in IDR that are near the two PAM2 motifs can diminish the S254 effects biochemically and biologically. Noticeably, JNK induced hyper-phosphorylation at multiple sites were found in the intrinsically disordered region of Tob2. This result suggests that those sites either play an opposite role in PABP interaction or are involved in other molecular processes, for example, phosphorylation-directed ubiquitination(121). Interestingly, the critical region for ubiquitination directed proteasome degradation on Tob2 was mapped to the end of C-terminal region(122), although the site for ubiquitination had not been solved. In Tob1 C-terminal, intrinsically disordered region was shown to interact with Skp2 E3 ligase and subjected to ubiquitin-mediated proteasome degradation(123). It was observed that Tob2 PM mutant protein expression level is much stronger than NP mutant when the same amount of plasmid was transfected into U2OS cell. It is possible that some of phosphorylation sites could control ubiquitination of Tob2 as a way of controlling the protein stability. Another important finding is that the two PAM2 motifs of Tob2 worked synergistically in PABP interaction. When S254 was not phosphorylated, the synergism was lost and the second PAM2 motif alone can no longer pull down PABP.

Lastly, this work suggests that CDK1 is likely a major cyclin-dependent kinase phosphorylating Tob2 at serine 254. Preliminary data from the transcriptome-based study supports the role of Tob2 in global mRNA decay and reveals the candidates of Tob2 targets. The present study also suggests that the anti-proliferation effect of Tob2 is not through arresting specific stage of cell cycle, but rather is linked to enhancing decay of cyclin mRNAs, thereby slowing down cell growth. Based on these notions, a Tob2 mRNP remodeling model can be proposed (Figure 4.20). When Tob2 S254 was not phosphorylated, only the first PAM2 motif interacted with PABP weakly. After

phosphorylation by CDK1, both PAM2 motifs gained strong ability to interact with PABP, thereby enhancing Caf1 nuclease processivity at this stage. During the process where the last PABP was being removed due to digestion of the poly(A) tail, the second PAM2 motif acquired the opportunity to interact with c-terminal MLLE domain of next PABP. Whenever cells encounter a condition in which JNK signaling pathway is activated, Tob2 will be phosphorylated at multiple sites located in intrinsically disorder region leading to decrease of deadenylation. This move could be a protective mechanism to give cells more responding room and time to react with turbulent environmental stresses. In conclusion, this study indicates that the deadenylation-promoting function of Tob2 is under the control of an orchestrated multi-layers phosphorylation mechanism.

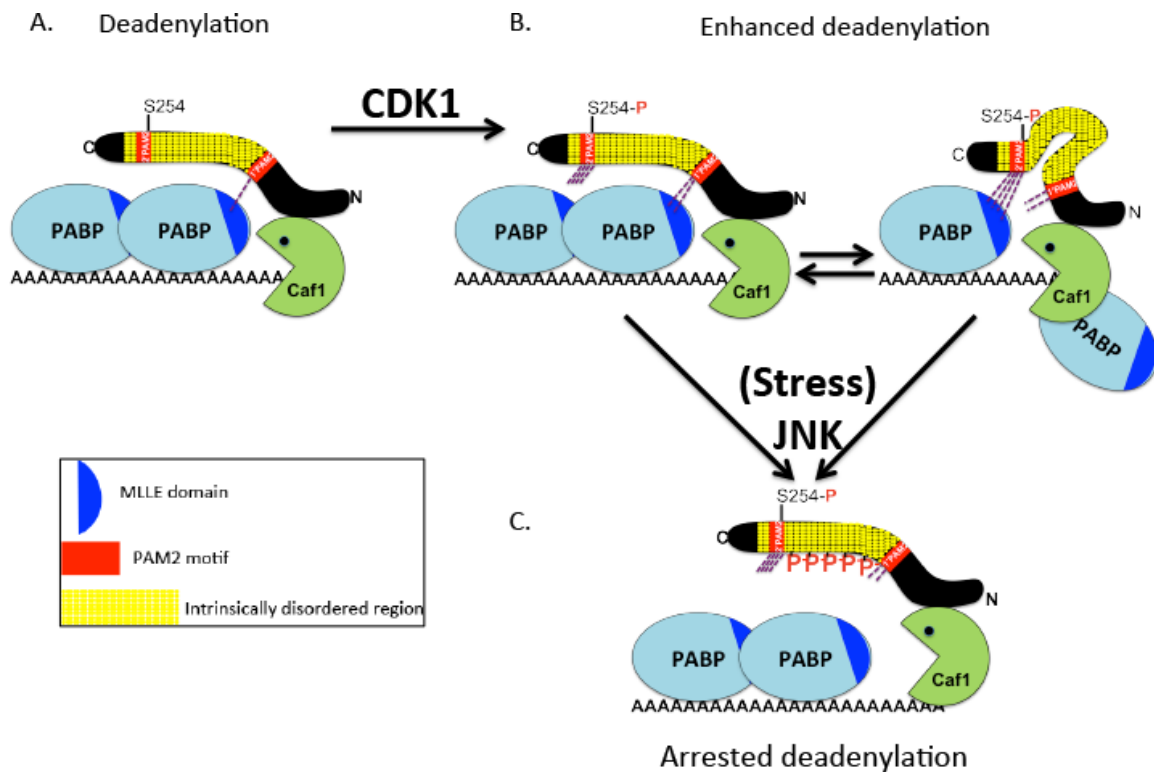


Figure 4.20 A model showing multi-layer regulations of Tob2 function in deadenylation. (A) Tob2 interacts with PABP through only first PAM2 motif when S254 is not phosphorylated. (B) Phosphorylation at S254 by CDK1 enables both PAM2 motifs work synergistically to enhance deadenylation function by interacting with PABP strongly. (C) In a circumstance when the JNK pathway is activated, Tob2 will be phosphorylated at

multiple sites in the intrinsically disordered region. The hyper-phosphorylated Tob2 will have diminished interaction with PABP. As a result, deadenylation is slowed down.

Chapter 5

Retrospectives and Perspectives

It is known that decay of majority mRNAs occurs after deadenylation. Besides, the poly(A) tail also determines each mRNA's location and translation efficiency. Poly(A) binding proteins (PABPs) on the tail orchestrate this delicate machinery by interacting with various proteins, mainly through C-terminal MLLE domain, to determine mRNA fate. The current model of on-poly(A) tail PABP interaction with PAM2 motif-containing proteins is that only the last one on tail have available MLLE domain free for interaction with PAM2 motif. Many different PAM2 motif-containing proteins have their own unique biological function, but only one PABP on each mRNA tail is available for binding. This raises the question of how the MLLE domain of PABP is regulated to selectively interact with various PAM2 motifs containing proteins? Initially, to test if phosphorylation in or adjacent to the MLLE domain of PABP regulates the selectivity, mutagenesis was carried out to change predicted phosphorylation sites in PABP C-terminal region, to either phospho-resistant or phospho-mimetic mutants. Co-immunoprecipitation assay was used to test whether these mutants have different affinity toward PAM2 motif-containing proteins, such as Tob2. While preliminary results show that these PABP mutants pulled down similar amount of Tob2, the Tob2 co-immunoprecipitated by PABP have a different phosphorylation pattern as compared to steady state pattern, and it seemed that PABP preferentially interacts with less phosphorylated Tob2. Thus, this study focused on the role of phosphorylation of PAM2 motif-containing proteins.

Previous prediction by our lab suggested that most of the PAM2 motif-containing proteins share the same feature with intrinsically disordered region (IDR) in their full structures. The IDR region is known for its flexible structure and the tendency to be post-translation modified by phosphorylation. Since PAM2 motifs are embedded in this region surrounded by many predicted phosphorylation sites, we further hypothesized that phosphorylation in the IDR region of PAM2 motif-containing proteins regulates its

interaction with PABP.

The work described in Chapter 3 of this dissertation demonstrated that indeed multiple phosphorylation in IDR region of well-known PAM2 motif-containing proteins Tob2, Pan3, and Tnrc6 diminish their interaction with PABP and decrease their biological functions. The work described in Chapter 4 of this dissertation used Tob2-PABP interaction as a model to find the critical phosphorylation site controlling the interaction of PAM2 motif-containing proteins with PABP because (1) Tob2 has a smaller IDR region and thus has less predicted phosphorylation sites than Pan3 and TNRC6; (2) Tob2 has a unique and distinct phosphorylation pattern. It is relatively easy to judge whether Tob2 is in hyper-phosphorylation status or hypo-phosphorylation status without using an antibody against the phosphorylation sites. We identified a critical phosphorylation site (S254) inside the second PAM2 motif of Tob2, which controls the ability of the second PAM2 motif to interact with PABP and the synergism of the two PAM2 motifs in terms of PABP interaction. The enhancement of PABP interaction by phosphorylation at S254 of Tob2 greatly enhances the Tob2 function in promoting deadenylation. In accordance with the hypothesis in Chapter 3 that multiple phosphorylations in the IDR region of PAM2 motif-containing proteins dampen their interaction with PABP, this study also found that hyper-phosphorylated Tob2 induced by JNK1 reduced its ability to interact with PABP. Mass Spectrometry analysis revealed that those phosphorylation sites are located in the IDR region adjacent to the PAM2 motif. Preliminary data from RNA deep sequencing analysis supports the notion that Tob2 anti-proliferation is correlated with mRNA destabilization of cyclins, which are known to control cell cycle progression, hence the rate of cell proliferation. These observations suggest that Tob2 anti-proliferation function is in part through destabilizing cyclins mRNA to decrease cyclins level.

Chapter 4 of this dissertation also described the finding that JNK1 can induce Tob2 hyper-phosphorylation *in vivo*. While other PAM2-containing proteins may share that same pathway for PABP-interaction, each PAM2 motif-containing protein could have its own unique upstream pathway, receiving different signaling cues and responding to the PABP-poly(A) tail mRNP. Thus, although multiple phosphorylation events in the IDR region of PAM2 motif-containing proteins seems to diminish interactions of all PAM2 with PABP, the phosphorylation events may be induced from different kinases by different stimuli.

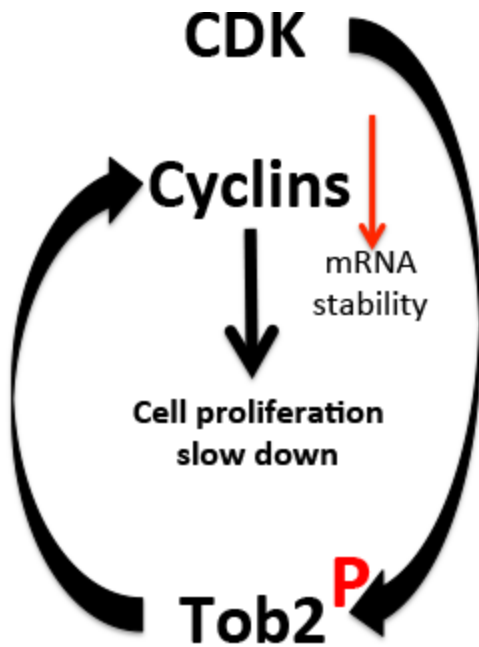


Figure 5.1. Diagram shows the hypothesis of the feedback loop of deadenylation regulation and its effect on cell proliferation. Cyclin-dependent kinase (CDK) phosphorylates Tob2 at Serine 254, resulting in enhancement of deadenylation toward cyclin mRNA. Decrease of cyclins' stability not only reduces cell proliferations rate but also disables the CDK kinase function. In return, Tob2 S254 is less phosphorylated and cyclins' transcripts gain their stability back and restore growth rate.

The work described in Chapter 4 also supports that Tob2 S254 can be phosphorylated by CDK. As our preliminary data support a role of Tob2 S254D phospho-mimetic mutant in destabilizing major cyclins, these observations suggest a feedback loop model between CDK1/cyclins and Tob2 (Figure 5.1). When CDK1/cyclins

phosphorylate Tob2 at S254, global deadenylation is promoted by Tob2 and cyclins mRNAs are destabilized; as a result, less proteins are available for CDK activity. Cell cycle progression is slowed down in all phases, resulting in anti-proliferation effect of Tob2. On the other hand, dephosphorylation of Tob2 S254 by phosphatase or turnover of Tob2 protein gives rise to non-phosphorylated S254 of Tob2, which impact the ability to promote deadenylation. Restoration of cyclins mRNA stability allows CDK protein to be expressed and thus to phosphorylate Tob2 again.

Bibliography

1. Goldstrohm, A. C., and Wickens, M. (2008) Multifunctional deadenylase complexes diversify mRNA control. *Nature reviews. Molecular cell biology* **9**, 337-344
2. McKee, A. E., and Silver, P. A. (2007) Systems perspectives on mRNA processing. *Cell research* **17**, 581-590
3. Shatkin, A. J. (1976) Capping of eucaryotic mRNAs. *Cell* **9**, 645-653
4. Chandler, D. S., McGuffin, M. E., and Mattox, W. (2001) Functionally antagonistic sequences are required for normal autoregulation of *Drosophila* tra-2 pre-mRNA splicing. *Nucleic acids research* **29**, 3012-3019
5. Mandel, C. R., Kaneko, S., Zhang, H., Gebauer, D., Vethantham, V., Manley, J. L., and Tong, L. (2006) Polyadenylation factor CPSF-73 is the pre-mRNA 3'-end-processing endonuclease. *Nature* **444**, 953-956
6. Bienroth, S., Keller, W., and Wahle, E. (1993) Assembly of a processive messenger RNA polyadenylation complex. *The EMBO journal* **12**, 585-594
7. Rigo, F., and Martinson, H. G. (2009) Polyadenylation releases mRNA from RNA polymerase II in a process that is licensed by splicing. *Rna* **15**, 823-836
8. Fuke, H., and Ohno, M. (2008) Role of poly (A) tail as an identity element for mRNA nuclear export. *Nucleic acids research* **36**, 1037-1049
9. Kloc, M., Zearfoss, N. R., and Etkin, L. D. (2002) Mechanisms of subcellular mRNA localization. *Cell* **108**, 533-544
10. Weill, L., Belloc, E., Bava, F. A., and Mendez, R. (2012) Translational control by changes in poly(A) tail length: recycling mRNAs. *Nature structural & molecular biology* **19**, 577-585

11. Fabian, M. R., Cieplak, M. K., Frank, F., Morita, M., Green, J., Srikumar, T., Nagar, B., Yamamoto, T., Raught, B., Duchaine, T. F., and Sonenberg, N. (2011) miRNA-mediated deadenylation is orchestrated by GW182 through two conserved motifs that interact with CCR4-NOT. *Nature structural & molecular biology* **18**, 1211-1217
12. Meyer, S., Temme, C., and Wahle, E. (2004) Messenger RNA turnover in eukaryotes: pathways and enzymes. *Critical reviews in biochemistry and molecular biology* **39**, 197-216
13. Chen, C. Y., Ezzeddine, N., and Shyu, A. B. (2008) Messenger RNA half-life measurements in mammalian cells. *Methods in enzymology* **448**, 335-357
14. Chen, C. Y., and Shyu, A. B. (2013) Deadenylation and P-bodies. *Advances in experimental medicine and biology* **768**, 183-195
15. Proudfoot, N. J. (2011) Ending the message: poly(A) signals then and now. *Genes & development* **25**, 1770-1782
16. Yamashita, A., Chang, T. C., Yamashita, Y., Zhu, W., Zhong, Z., Chen, C. Y., and Shyu, A. B. (2005) Concerted action of poly(A) nucleases and decapping enzyme in mammalian mRNA turnover. *Nature structural & molecular biology* **12**, 1054-1063
17. Chen, C. Y., and Shyu, A. B. (2011) Mechanisms of deadenylation-dependent decay. *Wiley interdisciplinary reviews. RNA* **2**, 167-183
18. Beelman, C. A., and Parker, R. (1995) Degradation of mRNA in eukaryotes. *Cell* **81**, 179-183
19. Collier, J., and Parker, R. (2004) Eukaryotic mRNA decapping. *Annual review of biochemistry* **73**, 861-890

20. Muhlrads, D., Decker, C. J., and Parker, R. (1994) Deadenylation of the unstable mRNA encoded by the yeast MFA2 gene leads to decapping followed by 5'→3' digestion of the transcript. *Genes & development* **8**, 855-866
21. Mitchell, P., Petfalski, E., Shevchenko, A., Mann, M., and Tollervey, D. (1997) The exosome: a conserved eukaryotic RNA processing complex containing multiple 3'→5' exoribonucleases. *Cell* **91**, 457-466
22. Schaeffer, D., Tsanova, B., Barbas, A., Reis, F. P., Dastidar, E. G., Sanchez-Rotunno, M., Arraiano, C. M., and van Hoof, A. (2009) The exosome contains domains with specific endoribonuclease, exoribonuclease and cytoplasmic mRNA decay activities. *Nature structural & molecular biology* **16**, 56-62
23. Baer, B. W., and Kornberg, R. D. (1980) Repeating structure of cytoplasmic poly(A)-ribonucleoprotein. *Proceedings of the National Academy of Sciences of the United States of America* **77**, 1890-1892
24. Mangus, D. A., Evans, M. C., and Jacobson, A. (2003) Poly(A)-binding proteins: multifunctional scaffolds for the post-transcriptional control of gene expression. *Genome biology* **4**, 223
25. Kozlov, G., Trempe, J. F., Khaleghpour, K., Kahvejian, A., Ekiel, I., and Gehring, K. (2001) Structure and function of the C-terminal PABC domain of human poly(A)-binding protein. *Proceedings of the National Academy of Sciences of the United States of America* **98**, 4409-4413
26. Derry, M. C., Yanagiya, A., Martineau, Y., and Sonenberg, N. (2006) Regulation of poly(A)-binding protein through PABP-interacting proteins. *Cold Spring Harbor symposia on quantitative biology* **71**, 537-543
27. Kuhn, U., Gundel, M., Knoth, A., Kerwitz, Y., Rudel, S., and Wahle, E. (2009) Poly(A) tail length is controlled by the nuclear poly(A)-binding protein regulating

- the interaction between poly(A) polymerase and the cleavage and polyadenylation specificity factor. *The Journal of biological chemistry* **284**, 22803-22814
28. Muniz, L., Davidson, L., and West, S. (2015) Poly(A) Polymerase and the Nuclear Poly(A) Binding Protein, PABPN1, Coordinate the Splicing and Degradation of a Subset of Human Pre-mRNAs. *Molecular and cellular biology* **35**, 2218-2230
 29. Apponi, L. H., Leung, S. W., Williams, K. R., Valentini, S. R., Corbett, A. H., and Pavlath, G. K. (2010) Loss of nuclear poly(A)-binding protein 1 causes defects in myogenesis and mRNA biogenesis. *Human molecular genetics* **19**, 1058-1065
 30. Kozlov, G., De Crescenzo, G., Lim, N. S., Siddiqui, N., Fantus, D., Kahvejian, A., Trempe, J. F., Elias, D., Ekiel, I., Sonenberg, N., O'Connor-McCourt, M., and Gehring, K. (2004) Structural basis of ligand recognition by PABC, a highly specific peptide-binding domain found in poly(A)-binding protein and a HECT ubiquitin ligase. *The EMBO journal* **23**, 272-281
 31. Hoshino, S., Imai, M., Kobayashi, T., Uchida, N., and Katada, T. (1999) The eukaryotic polypeptide chain releasing factor (eRF3/GSPT) carrying the translation termination signal to the 3'-Poly(A) tail of mRNA. Direct association of erf3/GSPT with polyadenylate-binding protein. *The Journal of biological chemistry* **274**, 16677-16680
 32. Deo, R. C., Bonanno, J. B., Sonenberg, N., and Burley, S. K. (1999) Recognition of polyadenylate RNA by the poly(A)-binding protein. *Cell* **98**, 835-845
 33. Smith, B. L., Gallie, D. R., Le, H., and Hansma, P. K. (1997) Visualization of poly(A)-binding protein complex formation with poly(A) RNA using atomic force microscopy. *Journal of structural biology* **119**, 109-117

34. Kuyumcu-Martinez, N. M., Joachims, M., and Lloyd, R. E. (2002) Efficient cleavage of ribosome-associated poly(A)-binding protein by enterovirus 3C protease. *Journal of virology* **76**, 2062-2074
35. Roy, G., De Crescenzo, G., Khaleghpour, K., Kahvejian, A., O'Connor-McCourt, M., and Sonenberg, N. (2002) Paip1 interacts with poly(A) binding protein through two independent binding motifs. *Molecular and cellular biology* **22**, 3769-3782
36. Albrecht, M., and Lengauer, T. (2004) Survey on the PABC recognition motif PAM2. *Biochemical and biophysical research communications* **316**, 129-138
37. Ezzeddine, N., Chang, T. C., Zhu, W., Yamashita, A., Chen, C. Y., Zhong, Z., Yamashita, Y., Zheng, D., and Shyu, A. B. (2007) Human TOB, an antiproliferative transcription factor, is a poly(A)-binding protein-dependent positive regulator of cytoplasmic mRNA deadenylation. *Molecular and cellular biology* **27**, 7791-7801
38. Ezzeddine, N., Chen, C. Y., and Shyu, A. B. (2012) Evidence providing new insights into TOB-promoted deadenylation and supporting a link between TOB's deadenylation-enhancing and antiproliferative activities. *Molecular and cellular biology* **32**, 1089-1098
39. Kozlov, G., Menade, M., Rosenauer, A., Nguyen, L., and Gehring, K. (2010) Molecular determinants of PAM2 recognition by the MLLE domain of poly(A)-binding protein. *Journal of molecular biology* **397**, 397-407
40. Martineau, Y., Derry, M. C., Wang, X., Yanagiya, A., Berlanga, J. J., Shyu, A. B., Imataka, H., Gehring, K., and Sonenberg, N. (2008) Poly(A)-binding protein-interacting protein 1 binds to eukaryotic translation initiation factor 3 to stimulate translation. *Molecular and cellular biology* **28**, 6658-6667

41. Khaleghpour, K., Svitkin, Y. V., Craig, A. W., DeMaria, C. T., Deo, R. C., Burley, S. K., and Sonenberg, N. (2001) Translational repression by a novel partner of human poly(A) binding protein, Paip2. *Molecular cell* **7**, 205-216
42. Kozlov, G., and Gehring, K. (2010) Molecular basis of eRF3 recognition by the MLLE domain of poly(A)-binding protein. *PloS one* **5**, e10169
43. Osawa, M., Hosoda, N., Nakanishi, T., Uchida, N., Kimura, T., Imai, S., Machiyama, A., Katada, T., Hoshino, S., and Shimada, I. (2012) Biological role of the two overlapping poly(A)-binding protein interacting motifs 2 (PAM2) of eukaryotic releasing factor eRF3 in mRNA decay. *Rna* **18**, 1957-1967
44. Chen, C. Y., Zheng, D., Xia, Z., and Shyu, A. B. (2009) Ago-TNRC6 triggers microRNA-mediated decay by promoting two deadenylation steps. *Nature structural & molecular biology* **16**, 1160-1166
45. Huang, K. L., Chadee, A. B., Chen, C. Y., Zhang, Y., and Shyu, A. B. (2013) Phosphorylation at intrinsically disordered regions of PAM2 motif-containing proteins modulates their interactions with PABPC1 and influences mRNA fate. *Rna* **19**, 295-305
46. Brown, C. J., Johnson, A. K., Dunker, A. K., and Daughdrill, G. W. (2011) Evolution and disorder. *Current opinion in structural biology* **21**, 441-446
47. Uversky, V. N. (2011) Intrinsically disordered proteins from A to Z. *The international journal of biochemistry & cell biology* **43**, 1090-1103
48. Dyson, H. J., and Wright, P. E. (2005) Intrinsically unstructured proteins and their functions. *Nature reviews. Molecular cell biology* **6**, 197-208
49. Iakoucheva, L. M., Radivojac, P., Brown, C. J., O'Connor, T. R., Sikes, J. G., Obradovic, Z., and Dunker, A. K. (2004) The importance of intrinsic disorder for protein phosphorylation. *Nucleic acids research* **32**, 1037-1049

50. Tompa, P., and Csermely, P. (2004) The role of structural disorder in the function of RNA and protein chaperones. *FASEB journal : official publication of the Federation of American Societies for Experimental Biology* **18**, 1169-1175
51. Castello, A., Fischer, B., Eichelbaum, K., Horos, R., Beckmann, B. M., Strein, C., Davey, N. E., Humphreys, D. T., Preiss, T., Steinmetz, L. M., Krijgsveld, J., and Hentze, M. W. (2012) Insights into RNA biology from an atlas of mammalian mRNA-binding proteins. *Cell* **149**, 1393-1406
52. Ubersax, J. A., and Ferrell, J. E., Jr. (2007) Mechanisms of specificity in protein phosphorylation. *Nature reviews. Molecular cell biology* **8**, 530-541
53. Doidge, R., Mittal, S., Aslam, A., and Winkler, G. S. (2012) The anti-proliferative activity of BTG/TOB proteins is mediated via the Caf1a (CNOT7) and Caf1b (CNOT8) deadenylase subunits of the Ccr4-not complex. *PloS one* **7**, e51331
54. Zheng, D., Ezzeddine, N., Chen, C. Y., Zhu, W., He, X., and Shyu, A. B. (2008) Deadenylation is prerequisite for P-body formation and mRNA decay in mammalian cells. *The Journal of cell biology* **182**, 89-101
55. Kuhn, U., and Wahle, E. (2004) Structure and function of poly(A) binding proteins. *Biochimica et biophysica acta* **1678**, 67-84
56. Wells, S. E., Hillner, P. E., Vale, R. D., and Sachs, A. B. (1998) Circularization of mRNA by eukaryotic translation initiation factors. *Molecular cell* **2**, 135-140
57. Brook, M., and Gray, N. K. (2012) The role of mammalian poly(A)-binding proteins in co-ordinating mRNA turnover. *Biochemical Society transactions* **40**, 856-864
58. Sonenberg, N., and Hinnebusch, A. G. (2009) Regulation of translation initiation in eukaryotes: mechanisms and biological targets. *Cell* **136**, 731-745

59. Wilusz, C. J., Wormington, M., and Peltz, S. W. (2001) The cap-to-tail guide to mRNA turnover. *Nature reviews. Molecular cell biology* **2**, 237-246
60. Tritschler, F., Huntzinger, E., and Izaurralde, E. (2010) Role of GW182 proteins and PABPC1 in the miRNA pathway: a sense of deja vu. *Nature reviews. Molecular cell biology* **11**, 379-384
61. Jinek, M., Fabian, M. R., Coyle, S. M., Sonenberg, N., and Doudna, J. A. (2010) Structural insights into the human GW182-PABC interaction in microRNA-mediated deadenylation. *Nature structural & molecular biology* **17**, 238-240
62. Khaleghpour, K., Kahvejian, A., De Crescenzo, G., Roy, G., Svitkin, Y. V., Imataka, H., O'Connor-McCourt, M., and Sonenberg, N. (2001) Dual interactions of the translational repressor Paip2 with poly(A) binding protein. *Molecular and cellular biology* **21**, 5200-5213
63. Eystathiou, T., Jakymiw, A., Chan, E. K., Seraphin, B., Cougot, N., and Fritzler, M. J. (2003) The GW182 protein colocalizes with mRNA degradation associated proteins hDcp1 and hLSm4 in cytoplasmic GW bodies. *Rna* **9**, 1171-1173
64. Uchida, N., Hoshino, S., and Katada, T. (2004) Identification of a human cytoplasmic poly(A) nuclease complex stimulated by poly(A)-binding protein. *The Journal of biological chemistry* **279**, 1383-1391
65. Ikematsu, N., Yoshida, Y., Kawamura-Tsuzuku, J., Ohsugi, M., Onda, M., Hirai, M., Fujimoto, J., and Yamamoto, T. (1999) Tob2, a novel anti-proliferative Tob/BTG1 family member, associates with a component of the CCR4 transcriptional regulatory complex capable of binding cyclin-dependent kinases. *Oncogene* **18**, 7432-7441

66. Radivojac, P., Iakoucheva, L. M., Oldfield, C. J., Obradovic, Z., Uversky, V. N., and Dunker, A. K. (2007) Intrinsic disorder and functional proteomics. *Biophysical journal* **92**, 1439-1456
67. Dunker, A. K., Brown, C. J., Lawson, J. D., Iakoucheva, L. M., and Obradovic, Z. (2002) Intrinsic disorder and protein function. *Biochemistry* **41**, 6573-6582
68. Gnäd, F., Gunawardena, J., and Mann, M. (2011) PHOSIDA 2011: the posttranslational modification database. *Nucleic acids research* **39**, D253-260
69. Hunter, T. (2007) The age of crosstalk: phosphorylation, ubiquitination, and beyond. *Molecular cell* **28**, 730-738
70. Temporini, C., Calleri, E., Massolini, G., and Caccialanza, G. (2008) Integrated analytical strategies for the study of phosphorylation and glycosylation in proteins. *Mass spectrometry reviews* **27**, 207-236
71. Reiland, S., Messerli, G., Baerenfaller, K., Gerrits, B., Endler, A., Grossmann, J., Gruissem, W., and Baginsky, S. (2009) Large-scale Arabidopsis phosphoproteome profiling reveals novel chloroplast kinase substrates and phosphorylation networks. *Plant physiology* **150**, 889-903
72. Sugiyama, N., Nakagami, H., Mochida, K., Daudi, A., Tomita, M., Shirasu, K., and Ishihama, Y. (2008) Large-scale phosphorylation mapping reveals the extent of tyrosine phosphorylation in Arabidopsis. *Molecular systems biology* **4**, 193
73. Johnson, L. N., and Lewis, R. J. (2001) Structural basis for control by phosphorylation. *Chemical reviews* **101**, 2209-2242
74. Romero, P., Obradovic, Z., and Dunker, A. K. (2004) Natively disordered proteins: functions and predictions. *Applied bioinformatics* **3**, 105-113

75. Xue, B., Dunbrack, R. L., Williams, R. W., Dunker, A. K., and Uversky, V. N. (2010) PONDR-FIT: a meta-predictor of intrinsically disordered amino acids. *Biochimica et biophysica acta* **1804**, 996-1010
76. Linding, R., Russell, R. B., Neduva, V., and Gibson, T. J. (2003) GlobPlot: Exploring protein sequences for globularity and disorder. *Nucleic acids research* **31**, 3701-3708
77. Mauxion, F., Faux, C., and Seraphin, B. (2008) The BTG2 protein is a general activator of mRNA deadenylation. *The EMBO journal* **27**, 1039-1048
78. Miyasaka, T., Morita, M., Ito, K., Suzuki, T., Fukuda, H., Takeda, S., Inoue, J., Semba, K., and Yamamoto, T. (2008) Interaction of antiproliferative protein Tob with the CCR4-NOT deadenylase complex. *Cancer science* **99**, 755-761
79. Okochi, K., Suzuki, T., Inoue, J., Matsuda, S., and Yamamoto, T. (2005) Interaction of anti-proliferative protein Tob with poly(A)-binding protein and inducible poly(A)-binding protein: implication of Tob in translational control. *Genes to cells : devoted to molecular & cellular mechanisms* **10**, 151-163
80. Sanduja, S., Blanco, F. F., and Dixon, D. A. (2011) The roles of TTP and BRF proteins in regulated mRNA decay. *Wiley interdisciplinary reviews. RNA* **2**, 42-57
81. Tiedje, C., Kotlyarov, A., and Gaestel, M. (2010) Molecular mechanisms of phosphorylation-regulated TTP (tristetraprolin) action and screening for further TTP-interacting proteins. *Biochemical Society transactions* **38**, 1632-1637
82. Suganuma, M., Fujiki, H., Furuya-Suguri, H., Yoshizawa, S., Yasumoto, S., Kato, Y., Fusetani, N., and Sugimura, T. (1990) Calyculin A, an inhibitor of protein phosphatases, a potent tumor promoter on CD-1 mouse skin. *Cancer research* **50**, 3521-3525

83. Brautigan, D. L. (2013) Protein Ser/Thr phosphatases--the ugly ducklings of cell signalling. *The FEBS journal* **280**, 324-345
84. Rose, K. M., Bell, L. E., and Jacob, S. T. (1977) Specific inhibition of chromatin-associated poly(A) synthesis in vitro by cordycepin 5'-triphosphate. *Nature* **267**, 178-180
85. Pillai, R. S., Artus, C. G., and Filipowicz, W. (2004) Tethering of human Ago proteins to mRNA mimics the miRNA-mediated repression of protein synthesis. *Rna* **10**, 1518-1525
86. Fabian, M. R., Mathonnet, G., Sundermeier, T., Mathys, H., Zipprich, J. T., Svitkin, Y. V., Rivas, F., Jinek, M., Wohlschlegel, J., Doudna, J. A., Chen, C. Y., Shyu, A. B., Yates, J. R., 3rd, Hannon, G. J., Filipowicz, W., Duchaine, T. F., and Sonenberg, N. (2009) Mammalian miRNA RISC recruits CAF1 and PABP to affect PABP-dependent deadenylation. *Molecular cell* **35**, 868-880
87. Huntzinger, E., Braun, J. E., Heimstadt, S., Zekri, L., and Izaurralde, E. (2010) Two PABPC1-binding sites in GW182 proteins promote miRNA-mediated gene silencing. *The EMBO journal* **29**, 4146-4160
88. Zekri, L., Huntzinger, E., Heimstadt, S., and Izaurralde, E. (2009) The silencing domain of GW182 interacts with PABPC1 to promote translational repression and degradation of microRNA targets and is required for target release. *Molecular and cellular biology* **29**, 6220-6231
89. Funakoshi, Y., Doi, Y., Hosoda, N., Uchida, N., Osawa, M., Shimada, I., Tsujimoto, M., Suzuki, T., Katada, T., and Hoshino, S. (2007) Mechanism of mRNA deadenylation: evidence for a molecular interplay between translation termination factor eRF3 and mRNA deadenylases. *Genes & development* **21**, 3135-3148

90. Liu, J., Rivas, F. V., Wohlschlegel, J., Yates, J. R., 3rd, Parker, R., and Hannon, G. J. (2005) A role for the P-body component GW182 in microRNA function. *Nature cell biology* **7**, 1261-1266
91. Mangus, D. A., Evans, M. C., Agrin, N. S., Smith, M., Gongidi, P., and Jacobson, A. (2004) Positive and negative regulation of poly(A) nuclease. *Molecular and cellular biology* **24**, 5521-5533
92. Braun, J. E., Huntzinger, E., Fauser, M., and Izaurralde, E. (2011) GW182 proteins directly recruit cytoplasmic deadenylase complexes to miRNA targets. *Molecular cell* **44**, 120-133
93. Chekulaeva, M., Mathys, H., Zipprich, J. T., Attig, J., Colic, M., Parker, R., and Filipowicz, W. (2011) miRNA repression involves GW182-mediated recruitment of CCR4-NOT through conserved W-containing motifs. *Nature structural & molecular biology* **18**, 1218-1226
94. Moretti, F., Kaiser, C., Zdanowicz-Specht, A., and Hentze, M. W. (2012) PABP and the poly(A) tail augment microRNA repression by facilitated miRISC binding. *Nature structural & molecular biology* **19**, 603-608
95. Brook, M., McCracken, L., Reddington, J. P., Lu, Z. L., Morrice, N. A., and Gray, N. K. (2012) The multifunctional poly(A)-binding protein (PABP) 1 is subject to extensive dynamic post-translational modification, which molecular modelling suggests plays an important role in co-ordinating its activities. *The Biochemical journal* **441**, 803-812
96. Burnett, G., and Kennedy, E. P. (1954) The enzymatic phosphorylation of proteins. *The Journal of biological chemistry* **211**, 969-980
97. Cozzzone, A. J. (1988) Protein phosphorylation in prokaryotes. *Annual review of microbiology* **42**, 97-125

98. Preiss, T., Muckenthaler, M., and Hentze, M. W. (1998) Poly(A)-tail-promoted translation in yeast: implications for translational control. *Rna* **4**, 1321-1331
99. Ajima, R., Ikematsu, N., Ohsugi, M., Yoshida, Y., and Yamamoto, T. (2000) Cloning and characterization of the mouse tob2 gene. *Gene* **253**, 215-220
100. Jia, S., and Meng, A. (2007) Tob genes in development and homeostasis. *Developmental dynamics : an official publication of the American Association of Anatomists* **236**, 913-921
101. Winkler, G. S. (2010) The mammalian anti-proliferative BTG/Tob protein family. *Journal of cellular physiology* **222**, 66-72
102. Mauxion, F., Chen, C. Y., Seraphin, B., and Shyu, A. B. (2009) BTG/TOB factors impact deadenylases. *Trends in biochemical sciences* **34**, 640-647
103. Suzuki, T., J, K. T., Ajima, R., Nakamura, T., Yoshida, Y., and Yamamoto, T. (2002) Phosphorylation of three regulatory serines of Tob by Erk1 and Erk2 is required for Ras-mediated cell proliferation and transformation. *Genes & development* **16**, 1356-1370
104. Maekawa, M., Nishida, E., and Tanoue, T. (2002) Identification of the Anti-proliferative protein Tob as a MAPK substrate. *The Journal of biological chemistry* **277**, 37783-37787
105. Aslam, A., Mittal, S., Koch, F., Andrau, J. C., and Winkler, G. S. (2009) The Ccr4-NOT deadenylase subunits CNOT7 and CNOT8 have overlapping roles and modulate cell proliferation. *Molecular biology of the cell* **20**, 3840-3850
106. Feng, M., Li, Z., Aau, M., Wong, C. H., Yang, X., and Yu, Q. (2011) Myc/miR-378/TOB2/cyclin D1 functional module regulates oncogenic transformation. *Oncogene* **30**, 2242-2251

107. Mayya, V., Lundgren, D. H., Hwang, S. I., Rezaul, K., Wu, L., Eng, J. K., Rodionov, V., and Han, D. K. (2009) Quantitative phosphoproteomic analysis of T cell receptor signaling reveals system-wide modulation of protein-protein interactions. *Science signaling* **2**, ra46
108. Franz-Wachtel, M., Eisler, S. A., Krug, K., Wahl, S., Carpy, A., Nordheim, A., Pfizenmaier, K., Hausser, A., and Macek, B. (2012) Global detection of protein kinase D-dependent phosphorylation events in nocodazole-treated human cells. *Molecular & cellular proteomics : MCP* **11**, 160-170
109. Mertins, P., Qiao, J. W., Patel, J., Udeshi, N. D., Clauser, K. R., Mani, D. R., Burgess, M. W., Gillette, M. A., Jaffe, J. D., and Carr, S. A. (2013) Integrated proteomic analysis of post-translational modifications by serial enrichment. *Nature methods* **10**, 634-637
110. Gossen, M., and Bujard, H. (1993) Anhydrotetracycline, a novel effector for tetracycline controlled gene expression systems in eukaryotic cells. *Nucleic acids research* **21**, 4411-4412
111. Harrold, S., Genovese, C., Kobrin, B., Morrison, S. L., and Milcarek, C. (1991) A comparison of apparent mRNA half-life using kinetic labeling techniques vs decay following administration of transcriptional inhibitors. *Analytical biochemistry* **198**, 19-29
112. Seiser, C., Posch, M., Thompson, N., and Kuhn, L. C. (1995) Effect of transcription inhibitors on the iron-dependent degradation of transferrin receptor mRNA. *The Journal of biological chemistry* **270**, 29400-29406
113. Chen, C. Y., Xu, N., and Shyu, A. B. (1995) mRNA decay mediated by two distinct AU-rich elements from c-fos and granulocyte-macrophage colony-

- stimulating factor transcripts: different deadenylation kinetics and uncoupling from translation. *Molecular and cellular biology* **15**, 5777-5788
114. Shyu, A. B., Greenberg, M. E., and Belasco, J. G. (1989) The c-fos transcript is targeted for rapid decay by two distinct mRNA degradation pathways. *Genes & development* **3**, 60-72
 115. Kawamura, H., Tomozoe, Y., Akagi, T., Kamei, D., Ochiai, M., and Yamada, M. (2002) Identification of the nucleocytoplasmic shuttling sequence of heterogeneous nuclear ribonucleoprotein D-like protein JKTBP and its interaction with mRNA. *The Journal of biological chemistry* **277**, 2732-2739
 116. Lin, Y. T., Wen, W. C., and Yen, P. H. (2012) Transcription-dependent nuclear localization of DAZAP1 requires an N-terminal signal. *Biochemical and biophysical research communications* **428**, 422-426
 117. Wang, Y., Pang, W. J., Wei, N., Xiong, Y., Wu, W. J., Zhao, C. Z., Shen, Q. W., and Yang, G. S. (2014) Identification, stability and expression of Sirt1 antisense long non-coding RNA. *Gene* **539**, 117-124
 118. Iio, A., Takagi, T., Miki, K., Naoe, T., Nakayama, A., and Akao, Y. (2013) DDX6 post-transcriptionally down-regulates miR-143/145 expression through host gene NCR143/145 in cancer cells. *Biochimica et biophysica acta* **1829**, 1102-1110
 119. Tani, H., Mizutani, R., Salam, K. A., Tano, K., Ijiri, K., Wakamatsu, A., Isogai, T., Suzuki, Y., and Akimitsu, N. (2012) Genome-wide determination of RNA stability reveals hundreds of short-lived noncoding transcripts in mammals. *Genome research* **22**, 947-956
 120. Lu, K. P., Liou, Y. C., and Zhou, X. Z. (2002) Pinning down proline-directed phosphorylation signaling. *Trends in cell biology* **12**, 164-172

121. Nguyen, L. K., Kolch, W., and Kholodenko, B. N. (2013) When ubiquitination meets phosphorylation: a systems biology perspective of EGFR/MAPK signalling. *Cell communication and signaling : CCS* **11**, 52
122. Sasajima, H., Nakagawa, K., and Yokosawa, H. (2002) Antiproliferative proteins of the BTG/Tob family are degraded by the ubiquitin-proteasome system. *European journal of biochemistry / FEBS* **269**, 3596-3604
123. Hiramatsu, Y., Kitagawa, K., Suzuki, T., Uchida, C., Hattori, T., Kikuchi, H., Oda, T., Hatakeyama, S., Nakayama, K. I., Yamamoto, T., Konno, H., and Kitagawa, M. (2006) Degradation of Tob1 mediated by SCFSkp2-dependent ubiquitination. *Cancer research* **66**, 8477-8483

Vita

Kai-Lieh Huang was born in Taipei, Taiwan on December 22, 1978, the only child of Kong Huang and Mei-Lan Chang. After completing his work at Municipal Chenggong High School, Taipei City, Taiwan in 1997, he entered the National Sun Yat-sen University in Kaohsiung, Taiwan. He received the degree of Bachelor of Science from the University in June 2001. He later jointed Dr. Chung-Lung Cho and Dr. Hong-Yo Kang's labs to study the mechanism of androgen-induced osteoblast proliferation, and received the Master of Science degree in June 2003. For the next four years, he worked as a research assistant in Academia Sinica, Taipei, Taiwan, where he first worked at the National Genotyping Center, and then moved to Dr. Yuh-Shan Jou's lab to study carcinogenesis of oral cancer. In September of 2008, he entered The University of Texas Graduate School of Biomedical Sciences at Houston. He was with Dr. Dina Lev for the first three years to perform a translational study in sarcoma. In May of 2011, he started this dissertation research with Dr. Chyi-Ying A. Chen and Dr. Ann-Bin Shyu.

Publications

1. **Huang KL**, Chadee AB, Chen CY, Zhang Y, Shyu AB. *Phosphorylation at intrinsically disordered regions of PAM2 motif-containing proteins modulates their interactions with PABPC1 and influences mRNA fate*. RNA. 2013 Mar;19(3):295-305.

2. Kivlin CM, Watson KL, Al Sannaa GA, Belousov R, Ingram DR, **Huang KL**, May CD, Bolshakov S, Landers SM, Kalam AA, Slopis JM, McCutcheon IE, Pollock RE, Lev D, Lazar AJ, Torres KE. *Poly (ADP) Ribose Polymerase Inhibition: A Potential Treatment of Malignant Peripheral Nerve Sheath Tumor*. Cancer Biol Ther. 2016 Feb;17(2):129-38.
3. Brewer Savannah KJ, Demicco EG, Lusby K, Ghadimi MP, Belousov R, Young E, Zhang Y, **Huang KL**, Lazar AJ, Hunt KK, Pollock RE, Creighton CJ, Anderson ML, Lev D. *Dual targeting of mTOR and aurora-A kinase for the treatment of uterine Leiomyosarcoma*. Clin Cancer Res. 2012 Sep 1;18(17):4633-45.
4. Torres KE, Liu J, Young E, **Huang KL**, Ghadimi M, Lusby K, Lazar AJ, Lev D. *Expression of 'druggable' tyrosine kinase receptors in malignant peripheral nerve sheath tumour: potential molecular therapeutic targets for a chemoresistant cancer*. Histopathology. 2011 Jul;59(1):156-9.
5. Zhu QS, Rosenblatt K, **Huang KL**, Lahat G, Brobey R, Bolshakov S, Nguyen T, Ding Z, Bill K, Lazar AJ, Dicker A, Mills GB, Hung MC, Lev D. *Vimentin is a Novel AKT1 Target Mediating Motility and Invasion*. Oncogene. 2011 Jan 27;30(4):457-70.
6. Lahat G, Zhu QS, **Huang KL**, Wang S, Bolshakov S, Liu J, Torres K, Langley RR, Lazar AJ, Hung MC, Lev D. *Vimentin is a novel anti-cancer therapeutic target; insights from in vitro and in vivo mice xenograft studies*. PLoS One. 2010 Apr 16;5(4):e10105.

7. Chen JYF, Hung CC, **Huang KL**, Chen YT, Liu SY, Chiang WF, Chen HR, Chen YC, Yen CY, Chung TT, Ko JY, Jou YS. *Src family kinases mediate betel quid-induced oral cancer cell motility and could be crucial for the early progression of oral carcinogenesis*. Neoplasia. 2008 Dec;10(12):1393-401.
8. Kang HY, Cho CL, **Huang KL**, Wang JC, Hu YC, Lin HK, Chang C, Huang KE. *Nongenomic androgen activation of phosphatidylinositol 3-kinase/Akt signaling pathway in MC3T3-E1 osteoblasts*. J Bone Miner Res. 2004 Jul;19(7):1181-90.

Permanent address:

12F., No.270, Han-sheng E. Rd.

Banqiao District, New Taipei City 22066

Taiwan